Source apportionment of PM2.5 and their associated metallic elements by positive matrix factorization at a traffic site in Constantine, Algeria

Lamri Naidja, Hocine Ali-Khodja, Salah Khardi, Fairouz Bencharif-Madani, Ahmed Terrouche, Kanza Lokorai, Mokhtar Bouziane, Aurélie Charron

Source apportionment of $PM_{2.5}$ and their associated metallic elements by positive matrix factorization at a traffic site in Constantine, Algeria

Lamri Naidja[1,2,3] · Hocine Ali-Khodja[1] · Salah Khardi[4] · Fairouz Bencharif-Madani[1] · Ahmed Terrouche[1] · Kanza Lokorai[1] · Mokhtar Bouziane[1] · Aurélie Charron[5]

Abstract

Chemical characterization of $PM_{2.5}$ (major and trace elements) was carried out for a source apportionment study of $PM_{2.5}$ at a traffic site in Constantine, Algeria, from March 2017 to March 2018. For this purpose, several tools were used of which PMF, *CPF*, *PSCF*, Spearman correlation matrix and HYSPLIT back trajectories. The mean annual concentration of $PM_{2.5}$ at the sampling site was 54.07 ± 28.81 μg/m^3. This value is much higher than the annual threshold recommended by the WHO of 10 μg/m^3. Based on the PMF modelling, five sources were identified: sea salts (15.1%), industrial activities (18.9%), non-exhaust emissions (wear of brakes, tires and road surfaces) (24.2%), exhaust emissions (mixed diesel and gasoline engine exhaust) (15.8%) and mineral dust (25.9%) as the main sources of metallic aerosols at the sampling site in Constantine. Our results revealed that anthropogenic activities (traffic and industry) contributed 59% to all emissions, while natural sources (mineral dust and sea salt) accounted for 41%. Traffic-related sources are the major contributor to anthropogenic emissions (40%) with non-exhaust emissions being the dominant source. As anthropogenic emissions are the leading sources, their control is of utmost importance for improving air quality. The concentrations of $PM_{2.5}$ tend to increase appreciably with temperature and wind speed for a relative humidity less than 60%. The contribution of vehicular emissions is affected by relative humidity and temperature while industrial emissions are affected mainly by wind intensity and direction. Relative humidity, temperature and wind speed are determining parameters of mineral dust. There are seasonal variations in the contributions of the PMF-derived sources. Summer undergoes significant contributions of three factors: sea salts, industrial emissions and mineral dust. Spring is affected mainly by industrial emissions and non-exhaust emissions. Winter experiences a drastic contribution of the exhaust emission factor. Autumn is the least affected season by mineral dust and sea salts. It is rather affected by industrial and traffic emissions.

Keywords Metallic aerosols · $PM_{2.5}$ · PMF · CPF · PSCF · Source apportionment · Traffic site

✉ Hocine Ali-Khodja
hocine_ak@yahoo.fr

[1] Laboratory of Pollution and Water Treatment, Department of Chemistry, Faculty of Exact Sciences, University of Mentouri Brothers-Constantine 1, 25017 Constantine, Algeria

[2] Centre de Recherche Scientifique Et Technique en Analyses Physico-Chimiques (CRAPC), Si`Ege Ex Pasna Zone Industrielle Bou-Ismail, BP 384, CP 42004 Tipaza, Algeria

[3] Centre de Recherche en Sciences Pharmaceutiques, Nouvelle Ville Ali Mendjli, Zone d'activités ZAM, Constantine, Algeria

[4] University Lyon, INSA Lyon, CNRS, LaMCoS, UMR5259, 69621, Villeurbanne, France

[5] Unité Mixte de Recherche Epidémiologique Et de Surveillance Transport Travail Environnement, University Gustave Eiffel Lyon Campus, Lyon, France

Introduction

Particulate matter (PM) is a complex mixture of small particles and liquid droplets whose physical and chemical characteristics vary by region and time. Common chemical constituents of PM include sulphates, nitrates, ammonium, other inorganic ions, metals, elemental carbon and organic compounds.

The health effects were related to the distribution of PM sizes, the latter were divided into two parts: PM_{10} (coarse particles) and $PM_{2.5}$ (fine particles). The potential impact of smaller particles on human health has been revealed by several authors (Biersteker 1976; Bevan and Manger 1985; Quackenboss et al. 1989). Boubel et al. (2013) showed that $PM_{2.5}$ could not be retained in the upper part of the

respiratory system and can accumulate in the lungs and enter the airways, due to Brownian motion, unlike PM_{10} which could be retained. Besides the size, the effect of aerosols on health is also a function of their chemical composition. Most heavy metals are dangerous because they tend to bio-accumulate in the human body. Metallic elements cannot be degraded, and can be transported by air, and enter water and human food supply. However, at higher (although relatively low) concentrations they can become toxic (Järup 2003). Many studies have linked certain metals to several health problems such as cardiovascular disease, heart disease, aggravated asthma and lung cancer (Kampa and Castanas 2008; Sudheer and Rengarajan 2012).

The problem of air pollution is clearly ignored by many African countries, largely because it is not seen as a priority over economic development. Therefore, these countries are clearly in no rush to solve air quality problems. In many African countries, air quality data is scarce and virtually absent, especially in sub-Saharan countries. The lack of data is therefore one of the main constraints to understanding the harmful effects on human health of fine particles.

Ambient air quality improvement strategies involve reducing emissions from primary sources. It is therefore essential to be able to identify and distribute the contributions of these sources and then implement effective regulations and policies that reduce the levels of particulate pollution. Receptor models are often presented as a reliable tools which allow the identification of the contribution of emission sources and which require speciation data for the aerosol fraction sampled at a receptor site (Hoke 2010).

In Algeria, few studies have been carried out to identify PM emission sources. Terrouche et al. (2016) used the varimax rotated factor analysis, a multivariate technique. Their study targeted only eight metallic elements. Bencharif-Madani et al. (2019) and Talbi et al. (2018) both used the PCA technique which did not differentiate separate sources. Moreover, these methods do not provide a quantitative distribution of mass contributions.

In addition, the absence of a non-negativity requirement implies that PCA can give factors with negative loadings and could promote physically unreasonable results (Paatero and Tapper 1994). To solve this problem, specific methods such as positive matrix factorization (PMF) have been specifically developed (Paatero and Hopke 2003). In order to distinguish between nearby and distant sources, the *CPF* and *PSCF* tools have been used.

Materials and methods

Description of the sampling site

Constantine is a city in northeastern Algeria, located about 390 km from Algiers, the country's capital (Fig. 1) and 63 km from the Algerian coast. This metropolis is the third most populous city in the country. The agglomeration of Constantine had 943,112 inhabitants in 2015, of which only 54% live in the municipality of Constantine (448,000 inhabitants). This city is characterized by a hot and dry semi-arid climate in summer with an average maximum temperature of 36 °C and a humidity of around 25% while

Fig. 1 Location of the sampling site and city of Constantine, Algeria

the winter is cold and wet. Precipitation totals 560 mm per year, with monthly precipitation varying from 0 to 80 mm (Bencharif-Madani et al. 2019).

To attain the objectives of our work, an urban traffic site was chosen in Zouaghi, Constantine (36° 31′ North, 6° 62′ East, 649 m above sea level). The site is located 5.65 km southwest of the city of Constantine (Fig. 1). It has around 26,000 inhabitants.

The national vehicle fleet is composed approximately of 50% vehicles running on gasoline and the remaining 50% on gas-oil. However, gas-oil represents 70% of total fuel consumption.

The nearest main road (national road N79) is about 5 m west of the study site and has two lanes of traffic in each direction (Fig. S1). This road connects the city of Constantine with the new town, Ali Mendjli, as well as other cities such as Batna, Oum El Bouaghi and Biskra. The East–West motorway is 1.7 km south of the site. The sampling site is also surrounded by three urban areas. These are located to the east, south and northwest of the site (Fig. S1). In addition, Mohamed Boudiaf Airport is located 2.86 km south of the sampling site.

Sampling campaign

$PM_{2.5}$ was collected on quartz fibre filters (WHATMAN®, diameter 47 mm, QMA grade) at the frequency of one sample every 3 days at the entrance of the Faculty of Earth Sciences in Zouaghi. The sampling campaign ran from March 15, 2017 to March 15, 2018, using a low volume LVS (low volume sampler) brand "Tactical Air Sampler" (Fig. S2). Each sampling was carried out for a period of 24 h with a suction flow rate of 5 l of air/min.

The sampler is attached to a metal pipe at a height of 1.80 m and at a distance of approximately 5 m from the N79 national road. It operates from a battery that can power the sampler for at least 24 h continuously, making the sampling site independent of mains power.

The exposed filter is recovered within hours of the end of the sampling period to prevent damage to the filter or change in particle mass due to passive absorption or volatilization. The exposed filters are placed in petri dishes, placed with the exposed side of the filter facing up and kept in the desiccator for 48 h. They are weighed before and after each sampling using a microbalance with an accuracy of 1 µg (Shimadzu AUW 120D) to determine the mass of particles captured on the filters. All precautions are taken during the installation and recovery of the filters (wearing gloves, using the pliers) to avoid any contamination. A total of 120 samples were collected throughout the sampling period of 12 months.

Mineralization protocol

We have chosen the mineralization method proposed by Querol et al. (2001). Kemmouche et al. (2017) were able to demonstrate that the chosen protocol is the most effective since it promotes the complete recovery of all the elements by the essential use of hydrofluoric acid (HF) which remains the only reagent capable of releasing major elements and traces linked to silica with recovery rates greater than 80%. This protocol is best suited for source distribution studies, which require a large number of elements and where it is strongly recommended to consider total dissolution of samples using HF to ensure reliability of results.

First, the filters are cut in half. Half undergo the digestion protocol and the other half are stored in the fridge at 3 °C for further analysis. The half-filters are digested in a solution containing 1 ml of nitric acid (HNO_3) and 2 ml of HF in closed Teflon-PFA (PerFluorAlkoxy) vials in the oven at 90 °C overnight (at least 8 h of time). After cooling, 1 ml of perchloric acid ($HClO_4$) is added. Then, the containers are heated for 4 h on a hotplate at 240 °C until the acids have completely evaporated. 2.5 ml of HNO_3 are then added to the remaining dry residue and then diluted in a 25-ml flask, making up the volume with ultra-pure water (MilliQ) to obtain 5% HNO_3 solutions. Then the contents of each vial are transferred to test tubes and centrifuged for 2 min at 3000 rpm to remove residues from the mineral filters. The solutions obtained are stored in polypropylene (PP) bottles fitted with tight caps.

Filter analysis

The 120 $PM_{2.5}$ samples, including the 5 blank filters, were analysed by two instruments, inductively coupled plasma emission spectroscopy (ICP-OES, Perkin Elmer Optima 4300 DV model) for sulphur (S) and plasma mass spectrometry with inductive coupling (ICP-MS, Perkin Elmer NexIon 300 X model) for the rest of the elements, at the CEREGE Sustainable Development Team laboratory (UM34 University of Aix Marseille), Technopole Environnement Arbois-Méditerranée. Twenty elements which include Na, Mg, P, K, Ca, Sr, Zr, Ba, Pb, Al, Ti, V, Cr, Mn, Fe, Ni, Cu, Zn, Mo and S were measured. The detection limits and measurement uncertainty of metallic elements analysed by ICP-MS and ICP-OES are reported in Table S1.

Computation of the concentration of mineral dust

Mineral dust from the Sahara/Sahel region is mainly composed of oxides (such as SiO_2, Al_2O_3, FeO, Fe_2O_3, CaO) and carbonates (such as $CaCO_3$, $MgCO_3$) allows the determination of the mineral load brought by the Sahara (Denier van der Gon et al. 2010; European Commission 2011). Among

all other elements, oxygen is present as an oxide and is never directly measured in particle samples (Denier van der Gon et al. 2010).

There is a formula that calculates the concentration of mineral dust in their oxide forms directly, given in the equation below. According to Remoundaki et al. (2011), these oxides represent the mineral dust portion of $PM_{2.5}$:

$$\text{Mineral Dust oxide} = [SiO_2] + [A1_2O_3] + [Fe_2O_3] + [K_2O] + [CaO + CaCO_3] + [MgO] + [Tio_2]$$

To estimate the calcium levels in its most abundant forms ($CaO + CaCO_3$), Ca was multiplied by a factor of 1.95 (Remoundaki et al. 2011).

The silicon concentration was not obtained by analysis because quartz filters are rich in silicon. In our study, silicon was estimated by multiplying the concentration of aluminium by a factor of 3 (Alastuey et al. 2005).

Data analysis by PMF

The PMF approach is a multivariate factor analysis technique that has been widely applied in numerous studies in recent years. The fundamental principle of PMF is to decompose the matrix of ambient data X comprising the measurements of concentration of n chemical species in m samples and their corresponding uncertainties, into two matrices, the matrix G which represents the contribution of each factor for each sample and the matrix F which represents the chemical composition of the profile of each factor. PMF calculates the site-specific source profiles with the temporal variations of these sources based on the correlations between the data as shown in equation:

$$x_{ij} = \sum_{k=1}^{p} g_{ik} f_{kj} + e_{ij} \quad (1)$$

where x_{ij} is the concentration of species j measured on sample i, g_{ik} is the relative contribution of any k factor to sample i, f_{kj} is the concentration of species j in the k factor profile, e_{ij} is the residue associated with the concentration of species j measured in sample i, and p is the number of independent sources.

The PMF model tries to reproduce x_{ij} by minimizing the sum of the squares of the scaled residuals (Q):

$$Q = \sum_{i=1}^{n} \sum_{j=1}^{m} \left(\frac{e_{ij}}{S_{ij}} \right)^2 \quad (2)$$

Thus, PMF identifies a set of p factors that best characterize $PM_{2.5}$ on our site. The results are constrained so that no sample can have a negative contribution to the source.

The identification of the main sources of particulate pollution as well as the contribution of each source to the levels of the $PM_{2.5}$ is based on the protocol compiled by Belis et al. (2013), the recommendations of the EPA PMF v.5 guide (Norris et al. 2014) as well as the recommendations of Brown et al. (2015).

The number of factors (p) was determined using two criteria: the interpretability of the resulting PMF factor profiles and the factor matching success rate for the bootstrap (BS), displacement (DISP) trials and combination two (BS—DISP).

The following approach has been used consistently. The solution with the greatest number of physically significant factors is the one chosen. This choice is confirmed by visual inspection of any sharp drop in the Q_{true}/Q_{exp} graphs, relative to the number of adjusted factors. A detailed examination of the model results and goodness of fit was performed for the solutions of 2 to 9 factors.

Two input files must be specified, a concentration file and a file of uncertainties associated with these concentrations in order to be able to use PMF (Huang et al. 2001; Poirot et al. 2001).

As the PMF solution is highly dependent on the concentration and uncertainties, their estimation is crucial to obtain reliable results. Initially, all available species and samples (20 chemical elements and 120 samples) in the dataset are considered for the $PM_{2.5}$ source apportionment, then data processing was performed to exclude species, samples or outliers.

To ensure a strong data signal, only samples with less than 10% data below zero or below the limit of detection (LD) are accepted; the uncertainty attributed to these values is given as follows:

$$\sigma a^2 = LDj^2 + \left(a_{ij} X_{ij} \right) \quad (3)$$

where LD_j is the detection limit of element j, α_{ij} is the measurement uncertainty (%) of the concentration of element j in sample i and X_{ij} is the concentration of element X_j in sample i.

In addition, the analytical determination also includes the subtraction of the concentrations of the metallic elements of the blank filters which are filters different from those used for sampling. Blanks entail an additional source of uncertainty σ_{blk} which must be propagated together with σ_a to obtain the analytical determination uncertainty σ_A: ${\sigma_A}^2 = {\sigma_a}^2 + {\sigma^2}_{blk}$.

In order to include additional sources of uncertainty, the overall uncertainty was estimated by the following formula (Amato et al. 2009):

$$\sigma_{ij}^2 = \sqrt{\frac{\sigma_A^2}{V_i^2}} + \left(\beta X_{ij} \right)^2 \quad (4)$$

where V_i is the volume of air sampled for each sample i and β is a coefficient estimated at 0.15.

Species with a concentration below the detection limit have been replaced by *LD*/2 and the uncertainty S_{ij} of these values is calculated as follows:

$$\sigma_{ij} = 5/6LD \quad (5)$$

The data obtained is systematically filtered to detect unusual events and instrument performance, and is validated before modelling. The Grubbs test was also applied to the data set to detect maximum outliers. These values are removed from the data set and the test is repeated until no outlier is detected. An outlier may indicate an unusual event that disturbed the observed phenomenon to the point of making it incomparable to others. In such cases, the extreme value is either corrected where possible, or removed from the dataset. In our study, the outliers obtained during desert dust intrusions or other uncommon events were examined and retained and the uncertainties calculated for these values were increased by a factor of 3 (Kim et al. 2004, 2005).

The time series of species were also plotted and studied to identify any unusual outliers. Time series of uncertainties attributed to species concentrations were also plotted to detect any data anomalies, in which case the sample date is reconsidered to justify the extreme observation. If the anomaly is not justified, the actual value is taken as such in the modelling procedure. Each data set was also analysed to find the number of missing information, the number of validated data and the number of samples with a concentration below the *LD* value. Only species for which 50% of the data are above the mean detection limit were taken into account. Samples for which data are missing were removed from the PMF analysis. The final datasets contain 95 samples and 20 species.

Conditional probability calculation

The conditional probability function (*CPF*) was used to locate potential local sources based on local meteorological data (wind direction and speed) (Begum et al. 2004; Kim and Hopke 2004). *CPF* calculates the probability of a source that is in a particular wind direction sector, $\Delta\Theta$:

$$CPF = \frac{m_{\Delta\Theta}}{n_{\Delta\Theta}} \quad (6)$$

where $n_{\Delta\Theta}$ is the number of times the wind passed through the direction sector, and $m_{\Delta\Theta}$ is the number of times the source contribution peaked as the wind passed through the sector (Ashbaugh et al. 1985). It should be noted that the *CPF* is not suitable for distant sources because the air particles can be diverted from their path. A good knowledge of local sources is necessary.

To ensure statistical reliability, 24-h average source contribution data was applied to all 60-min wind direction averages measured at the site for each date. The wind direction range has been divided into 24 sectors of 15°. All periods associated with wind speeds less than 1 m/s were removed from the dataset. *CPF* is useful for determining the direction of a source from a receiving site. However, it cannot determine the actual location of the source.

Similarly to *CPF*, *PSCF* is a conditional probability function. In this case, regional potential sources are examined using backward trajectories. Potential source contribution function (*PSCF*) analysis has been widely used to identify regional sources that increase the level of pollutant concentration. *PSCF* is calculated with the probability of concentration at each cell and is calculated using the following equation:

$$\mathrm{PCSF}_{ij} = \frac{m_{ij}}{n_{ij}} \quad (7)$$

where m_{ij} is the number of points whose concentration is greater than a threshold and n_{ij} is the number of endpoints of the return paths that pass through each cell of the grid (Karnae and John 2011). The back trajectories required for the analysis are generated using a model developed by the National Oceanic and Atmospheric Administration (NOAA), called a hybrid single-particle Lagrangian integrated trajectory model (HYSPLIT4). The level of pollutant concentration in each of the parameters is calculated. Using the geographic information system (GIS), a spatial grid of required resolution is generated and a 90th percentile threshold is established for the distributed mass of each source.

The emission source contributions from the PMF analysis were analysed using the conditional probability function (*CPF*) and the potential source contribution function (*PSCF*) to identify the geographic locations of likely sources. The simultaneous use of these two tools is an effective way to identify local and regional sources affecting the sampling site (Wimolwattanapun et al. 2011). The *CPF* was applied at the 75 percentile of contributions and the *PSCF* at the 90 percentile (Pekney et al. 2006).

It should be noted that very few PMF studies have been conducted in Africa. The only source apportionment study conducted in Constantine is that of Bencharif-Madani et al. (2019), in which the authors used principal component analysis (PCA) to perform chemical speciation and identification of sources of PM_{10}.

Results and discussion

Characterization and temporal trend of $PM_{2.5}$ and metallic elements

The mean annual concentration of $PM_{2.5}$ at the Zouaghi sampling site was 54.07 ± 28.81 µg/m^3. It should be noted that the

relatively high standard deviation is due to a strong seasonal variation of $PM_{2.5}$ and the recording of high concentrations of $PM_{2.5}$ during unusual events. The maximum and minimum concentrations were 132.52 and 16.91 µg/m^3, respectively.

Figure 2 illustrates the average monthly $PM_{2.5}$ concentrations observed between 3/15/2017 and 3/15/2018 at the sampling site. The highest averages were recorded during the dry period (June-July–August). The mean annual concentration of $PM_{2.5}$ obtained in this campaign is higher than those measured at the traffic sites of other Algerian cities, such as Algiers (32.85 µg/m^3) (Talbi et al. 2018), Algiers (10.22 µg/m^3) (Belarbi et al. 2020) and Tiaret (33.57 µg/m^3) (Khadidja et al. 2019), and comparable to other North African cities such as Kenitra (51 µg/m^3) (Zghaid et al. 2009), Kenitra (50.73 µg/m^3) (Tahri et al. 2013), Cairo, Egypt (51 µg/m^3) (Boman et al. 2013) and Giza, Egypt (61.31 µg/m^3) (Hassan and Khoder 2017). This value is much higher than the annual threshold recommended by the WHO of 10 µg/m^3, the American annual limit (NAAQS) for $PM_{2.5}$ (32 µg/m^3) and exceeds by a factor of 2 the standard decreed by the European Commission (25 µg/m^3). However, this value is lower than the limit value set by Algerian regulations (80 µg/m^3). According to the study carried out by the Health Effects Institute and the Global Burden of Disease (GBD) project of the Institute for Health Metrics and Evaluation (IHME) in 2019, 90% of the world's population lives in an environment where annual average $PM_{2.5}$ concentrations exceed the WHO recommended threshold. Algeria is among the countries most exposed to fine particles in the world, with average annual concentrations between 35 and 45 µg/m^3 in the north and exceeding 70 µg/m^3 in the south. The areas most polluted in the world by fine particles are South and Southeast Asia, North Africa, the Middle East and the countries of sub-Saharan Africa. The highest annual levels were recorded in Nepal (100 µg/m^3), Niger (94 µg/m^3), India (91 µg/m^3), Qatar (91 µg/m^3), Saudi Arabia (88 µg/m^3), Egypt (87 µg/m^3), Cameroon (73 µg/m^3) and Nigeria (72 µg/m^3) (Health Effects Institute 2019).

The WHO recommended daily limit (25 µg/m^3) was exceeded 83 times during the sampling period, representing 69.17% of all sampling days.

Elemental analysis of $PM_{2.5}$ revealed that Ca, Na and Al predominate, followed by the elements S, Fe, K, Ba and Mg (Table 1). The terrigenous species Al, Ca, Fe, K, Mg and Ti are important as they represent about 62% of the total mass of metallic elements and the mineral dust component represents 16.6% of the mass of $PM_{2.5}$. Similar results were also observed in Barcelona (Pérez et al. 2008; Querol et al. 2004a). The concentrations of trace metals are in decreasing order Pb > P > Mo > Zn > Zr > Cr > Sr > Mn > Ni > Cu > V and are between 0.3 and 42 ng/m^3. The concentrations of Pb and Ni are not alarming. Their maximum values are 124 ng/m^3 and 14 ng/m^3, respectively.

The annual Pb concentration is well below the limit of 500 ng/m^3 recommended by the WHO and the limit set by the European Commission (200 ng/m^3). This value is lower than those reported in $PM_{2.5}$ nearby traffic sites in Algiers (371 ng/m^3, Talbi et al. 2018; 283 ng/m^3, Oucher et al. 2015), but it is close to that recorded in Barcelona (37 ng/m^3) (Querol et al. 2008). In Algeria, the main source of Pb emissions is leaded gasoline commonly used by vehicles (Naidja et al. 2018; Bencharif-Madani et al. 2019). Pb is not a tracer element for the combustion of gasoline in other countries where its use is prohibited.

The measured annual average concentrations of Cr, Ni and Zn are 6 ng/m^3, 3 ng/m^3 and 16 ng/m^3, respectively. They are

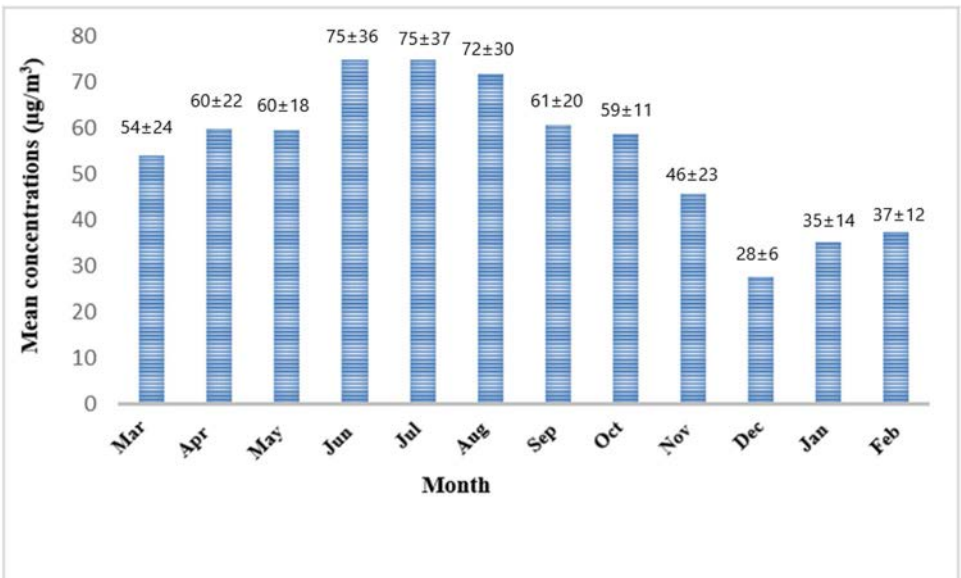

Fig. 2 Mean monthly concentrations of $PM_{2.5}$

Table 1 Statistical data on the concentrations of $PM_{2.5}$ (μg/m^3) and their components (ng/m^3)

Species	Min	25th	Mean	75th	Max	Standard deviation
$PM_{2.5}$	17	33	54	71	132	29
Na	10	352	769	987	2440	399
Mg	33	74	113	123	343	46
P	5	21	32	38	129	13
K	39	115	183	221	605	79
Ca	175	774	1249	1534	3771	496
Sr	2	4	6	7	14	2
Zr	7	10	14	17	27	4
Ba	11	65	120	139	442	54
Pb	0	30	46	58	123	19
Al	445	549	765	884	1767	220
Ti	7	13	20	22	62	8
V	0.14	0.3	0.6	0.7	2	0.3
Cr	0.01	4	6	7	28	2
Mn	2	4	5	6	49	2
Fe	57	122	158	218	5399	102
Ni	0.08	2	3	4	13	1
Cu	0.20	1	3	4	17	2
Zn	0	10	19	22	98	10
Mo	9	28	30	32	81	3
S	137	191	254	294	601	67

lower than those recorded in Algiers (46 ng/m^3, 14 ng/m^3, 78 ng/m^3) (Talbi et al. 2018) and in Kenitra, Morocco (84 ng/m^3, 166 ng/m^3, 1413 ng/m^3) (Zghaid et al. 2009). Spearman correlations between $PM_{2.5}$, mineral dust (MD), measured metals and meteorological parameters are presented in Fig. 3. This figure illustrates a strong correlation between mineral dust (MD) and terrigenous elements such as Al, Ca, Mg, Ti and K ($0.76 < r < 0.93$), except Fe ($r = 0.36$). Fe is influenced by various anthropogenic sources (traffic and industry in particular). Kandler et al. (2007) analysed dust plumes from the Sahara and observed the predominance of the major elements Al, Si, Fe, Ti, Ca, S, Na and Mg to which are added some trace elements Sr, Zr, Ba, La, Th and Nd. In addition, a strong correlation between Fe and mineral dust was recorded in summer and in autumn ($r = 0.91$ and 0.81, respectively) (Figs. S3, S4) while in spring, this correlation is medium (0.51) (Fig. S5).

There is no significant correlation between Fe and mineral dust during winter, while they are fairly well correlated during the other seasons (Figs. S3-S6). This trend has been highlighted by Bencharif-Madani et al. (2019) who observed high concentrations of this element at the same site during spring, summer and autumn, a phenomenon which could be explained by the frequency of Saharan dust episodes in Algeria during these seasons. Fe has an excellent correlation with Mn ($r = 0.97$). Mn is often an alloy with Fe to make steel. A probable source of emission of these two elements is the agricultural tractor company of Oued Hmimime, 10 km southeast from our sampling site.

Apart from Cr and Ni, which are fairly well correlated (59%), the trace elements Pb, Mo, Cu and Zn do not show a good correlation between them, with Ni and Cr and the major elements. This reflects the diversity of the sources of emission of these trace elements unlike the major elements which mainly come from the earth's crust. Figure 4 illustrates a similar time course for the major elements Na, Al, K and Mg indicating the existence of a common source. The major elements Ca, Fe, Ba and S do not follow the same pattern of temporal variation. This is due to the diversity of the sources of these major elements. Indeed, Fe, Ba and S are linked to traffic, industrial and natural emissions. V and Ti are, on the other hand, closely linked from the point of view of time evolution and also show a good correlation (76%). Several major elements (Na, Ca, Al, S, K, Mg, Ba) and traces (Sr, Ti, V, Cr) reach a peak during the period of July–August (Figs. 4, 5). As this season is known to be strongly impacted by desert dust (Lokorai et al. 2021) and temperature peaks favourable to the lifting of soil dust, it follows that these elements are essentially linked to sources of wind emissions.

Influence of meteorological conditions on $PM_{2.5}$ concentrations

Conventional meteorological parameters such as temperature, wind speed, wind direction, relative humidity and precipitation level have a strong effect on PM concentrations (Tran and Mölders 2011; Kassomenos et al. 2014).

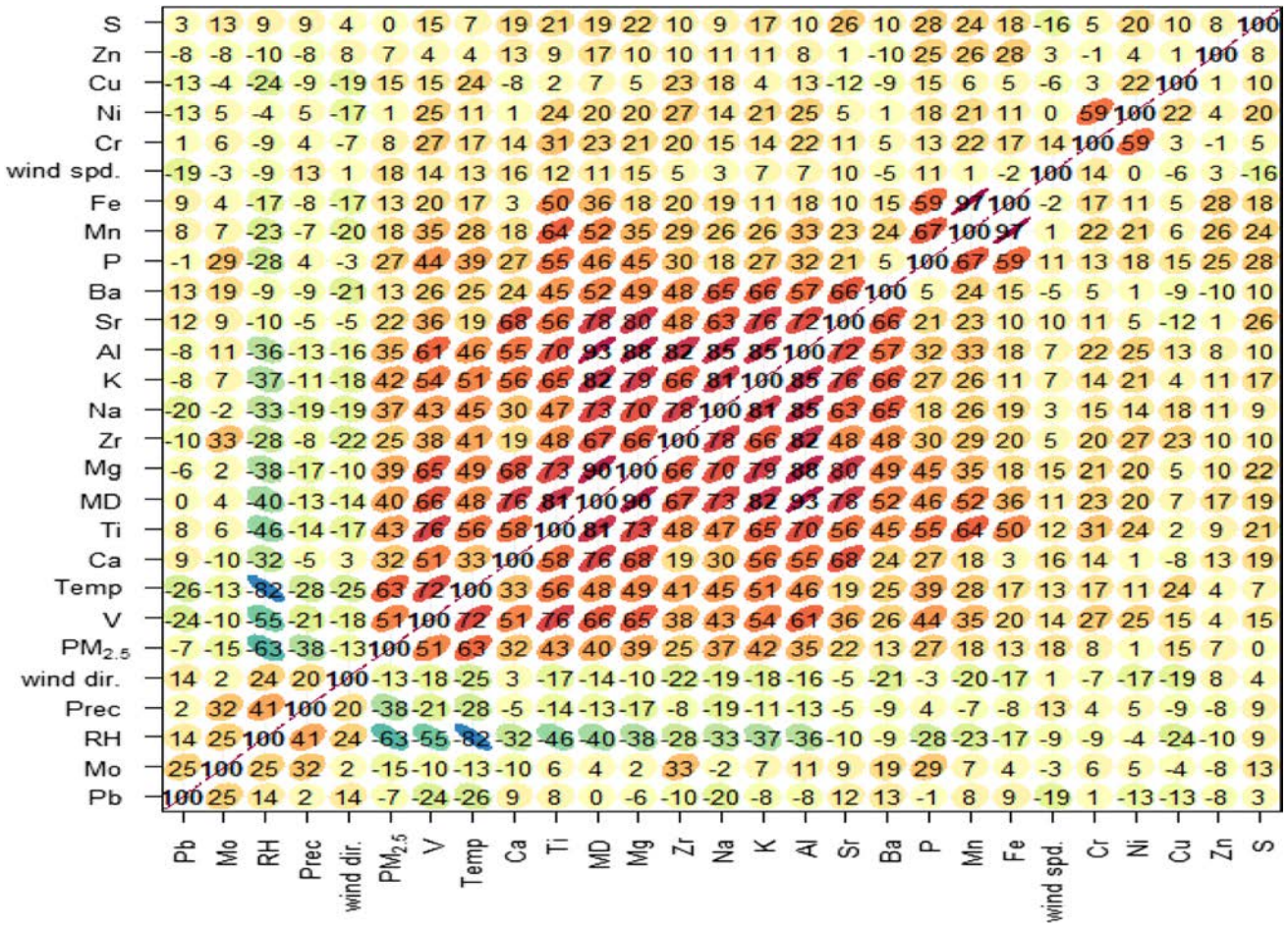

Fig. 3 Spearman correlation matrix showing the relationships between annual average concentrations of $PM_{2.5}$ components and different meteorological parameters

The variations of these factors over the course of a year have an impact on the seasonality of the annual profiles. This trend was also observed in our study. The sampling period was characterized by a low level of precipitation as a total volume of 476.62 mm was recorded. The average daily value of relative humidity varies between 22.40 and 91.21% with an annual average of 60.18 ± 18.12, the high values being recorded during winter. The wind rose specific to our site (Fig. S7) indicates that the prevailing winds are north-westerly (19.38%), north (18.95%) and west (15.61%), respectively. The mean annual wind speed was 3.96 m/s.

The figure of correlations between $PM_{2.5}$ and its metal compounds and several meteorological variables indicates that relative humidity (RH) and precipitation (Prec) have a negative correlation with most pollutants during the entire study period (Fig. 3). This was predictable due to the leaching of the atmosphere by precipitation (Dawson et al. 2007; Feng and Wang 2012). In addition, humidity promotes the agglomeration of particles in the air and their wet or dry deposition (Anda et al. 2015; Kang et al. 2015) or considerably reduces resuspension of dust by the wind (Hieu and Lee 2010). According to Chu (1997), a decrease in relative humidity (40–60%) led to higher PM concentrations. Positive correlations were found between RH and $PM_{2.5}$ leading to an exacerbation of PM pollution until sufficient hygroscopic growth, aggregation and merging of small-sized particles led to PM deposition (Lou et al. 2017). The highest concentrations of $PM_{2.5}$ were observed at elevated temperatures, thus facilitating the resuspension of soil dust by the wind.

Fig. S8 shows the combined effects of temperature, wind speed and relative humidity on $PM_{2.5}$ concentrations. These results showed that, for an $RH < 60\%$, the concentrations of $PM_{2.5}$ tend to (i) increase appreciably with T and (ii) increase with wind speed (WS). For an $RH > 60\%$, the concentrations of $PM_{2.5}$ tend to (i) increase slightly with T but (ii) they are independent of the wind speed.

For temperatures below 15 °C, $PM_{2.5}$ concentrations are independent of wind speed and relative humidity. Above

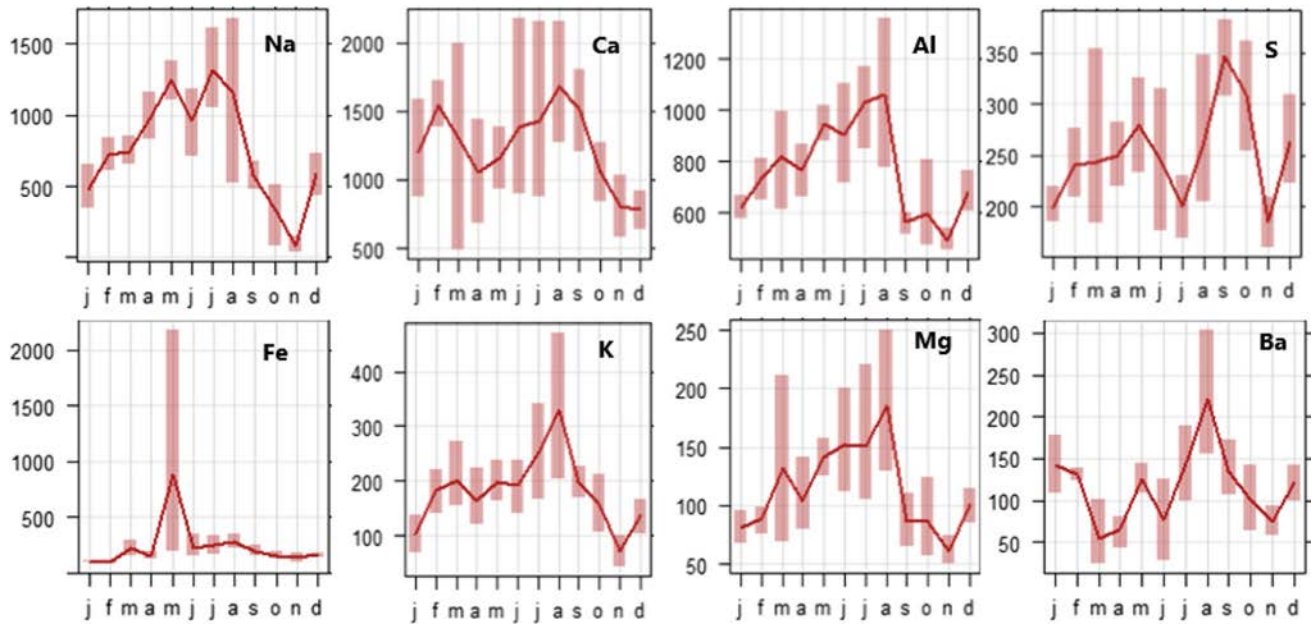

Fig. 4 Monthly average concentrations of major elements. The histogram represents the monthly minimum and maximum average values

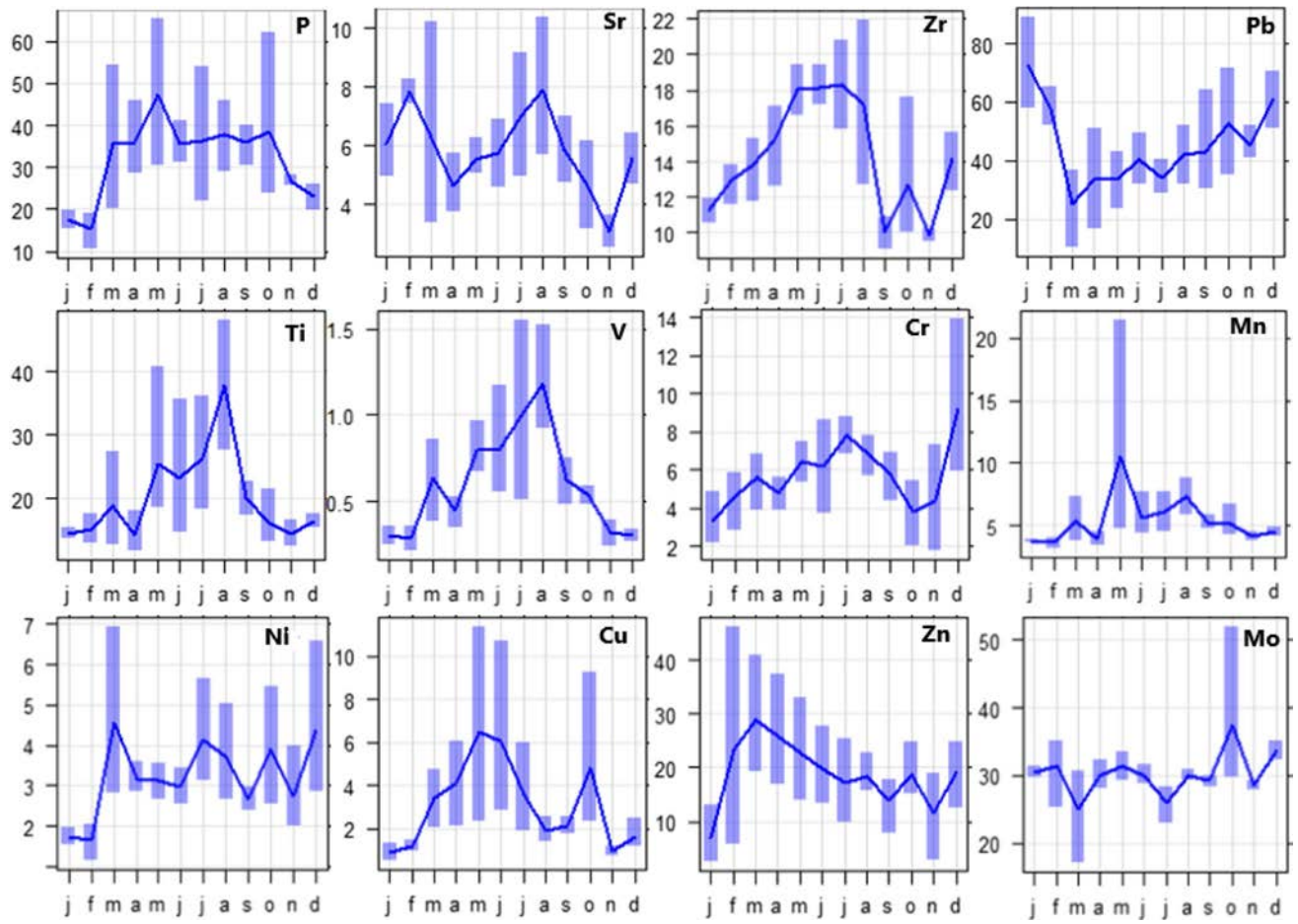

Fig. 5 Monthly average concentrations of trace elements. The histogram represents the monthly minimum and maximum average values

15 °C, $PM_{2.5}$ concentrations decrease with relative humidity but increase with wind speed.

In addition, the concentrations of $PM_{2.5}$ are not affected by the wind speed for a temperature < 15 °C and a relative humidity > 60%. In the latter case, relative humidity is linked to the agglomeration of particles, which weakens the influence of wind speed. This behaviour of $PM_{2.5}$ with respect to wind speed and relative humidity has been highlighted by Wang and Ogawa (2015) and Chen et al. (2018).

Identification of emission sources (profiles/contributions)

The high levels of particulate air pollution in Constantine are influenced by Saharan dust episodes (Ali-Khodja et al. 2008; Terrouche et al. 2016; Bencharif-Madani et al. 2019). The geographic proximity of North Africa to particularly active desert dust emission areas (Engelstaedter et al. 2006) such as the Libyan desert, Niger and Mali explains the high levels of particles in the air in this region (Safar and Labib 2010; Evan et al. 2015). In addition, the semi-arid climate, hot and dry in summer and cold and humid in winter where the frequency and intensity of precipitation is concentrated over a short period (on average 20 days per year), which characterizes the city of Constantine promotes the resuspension of dust and increases the concentrations of particles in the ambient air. It should be noted that activities related to agriculture are also an important source of dust and lead to soil erosion (Webb and Strong 2011; Ginoux et al. 2012; Avecilla et al. 2015). Constantine is traditionally an agricultural town. Agricultural land represents 82% of the total area of the province, of which forests only occupy nearly 8%, or 17,858 hectares (ANDI 2013). These factors explain the significant presence of dust raised by the winds, especially in dry weather.

The choice of the optimal solution is based on the knowledge available a priori of the profile of the chemical composition of the sources and on the results of the error estimation methods. This subjectivity is part of the process of choosing the optimal solution (Ulbrich et al. 2009). The discussion above indicates that the five-factor solution is more stable and realistic than the six- and seven-factor solutions, due to the lower random errors and rotational ambiguity (Fig. S9). In addition, the scaled residuals (d) for all elements are in the range $-3 < d < +3$ and mostly obey a normal distribution, adding credibility to the chosen solution.

Five factors were shown to be physically significant (Fig. 6). The PMF model identified sea salts (15.1%), industrial activities (18.9%), non-exhaust emissions (24.2%), exhaust emissions (15.8%) and mineral dust (25.9%) as the main sources of metallic aerosols near road traffic in Constantine. Mineral dust and non-exhaust emissions were found to be the two main contributors to $PM_{2.5}$. The results also show that 40% of the mass of $PM_{2.5}$ is attributable to vehicle emissions.

Sea salt

The species contributing to the first factor mainly include Na (86.7%), K (56%) and Mg (42.3%) (Fig. 7). This source is attributed to sea salts and contributes 15.1% to the concentration of $PM_{2.5}$. Indeed, the back trajectories of marine aerosols (85th percentiles) show that in many cases, the contribution of the Mediterranean Sea is undeniable (Fig. S10).

However, the contribution of the salt lakes in the region and the great chott of El Djerid which is crossed by southeastern air masses cannot be overlooked (Trousset 1995). The importance of this source is explained by the proximity of the city of Constantine to the Mediterranean Sea (60 km). Na, K and Mg are commonly used as sea salts tracer elements (Saradhi et al. 2008; Gupta et al. 2012). Several authors have used the Mg/Na ratio (Buat-Menard et al. 1974; Savoie and Prospero 1980). Marine aerosols are generally characterized by a Mg/Na ratio close to 0.12 (Brewer et al. 1975). A ratio equal to 0.129 was recorded on the island of Lampedusa (Kishcha et al. 2011), while in Athens, Basel and Helsinki, this ratio was between 0.11 and 0.14 (Ilacqua et al. 2007). In our study, the Mg/Na ratio is 0.066. The enrichment of Na in this factor could be explained by the high Na content in soil dust as well as in aerosols from salt lakes and anthropogenic sources (Hoffman and Duce 1972). According to the latter authors, continental dust transported across the Pacific is the source of excess Na in sea salts. In Algeria, the "sabkha" salt lakes have high concentrations of Na (Demdoum et al. 2015; Lamini and Hacini 2018). Doumbia (2012) found a ratio equal to 0.33 and concluded that salt lakes are the main source of Na, Mg and Cl. Other studies

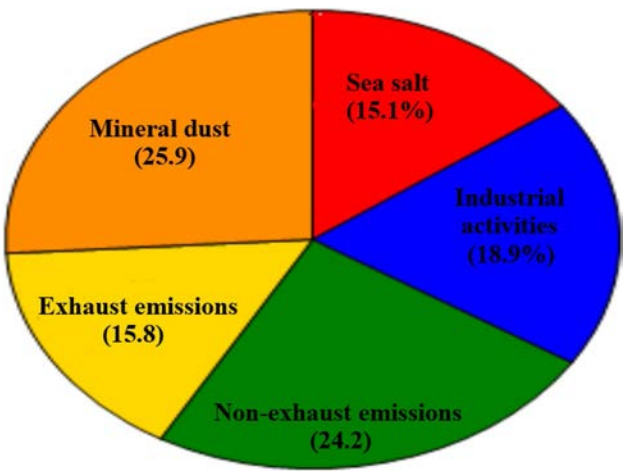

Fig. 6 Contributions of the five emission sources to $PM_{2.5}$

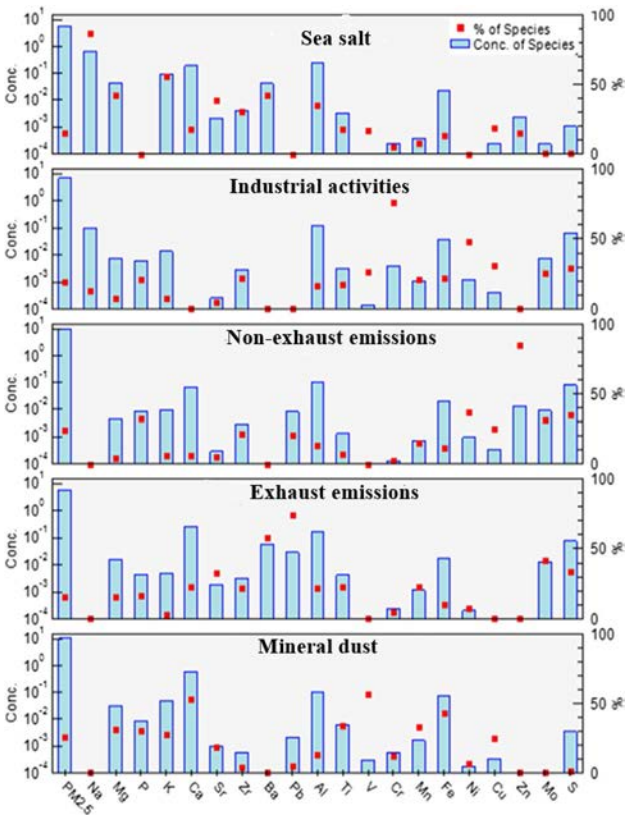

Fig. 7 PMF factor profiles for identified sources

have confirmed the association between high Na levels and salt lakes (Wen 1989; Cao et al. 2008).

The presence of elements such as Sr, Zr, Ca, Ba, Al and Ti in this factor could be linked to desert dust, which may be raised by air masses from the Mediterranean Sea. The Ca/Al ratio (0.77) calculated in this factor is in agreement with the reports of other studies (0.84 (Kong et al. 2011), 0.81 (Xu et al. 2004) and 0.76 (Shen et al. 2007)) which reflect the determining contribution of desert dust. Fig. S11 indicates that the Mediterranean Sea is the main source of this factor, the eastern contribution being more decisive than the northern contribution despite its remoteness from the sampling site. The contribution of the Sahara is not to be overlooked, either. The first factor can therefore, be considered as a mixture of sea salt and mineral dust.

The "sea salts" factor is more significant during the months of May, July and August as shown in Fig. S12. The scarcity of precipitation during the dry season facilitates wind erosion of soil and salt lakes.

Regarding the "sea salt" factor, its contribution tends to increase when RH < 30%, T > 20 °C and WS > 3 m/s (Fig. S13).

When RH decreases, sea salts tend to change from biphasic (saline) to crystals that can stay longer in the atmosphere and reach areas farther from the sea (Zezza and Macrì 1995; Morcillo et al. 2000). The temperature increase coincides with the warm seasons (summer and spring) when the recorded precipitation is lower. As a result, leaching of the atmosphere is less frequent and leads to a higher concentration of sea salts in the air (Zezza and Macrì 1995; Gong et al. 1997; Feliu et al. 1999). Furthermore, the wind speed favours the production of marine aerosols and this effect is observed at wind speeds greater than 3 m/s (McKay et al. 1994; Gustafsson and Franzén 1996; Morcillo et al. 2000). Moreover, according to these authors, sea salt concentrations increase exponentially with wind speed above 3 m/s.

Industrial activities

The second factor is attributed to industrial emissions, which are characterized by high contributions of Cr (76.1%), Ni (48.3%), Cu (31.2%), S (29.3%), V (26.4%), Mo (25.9%), Fe (22.1%) and Mn (21.3%) (Fig. 7). Industrial emissions are generally heterogeneous and differ depending on the manufacturing process and the type of fuel used (Singh et al. 2017). In contrast, the choice of metal tracers specific to an industrial source is often difficult (Banerjee et al. 2015). S, Ni, Mo and V are linked to anthropogenic activities such as combustion and industrial processes (Marcazzan et al. 2003). Ni and V are natural constituents of petroleum and are found in all of its by-products (Turunen et al. 1995; Vale et al. 2004).

Ni and V are widely associated with fuel oil combustion and the refining industry (Celis et al. 2004; Pey et al. 2009). The V/Ni ratio in this factor is 0.11 and cannot be representative of diesel emissions with a characteristic factor > 4 (Moreno et al. 2010). A ratio of < 2 reflects the presence of Ni enriched by emissions from the surface treatment industry located west-southwest of our sampling site (Bencharif-Madani et al. 2019). The Cr and Ni pollution rose indicates a similar concentration profile indicating that these two elements have a common emission source (Fig. S14). Ten kilometres from our site and in this direction is a large mechanical industrial pole within the Ain Smara industrial area.

In general, Ni, Cr, Fe, Mn, Zn, Fe, S, Cu and Mo are used as tracers of industrial emissions (Song et al. 2006; Tauler et al. 2009; Sharma et al. 2014). Metals like Cr, Fe, Mn, Mo and Ni are associated with the metallurgical and steel industries (Lodhi et al. 2009; Mansha et al. 2012). The production of iron and steel is an important source of particles in the ambient air around industrial areas (Kumar et al. 2001; Mazzei et al. 2006). Studies have reported that the particles emitted by the steel smelter in the region of Cornigliano, Italy, represent 60% of the mass of PM_{10} (Prati et al. 2000) and 45% of the mass of PM_{10} in Port Talbot, UK (Taiwo et al. 2014). Cr, Ni and Cu are generally used in the

metallurgical industry and in foundries as a highly corrosion-resistant element in the steel plating process (Wadden et al. 1991; Kulshrestha et al. 2009). Fe, Cr, Ni and Cu are probably from construction sites (Kulshrestha et al. 2009) in Didouche Mourad and El Khroub city (Fig. S15). They can also be emitted by the cement and glass industries as well as brickworks in the industrial zone of Didouche Mourad (Tian et al. 2012; Hasheminassab et al. 2014).

Mo is used as an additive in lubricants (Zainal et al. 2018) and it may be released into the environment by the combustion of fossil fuels used in industry, explaining its significant presence in this factor (Salminen et al. 2005). S in the form of SO_2 is a pollutant emitted by power plants, petroleum refineries as well as industrial activities such as steel processing (Salminen et al. 2005; Shahbazi et al. 2016). Finally, Fe and Mn are tracers in the steel industry (Owoade et al. 2015).

Summer and spring have the highest concentrations of this factor. The impact of an industrial zone is closely linked to the frequency of the winds that pass through it. Indeed, the wind rose (Fig. S16) indicates that N, N-NE and SE winds are more frequent during summer compared to fall and winter. The industrial zones of Didouche Mourad, Skikda and El Khroub located in these respective directions are believed to be responsible for this marked increase in this factor in summer. In the spring, NN-E and SE winds are more frequent than in the fall and winter. The contribution of the Skikda industrial zones and El Khroub would be decisive. Moreover, Fig. S17 perfectly illustrates the nuanced increase in this factor between summer and spring.

The factor "industrial activities" does not seem to be affected by the meteorological parameters. No particular trend is observed with the variation of these parameters (Fig. S18).

Wind direction and emission intensity are the determining factors for particulate matter concentrations from industrial areas. Fig. S19 shows the sources of the emissions contributing to this factor. These sources are located in the industrial zones of El Khroub (south-west), Didouche Mourad (north), Palma (north-west) and construction sites in Ali Mendjeli (south-west), in Didouche Mourad (north–north-east), the El Hadaba plateau (north-west) and the quarry of the National Aggregates Company (south-east).

The contribution of industrial activities to $PM_{2.5}$ in the study site (18.9%) is much less than that reported by Tahri et al. (2013) (52%) in Kenitra City, Morocco, who asserts that a significant number of small industrial facilities involved in metal works surround the sampling site located close to a bus station.

Non-exhaust emissions

The third factor includes elements resulting from the wear of brakes, tires and road surfaces as well as the resuspension of soil particles. Querol et al. (2004b) showed that in European cities, non-exhaust sources account for half of all traffic emissions. Harrison et al. (2001) also estimate that particles resuspended by vehicles represent a fraction equivalent to that of exhaust emissions. Rehn et al. (2014) also found that the contribution of non-exhaust emissions was equivalent to that of exhaust emissions. In some northern European countries, non-exhaust particulate concentrations in PM_{10} can represent up to 90% of airborne particles near the road (Forsberg et al. 2005; Omstedt et al. 2005). The contribution of this source at our sampling site is estimated at 24.2% of the total mass of $PM_{2.5}$ (Fig. 6) and represents more than 60% of the total emissions related to road traffic. This factor is mainly characterized by high loads of Zn (84.6%), Ni (37%), S (34.5%), P (32.5%), Cu (22.5%), Mo (31.8%), Zr (21.2%) and Pb (20.8%) (Fig. 7). The main sources of non-exhaust emissions are brake and tire wear and pavement abrasion (Thorpe and Harrison 2008; Pant et al. 2017). Several studies have indicated that Fe, Cu, Pb and Zn are basic tracers and reliable markers of brake wear (Hildemann et al. 1991; Legret and Pagotto 1999; Westerlund and Johansson 2002). Hulskotte et al. (2014) reported that Cu, Zn, Fe and Sn represent 80 to 90% of the metals present in brake pads. Furthermore, Hjortenkrans et al. (2007) reported that brake dust contains significant amounts of Cu, Sb, Ba, Al, Si, S, Ti, Zn, Ni, Cr and Pb. Kennedy and Gadd (2003) reported that concentrations of Cu are 11 mg/kg (25% by mass). Other studies have revealed that Cu is the most abundant species and represents 11.8% (Westerlund and Johansson 2002), 14.2% (Legret and Pagotto 1999) and 2.4% of the total mass of brake linings (von Uexküll et al. 2005). A wide variety of components is commonly used in brake linings (Chan and Stachowiak 2004). This contributes to the difficulty of identifying the chemical composition of the resulting particles. The presence of Zr as zirconium oxide can be attributed to brake wear (Eriksson et al. 1999) or road wear (Huzita and Kasama 1983).

Zn is considered, according to several studies, to be the main indicator of tire wear in traffic areas or urban areas (Adamiec et al. 2016). Tires contain between 0.4 and 4.3% Zn (Smolders and Degryse 2002; Ozaki et al. 2004). These high contents result from the addition of ZnO and ZnS to the tire during vulcanization (Heideman et al. 2004, 2005). Zn, Cd, Co, Cr, Cu, Hg, Mo, Ni and Pb are associated with tire wear (Adachi and Tainosho 2004; Hjortenkrans et al. 2007). Amato et al. (2011) showed the predominance of Zn, Sb, Cu, S, Ni and Cr in the factor representative of tire wear. Similar results have been reported in source allocation studies using PMF (Bukowiecki et al. 2010; Doumbia 2012). On the other hand, the absence of other metals characteristic of tire wear and, consequently, of elementary ratios makes it difficult to use it as a tire tracer when it emanates from other anthropogenic or natural sources. This factor also contains

terrigenous species such as Ca, Al, Ti, Fe and Mn as well as other trace elements such as Ni, Mo, S, Zr and P related to pavement wear (Lindgren 1996; Arditsoglou and Samara 2005; Amato et al. 2011). Fe and Mn are generally associated with the mechanical wear of engine parts and various seals (Hildemann et al. 1991).

According to Fig. S20, the main sources of the "non-exhaust" factor are the entrance to the faculty, the parking, the traffic roundabout in front of the entrance to the faculty and the pedestrian crossing. Indeed, emissions increase significantly during braking and deceleration, especially at the traffic roundabout.

Fig. S21 illustrates the seasonal effect of the "non-exhaust emissions" factor on the temporal evolution of the contribution. The latter is minimum in winter during the months of January and February and maximum in spring during the months of March to June. In summer, a decrease in this contribution is observed, because it corresponds to a notable drop in traffic, which coincides with the holiday period. In winter, the effect of precipitation on particles generated by the wear of various components is evident.

The contribution of emissions to the "non-exhaust emissions" factor increases when RH < 50% and the temperature is below 15 °C (Fig. S22). This is because low temperatures reduce the elasticity of the pavement surface, exacerbating friction on the harder inner layer. In addition, low temperatures tend to harden the tires thereby increasing the frictional force (Gustafsson et al. 2008). The effect of relative humidity is such that its decrease leads to favourable soil conditions for the resuspension of particles produced by various wear processes (Jeong et al. 2019). However, wind speed does not seem to have any effect (Fig. S22).

Exhaust emissions

The fourth factor is dominated by the presence of Pb, Ba, Mo, S, Sr and Mn, which contribute 73.9%, 57.6%, 41.5%, 33.9%, 32.4% and 22.9%, respectively, reflecting exhaust emissions. In India, vehicle emissions have been identified by Pb, Ni, Cu, Zn and Mn (Deshmukh et al. 2013; Sharma et al. 2016). Ba, Cd, Pb, Sb and Zn have been used as tracers of vehicular emissions in Pakistan (Lodhi et al. 2009; Mansha et al. 2012). In Sri Lanka, Seneviratne et al. (2011) identified K, Pb, Fe and S as tracers of vehicular emissions.

Pb, Ba and Mn are used as fuel additives to improve engine performance (Karar et al. 2006; Belis et al. 2013). The combustion of leaded gasoline remains the main source of lead emissions in the world (Pacyna and Pacyna 2001). It is an element that is often used as a marker of automotive emissions (Sabin et al. 2006; Zhu et al. 2018). Algeria is one of the few countries still using leaded gasoline (Naidja et al. 2018). Ba is considered to be a potential tracer of emissions from gasoline and LPG engines (Lin et al. 2005; Cheng et al. 2010). It is also used as a corrosion inhibitor in engine lubricating oils (Bem et al. 2003).

The profile of this factor also contains a substantial proportion of terrigenous elements such as Ca (23%), Ti (22.5%), Al (22%), P (16%) and Mg (15.4%) revealing the significant contribution of dust resuspended by road traffic. In our study, the Ca/Al ratio = 1.56 is close to those announced by Ho et al. (2003) (1.19) and by Kong et al. (2011) (1.29) which they attribute to dust from paved roads.

Fig. S23 shows the probability of the different directions contributing to the "exhaust emissions" factor at the local scale. The main sources are the road along the faculty as well as the roundabout in front of its entrance.

Winter experiences a drastic increase in concentrations of the "exhaust emissions" factor resolved by PMF (Fig. S24). Road traffic is usually intense during this season (Bencharif-Madani et al. 2019). This factor, associated with the reduction in the height of the atmospheric boundary layer and the stability of the lower atmospheric layers, increases remarkably during winter. In addition, the wind rose during winter is characterized by prevailing westerly winds where the main source of emissions contributing to the "exhaust emissions" factor is found, namely, the national road N79.

As for the "exhaust emissions" factor, its contribution increases when RH > 60% and T < 10 °C (Fig. S25). At low temperatures, meteorological conditions are more stable than in summer (Taghvaee et al. 2018). This results in a poor dispersion, which is at the origin of high concentrations of primary and secondary particles emitted directly into the atmosphere. The mixing of the hot vapours in the exhaust with the cold air considerably favours the nucleation phenomena for the atmospheric aerosols (Nilsson and Kulmala 1998; Charron and Harrison 2003). It is believed that nucleation increases the total mass of particles (Kulmala et al. 2001). Low temperatures associated with high relative humidity favour the formation of new particles (Easter and Peters 1994). In addition, high relative humidity promotes binary nucleation of sulphuric acid and water (Easter and Peters 1994; Hinds 1999; Seinfeld and Pandis 2016). Jamriska et al. (2008) suggest that the significant influence of RH on exhaust emissions may be related to particle agglomeration and changes in the hygroscopic properties of primary particles emitted by traffic which become hydrophilic under high-rate humidity conditions.

Mineral dust

The fifth factor represents 25.9% of the total mass of $PM_{2.5}$ and is dominated by V (56.7%), Ca (52.6%), Fe (43%), Ti (34.2%), Mn (32.9%), Mg (30.8%), P (30.3%) and K (27.7%) which are all terrigenous elements (Fig. 7). Therefore, this factor could be associated with the resuspension of soil dust. According to Lough et al. (2005), these dusts contain most

of the terrigenous elements Fe, Ca, Na, Mg, Al and K at high concentrations. Apart from K, these are the same terrigenous elements which are considered as tracers of soil dust: Al, Si, Ca, Mg, Fe and Na by Begum et al. (2006). A ratio of *x*/Al (where *x* is any element) could be considered a good criterion to distinguish the different sources of dust (Wang et al. 2006; Shen et al. 2016). The elementary ratios calculated in this study are more or less close to the ratios shown in Table 2.

The Ca/Al ratio of our study site is relatively higher compared to those of other sites. This is explained by the influence of anthropogenic emissions (Athanasopoulou et al. 2010). According to Fig. S26, we can assume that the construction sites near the sampling site (Ali Mendjeli, El Khroub), the quarries near El Khroub in the south-east and Ain Smara in the south-west and the area industrial plant of Didouche Mourad in the north (cement plant, brickyard, quarries) are the nearby sources that contribute the most to this factor.

On a regional scale, Fig. S27 reveals that the eastern region of Constantine contributes strongly to the "mineral dust" factor. This region is located in North Africa, between eastern Tunisia and eastern Algeria, and is considered a particularly intense and persistent source of dust (Prospero et al. 2002).

In fact, the prevailing synoptic winds are from the north-west (41.5%), east (39.4%) and west (19.1%) (Fig. S28).

The temporal evolution of mineral dust contributions perfectly illustrates the influence of the hot season on this factor. The period from June to September is the most favourable for the lifting of soil dust (Fig. S29).

The contribution to the "mineral dust" factor is favoured by $RH < 35\%$ and $T > 15$ °C and a wind speed > 3 m/s (Fig. S30). The influence of relative humidity on dust levels has been highlighted by several authors due to its impact on the moisture content of the soil surface, and therefore on the cohesion of soil particles (Ravi et al. 2004; McKenna Neuman and Sanderson 2008). According to Csavina et al. (2014). Conversely, when RH is relatively low, soil particles are looser and more easily dispersed by the wind.

Moreover, wind speed is a main factor in the resuspension of soil dust (Yin et al. 2007). Temperature is also strongly correlated with dust concentrations (Hussein et al. 2006). The contribution of this factor increases in the hot season due to the absence of leaching of the atmosphere which leads to the accumulation of dust in the air. Associated with strong winds, dry soil generates more dust in hot weather (Kassomenos et al. 2014; Li et al. 2015).

The influence of Saharan dust episodes, which are generally more frequent in summer, has been highlighted by several authors (Matassoni et al. 2009; Kopanakis et al. 2018; Querol et al. 2019).

Conclusion

The PMF model identified natural sources related to sea salt and mineral dust (41%) and vehicular emissions (exhaust and non-exhaust) (40%) as the main contributors to $PM_{2.5}$. Industrial emissions account for less than half of the contribution of each of these sources. The Mediterranean Sea is the main source of sea salt. The contribution of the Sahara is not to be overlooked, either. Emissions from natural sources are exacerbated during the hot season. The decrease of relative humidity and the increase of temperature favour sea salt particles and mineral dust resuspension. During winter, exhaust emissions are highest while non-exhaust emissions are lowest. These two components of vehicular emissions are affected in opposite ways by relative humidity and temperature. None of these parameters has an effect on industrial emissions which are mainly determined by wind intensity and direction. Moreover, the metallic tracers of different sources have been identified. These are Na for sea salt, Cr for industrial activities, Zn for non-exhaust emissions, Pb for exhaust emissions and Ca for mineral dust. It should be noted that Pb originates mainly from gasoline before its ban in August 2021. Ba and Mo could alternatively serve as metallic tracers for such exhaust emissions.

In order to be able to discriminate between influential sources, it would be wise to analyse a larger number of metallic elements and if possible other pollutants such as cations and anions. The analysis of organic tracers could be considered and integrated into future studies to better determine the influence of combustion sources.

A sufficiently large number of data can also allow separate studies according to the seasons. From a broader perspective, it appears very desirable to continue measurements

Table 2 Comparison between elementary ratios

	K/Al	Ca/Al	Ti/Al	Mn/Al	Fe/Al	Pb/Al	References
Constantine	0.48	5.92	0.06	0.02	0.75	0.021	This study
Hong Kong	0.40	1.93	0.05	0.03	1.54	0.030	Ho et al. (2003)
North-west China	0.73	3.73	0.12	0.04	1.35	0.008	Shen et al. (2016)
North-east China	0.41	2.65	0.09	0.03	0.95	0.004	Shen et al. (2016)
North China	0.47	3.07	0.10	0.03	1.14	0.006	Shen et al. (2016)

of the chemical composition of PM over the long term with, if necessary, a higher temporal resolution.

Acknowledgements This work was supported by the PHC-Tassili, a cooperation program between Algeria and France.

Funding This work was supported by the PHC Tassili project (Hubert Curien Tassili Partnership) referenced under number 16MDU969, a cooperation program between Algeria and France.

Data availability All data generated or analysed during this study are included in this published article (and its supplementary information files).

Declarations

Ethics approval and consent to participate This study did not require ethics approval. Informed consent was obtained from all individual participants included in the study.

Consent for publication Consent to publish has been received from all participants.

Competing interests The authors declare no competing interests.

References

Adachi K, Tainosho Y (2004) Characterization of heavy metal particles embedded in tire dust. Environ Int 30:1009–1017

Adamiec E, Jarosz-Krzemińska E, Wiesza\la R, (2016) Heavy metals from non-exhaust vehicle emissions in urban and motorway road dusts. Environ Monit Assess 188:1–11

Alastuey A, Querol X, Castillo S et al (2005) Characterisation of TSP and PM2.5 at Izaña and Sta. Cruz de Tenerife (Canary Islands, Spain) during a Saharan Dust Episode (July 2002). Atmos Environ 39:4715–4728

Ali-Khodja H, Belaala A, Demmane-Debbih W et al (2008) Air quality and deposition of trace elements in Didouche Mourad, Algeria. Environ Monit Assess 138:219–231

Amato F, Pandolfi M, Escrig A et al (2009) Quantifying road dust resuspension in urban environment by multilinear engine: a comparison with PMF2. Atmos Environ 43:2770–2780

Amato F, Pandolfi M, Moreno T et al (2011) Sources and variability of inhalable road dust particles in three European cities. Atmos Environ 45:6777–6787

Anda A, Soos G, da Silva JAT, Kozma-Bognar V (2015) Regional evapotranspiration from a wetland in Central Europe, in a 16-year period without human intervention. Agric for Meteorol 205:60–72

ANDI (2013) La vile de Constantine. Agence Nationale de Développement et de l'Investissement. Wiley Online Library

Arditsoglou A, Samara C (2005) Levels of total suspended particulate matter and major trace elements in Kosovo: a source identification and apportionment study. Chemosphere 59:669–678

Ashbaugh LL, Malm WC, Sadeh WZ (1985) A residence time probability analysis of sulfur concentrations at Grand Canyon National Park. Atmos Environ 19(8):1263–1270

Athanasopoulou E, Tombrou M, Russell AG, et al (2010) Implementation of road and soil dust emission parameterizations in the aerosol model CAMx: applications over the greater Athens urban area affected by natural sources. Journal of Geophysical Research: Atmospheres 115:

Avecilla F, Panebianco JE, Buschiazzo DE (2015) Variable effects of saltation and soil properties on wind erosion of different textured soils. Aeol Res 18:145–153

Banerjee T, Murari V, Kumar M, Raju MP (2015) Source apportionment of airborne particulates through receptor modeling: Indian scenario. Atmos Res 164:167–187

Begum BA, Kim E, Biswas SK, Hopke PK (2004) Investigation of sources of atmospheric aerosol at urban and semi-urban areas in Bangladesh. Atmos Environ 38:3025–3038

Begum BA, Biswas SK, Hopke PK, Cohen DD (2006) Multi-element analysis and characterization of atmospheric particulate pollution in Dhaka. Aerosol Air Qual Res 6(4):334–359

Belarbi N, Belamri M, Dahmani B, Benamar MA (2020) Road traffic and PM10, PM2.5 emission at an urban area in Algeria: identification and statistical analysis. Pollution 6:651–660

Belis CA, Karagulian F, Larsen BR, Hopke PK (2013) Critical review and meta-analysis of ambient particulate matter source apportionment using receptor models in Europe. Atmos Environ 69:94–108

Bem H, Gallorini M, Rizzio E, Krzemińska M (2003) Comparative studies on the concentrations of some elements in the urban air particulate matter in Lodz City of Poland and in Milan, Italy. Environ Int 29:423–428

Bencharif-Madani F, Ali-Khodja H, Kemmouche A et al (2019) Mass concentrations, seasonal variations, chemical compositions and element sources of PM10 at an urban site in Constantine, northeast Algeria. J Geochem Explor 206:106356

Bevan DR, Manger WE (1985) Effect of particulates on metabolism and mutagenicity of benzo [a] pyrene. Chem Biol Interact 56:13–28

Biersteker K (1976) Sulfur dioxide and suspended particulate matter: where do we stand? Environ Res 11:287–304

Boman J, Shaltout AA, Abozied AM, Hassan SK (2013) On the elemental composition of PM2.5 in central Cairo. Egypt X-Ray Spectrometry 42:276–283

Boubel RW, Vallero D, Fox DL, Turner B, Stern AC (2013) Fundamentals of air pollution. Elsevier, New York

Brewer PG, Riley JP, Skirrow G (1975) Chemical oceanography

Buat-Menard P, Morelli J, Chesselet R (1974) Water-soluble elements in atmospheric particulate matter over tropical and equatorial Atlantic. J Rech Atmosph 8:661–673

Bukowiecki N, Lienemann P, Hill M et al (2010) PM10 emission factors for non-exhaust particles generated by road traffic in an urban street canyon and along a freeway in Switzerland. Atmos Environ 44:2330–2340

Cao JJ, Chow JC, Watson JG et al (2008) Size-differentiated source profiles for fugitive dust in the Chinese Loess Plateau. Atmos Environ 42:2261–2275

Celis JE, Morales JR, Zaror CA, Inzunza JC (2004) A study of the particulate matter PM10 composition in the atmosphere of Chillán, Chile. Chemosphere 54:541–550

Chan D, Stachowiak GW (2004) Review of automotive brake friction materials Proceedings of the Institution of Mechanical Engineers, Part d. J Automob Eng 218:953–966

Charron A, Harrison RM (2003) Primary particle formation from vehicle emissions during exhaust dilution in the roadside atmosphere. Atmos Environ 37:4109–4119

Csavina J, Field J, Félix O, Corral-Avitia AY, Sáez AE, Betterton EA (2014) Effect of wind speed and relative humidity on atmospheric dust concentrations in semi-arid climates. Sci Total Environ 487:82–90

Chen G, Li S, Knibbs LD, Hamm NA, Cao W, Li T et al (2018) A machine learning method to estimate PM2.5 concentrations across China with remote sensing, meteorological and land use information. Sci Total Environ 63:52–60

Cheng Y, Lee SC, Ho KF et al (2010) Chemically-speciated on-road PM2.5 motor vehicle emission factors in Hong Kong. Sci Total Environ 408:1621–1627

European Commission (2011) Commission staff working paper establishing guidelines for determination of contributions from the re-suspension of particulates following winter sanding or salting of roads under the Directive 2008/50/EC on ambient air quality and cleaner air for Europe. Citeseer

Dawson JP, Adams PJ, Pandis SN (2007) Sensitivity of PM 2.5 to climate in the Eastern US: a modeling case study. Atmos Chem Phys 7:4295–4309

Demdoum A, Hamed Y, Feki M et al (2015) Multi-tracer investigation of groundwater in El Eulma Basin (Northwestern Algeria), North Africa. Arab J Geosci 8:3321–3333

Denier van der Gon H, Jozwicka M, Hendriks E, et al (2010) Mineral dust as a component of particulate matter. Delft, the Netherlands

Deshmukh DK, Deb MK, Mkoma SL (2013) Size distribution and seasonal variation of size-segregated particulate matter in the ambient air of Raipur city, India. Air Qual Atmos Health 6:259–276

Doumbia EHT (2012) Caractérisation physico-chimique de la pollution atmosphérique en Afrique de l'Ouest et étude d'impact sur la santé. PhD Thesis, Université de Toulouse, Université Toulouse III-Paul Sabatier

Easter RC, Peters LK (1994) Binary homogeneous nucleation: temperature and relative humidity fluctuations, nonlinearity, and aspects of new particle production in the atmosphere. J Appl Meteorol Climatol 33:775–784

Engelstaedter S, Tegen I, Washington R (2006) North African dust emissions and transport. Earth Sci Rev 79:73–100

Eriksson M, Bergman F, Jacobson S (1999) Surface characterisation of brake pads after running under silent and squealing conditions. Wear 232:163–167

Evan AT, Fiedler S, Zhao C et al (2015) Derivation of an observation-based map of North African dust emission. Aeol Res 16:153–162

Feliu S, Morcillo M, Chico B (1999) Effect of distance from sea on atmospheric corrosion rate. Corrosion 55:883–891

Feng X, Wang S (2012) Influence of different weather events on concentrations of particulate matter with different sizes in Lanzhou, China. J Environ Sci 24:665–674

Forsberg B, Hansson H-C, Johansson C et al (2005) Comparative health impact assessment of local and regional particulate air pollutants in Scandinavia. AMBIO A Human Environ 34:11–19

Ginoux P, Prospero JM, Gill TE, et al (2012) Global-scale attribution of anthropogenic and natural dust sources and their emission rates based on MODIS Deep Blue aerosol products. Reviews of Geophysics 50:

Gong SL, Barrie LA, Blanchet J-P (1997) Modeling sea-salt aerosols in the atmosphere: 1. Model development. Journal of Geophysical Research: Atmospheres 102:3805–3818

Gupta I, Salunkhe A, Kumar R (2012) Source apportionment of PM10 by positive matrix factorization in urban area of Mumbai, India. The Scientific World Journal 2012:

Gustafsson ME, Franzén LG (1996) Dry deposition and concentration of marine aerosols in a coastal area, SW Sweden. Atmos Environ 30:977–989

Gustafsson M, Blomqvist G, Gudmundsson A, Dahl A, Swietlicki E, Bohgard M et al (2008) Properties and toxicological effects of particles from the interaction between tyres, road pavement and winter traction material. Sci Total Environ 393(2-3):226–240

Harrison RM, Yin J, Mark D, Stedman J, Appleby RS, Booker J, Moorcroft S (2001) Studies of the coarse particle (2.5–10 μm) component in UK urban atmospheres. Atmos Environ 35(21):3667–3679

Hasheminassab S, Daher N, Saffari A et al (2014) Spatial and temporal variability of sources of ambient fine particulate matter (PM 2.5) in California. Atmos Chem Phys 14:12085–12097

Hassan SK, Khoder MI (2017) Chemical characteristics of atmospheric PM2.5 loads during air pollution episodes in Giza. Egypt Atmos Environ 150:346–355

Heideman G, Noordermeer JW, Datta RN, van Baarle B (2004) Zinc loaded clay as activator in sulfur vulcanization: a new route for zinc oxide reduction in rubber compounds. Rubber Chem Technol 77:336–355

Heideman G, Datta RN, Noordermeer JW, van Baarle B (2005) Influence of zinc oxide during different stages of sulfur vulcanization. Elucidated by model compound studies. J Appl Polym Sci 95:1388–1404

Hieu NT, Lee B-K (2010) Characteristics of particulate matter and metals in the ambient air from a residential area in the largest industrial city in Korea. Atmos Res 98:526–537

Hildemann LM, Markowski GR, Cass GR (1991) Chemical composition of emissions from urban sources of fine organic aerosol. Environ Sci Technol 25:744–759

Hinds WC (1999) Aerosol technology: properties, behavior, and measurement of airborne particles. John Wiley & Sons

Hjortenkrans DS, Bergbäck BG, Häggerud AV (2007) Metal emissions from brake linings and tires: case studies of Stockholm, Sweden 1995/1998 and 2005. Environ Sci Technol 41:5224–5230

Ho KF, Lee SC, Chow JC, Watson JG (2003) Characterization of PM10 and PM2.5 source profiles for fugitive dust in Hong Kong. Atmos Environ 37:1023–1032

Hoffman GL, Duce RA (1972) Consideration of the chemical fractionation of alkali and alkaline earth metals in the Hawaiian marine atmosphere. J Geophys Res 77:5161–5169

Hoke PK (2010) The application of receptor modeling to air quality data. Pollution Atmospherique 91–109

Huang S, Arimoto R, Rahn KA (2001) Sources and source variations for aerosol at Mace Head, Ireland. Atmos Environ 35:1421–1437

Hussein T, Karppinen A, Kukkonen J et al (2006) Meteorological dependence of size-fractionated number concentrations of urban aerosol particles. Atmos Environ 40:1427–1440

Huzita K, Kasama T (1983) Geology of the Kobe district. Quadrangle series (115 pp) Geol Surv Jpn 1:

Ilacqua V, Hänninen O, Saarela K et al (2007) Source apportionment of population representative samples of PM2.5 in three European cities using structural equation modelling. Sci Total Environ 384:77–92

Health Effects Institute (2019) State of global air 2019. Special report

Jamriska M, Morawska L, Mergersen K (2008) The effect of temperature and humidity on size segregated traffic exhaust particle emissions. Atmos Environ 42(10):2369–2382

Järup L (2003) Hazards of heavy metal contamination. Br Med Bull 68:167–182

Jeong C-H, Wang JM, Hilker N et al (2019) Temporal and spatial variability of traffic-related PM2.5 sources: comparison of exhaust and non-exhaust emissions. Atmos Environ 198:55–69

Kampa M, Castanas E (2008) Human health effects of air pollution. Environ Pollut 151:362–367

Kang X, Cui L, Zhao X et al (2015) Effects of wetlands on reducing atmospheric fine particles PM2.5 in Beijing. Chin J Ecol 34:2807–2813

Karar K, Gupta AK, Kumar A, Biswas AK (2006) Characterization and identification of the sources of chromium, zinc, lead, cadmium, nickel, manganese and iron in PM 10 particulates at the two sites of Kolkata, India. Environ Monit Assess 120:347–360

Karnae S, John K (2011) Source apportionment of fine particulate matter measured in an industrialized coastal urban area of South Texas. Atmos Environ 45:3769–3776

Kassomenos PA, Vardoulakis S, Chaloulakou A et al (2014) Study of PM10 and PM2.5 levels in three European cities: analysis of intra and inter urban variations. Atmos Environ 87:153–163

Kemmouche A, Ali-Khodja H, Bencharif-Madani F, Mahía PL, Querol X (2017) Comparative study of bulk and partial digestion methods for airborne PM10-bound elements in a high mineral dust urban site in Constantine. Algeria. Int J Environ Anal Chem 97(12):1132–1150

Khadidja N, Maatoug M, Lazreg B et al (2019) Quantification of mass concentrations aerosols PM2.5 in primary schools. Case study: Tiaret city (Algeria). Environ Res Eng Manag 75:47–59

Kim E, Hopke PK (2004) Comparison between conditional probability function and nonparametric regression for fine particle source directions. Atmos Environ 38:4667–4673

Kim E, Hopke PK, Edgerton ES (2004) Improving source identification of Atlanta aerosol using temperature resolved carbon fractions in positive matrix factorization. Atmos Environ 38:3349–3362

Kim E, Hopke PK, Kenski DM, Koerber M (2005) Sources of fine particles in a rural midwestern US area. Environ Sci Technol 39:4953–4960

Kishcha P, Nickovic S, Starobinets B et al (2011) Sea-salt aerosol forecasts compared with daily measurements at the island of Lampedusa (Central Mediterranean). Atmos Res 100:28–35

Kong S, Ji Y, Lu B et al (2011) Characterization of PM10 source profiles for fugitive dust in Fushun-a city famous for coal. Atmos Environ 45:5351–5365

Kopanakis I, Mammi-Galani E, Pentari D et al (2018) Ambient particulate matter concentration levels and their origin during dust event episodes in the eastern Mediterranean. Aerosol Sci Eng 2:61–73

Kulmala M, Maso MD, Mäkelä JM et al (2001) On the formation, growth and composition of nucleation mode particles. Tellus B 53:479–490

Kulshrestha A, Satsangi PG, Masih J, Taneja A (2009) Metal concentration of PM2.5 and PM10 particles and seasonal variations in urban and rural environment of Agra. India Sci Total Environ 407:6196–6204

Kumar AV, Patil RS, Nambi KSV (2001) Source apportionment of suspended particulate matter at two traffic junctions in Mumbai, India. Atmos Environ 35:4245–4251

Lamini A, Hacini M (2018) Geology and geochemistry of endoroique basin case of Baghdad chott southern of Algeria. In: AIP Conference Proceedings. AIP Publishing LLC, p 020006

Legret M, Pagotto C (1999) Evaluation of pollutant loadings in the runoff waters from a major rural highway. Sci Total Environ 235:143–150

Li R, Li Z, Gao W et al (2015) Diurnal, seasonal, and spatial variation of PM2.5 in Beijing. Sci Bull 60:387–395

Lin C-C, Chen S-J, Huang K-L et al (2005) Characteristics of metals in nano/ultrafine/fine/coarse particles collected beside a heavily trafficked road. Environ Sci Technol 39:8113–8122

Lindgren Å (1996) Asphalt wear and pollution transport. Sci Total Environ 189:281–286

Lodhi A, Ghauri B, Khan MR et al (2009) Particulate matter (PM2.5) concentration and source apportionment in Lahore. J Braz Chem Soc 20:1811–1820

Lokorai K, Ali-Khodja H, Khardi S et al (2021) Influence of mineral dust on the concentration and composition of PM10 in the city of Constantine. Aeol Res 50:100677

Lou C, Liu H, Li Y et al (2017) Relationships of relative humidity with PM2.5 and PM10 in the Yangtze River Delta. China Environ Monit Assess 189:1–16

Mansha M, Ghauri B, Rahman S, Amman A (2012) Characterization and source apportionment of ambient air particulate matter (PM2.5) in Karachi. Sci Total Environ 425:176–183

Marcazzan GM, Ceriani M, Valli G, Vecchi R (2003) Source apportionment of PM10 and PM2.5 in Milan (Italy) using receptor modelling. Sci Total Environ 317:137–147

Matassoni L, Pratesi G, Centioli D et al (2009) Saharan dust episodes in Italy: influence on PM 10 daily limit value (DLV) exceedances and the related synoptic. J Environ Monit 11:1586–1594

Mazzei F, D'Alessandro A, Lucarelli F et al (2006) Elemental composition and source apportionment of particulate matter near a steel plant in Genoa (Italy). Nucl Instrum Methods Phys Res, Sect B 249:548–551

McKay WA, Garland JA, Livesley D et al (1994) The characteristics of the shore-line sea spray aerosol and the landward transfer of radionuclides discharged to coastal sea water. Atmos Environ 28:3299–3309

McKenna Neuman C, Sanderson S (2008) Humidity control of particle emissions in aeolian systems. Journal of Geophysical Research: Earth Surface 113:

Morcillo M, Chico B, Mariaca L, Otero E (2000) Salinity in marine atmospheric corrosion: its dependence on the wind regime existing in the site. Corros Sci 42:91–104

Moreno T, Querol X, Alastuey A et al (2010) Variations in vanadium, nickel and lanthanoid element concentrations in urban air. Sci Total Environ 408:4569–4579

Naidja L, Ali-Khodja H, Khardi S (2018) Sources and levels of particulate matter in North African and Sub-Saharan cities: a literature review. Environ Sci Pollut Res 25:12303–12328

Nilsson ED, Kulmala M (1998) The potential for atmospheric mixing processes to enhance the binary nucleation rate. Journal of Geophysical Research: Atmospheres 103:1381–1389

Norris GA, Duvall R, Brown SG, Bai S (2014) Positive matrix factorization (PMF) 5.0 fundamentals and user guide prepared for the US Environmental Protection Agency. USEPA, Office Res Dev, Washington DC

Omstedt G, Bringfelt B, Johansson C (2005) A model for vehicle-induced non-tailpipe emissions of particles along Swedish roads. Atmos Environ 39:6088–6097

Oucher N, Kerbachi R, Ghezloun A, Merabet H (2015) Magnitude of air pollution by heavy metals associated with aerosols particles in Algiers. Energy Procedia 74:51–58

Owoade KO, Hopke PK, Olise FS et al (2015) Chemical compositions and source identification of particulate matter (PM2.5 and PM2.5–10) from a scrap iron and steel smelting industry along the Ife-Ibadan highway. Nigeria Atmos Pollut Res 6:107–119

Ozaki H, Watanabe I, Kuno K (2004) Investigation of the heavy metal sources in relation to automobiles. Water Air Soil Pollut 157:209–223

Paatero P, Tapper U (1994) Positive matrix factorization: a non-negative factor model with optimal utilization of error estimates of data values. Environmetrics 5:111–126

Paatero P, Hopke PK (2003) Discarding or downweighting high-noise variables in factor analytic models. Anal Chim Acta 490:277–289

Pacyna JM, Pacyna EG (2001) An assessment of global and regional emissions of trace metals to the atmosphere from anthropogenic sources worldwide. Environ Rev 9:269–298

Pant P, Shi Z, Pope FD, Harrison RM (2017) Characterization of traffic-related particulate matter emissions in a road tunnel in Birmingham, UK: trace metals and organic molecular markers. Aerosol Air Qual Res 17:117–130

Pekney NJ, Davidson CI, Zhou L, Hopke PK (2006) Application of PSCF and CPF to PMF-modeled sources of PM2.5 in Pittsburgh. Aerosol Sci Technol 40:952–961

Pérez N, Pey J, Querol X, Alastuey A, López JM, Viana M (2008) Partitioning of major and trace components in PM10–PM2.5–PM1

at an urban site in Southern Europe. Atmos Environ 42(8):1677–1691
Pey J, Querol X, Alastuey A et al (2009) Source apportionment of urban fine and ultra-fine particle number concentration in a Western Mediterranean city. Atmos Environ 43:4407–4415
Poirot RL, Wishinski PR, Hopke PK, Polissar AV (2001) Comparative application of multiple receptor methods to identify aerosol sources in northern Vermont. Environ Sci Technol 35:4622–4636
Prati P, Zucchiatti A, Lucarelli F, Mando PA (2000) Source apportionment near a steel plant in Genoa (Italy) by continuous aerosol sampling and PIXE analysis. Atmos Environ 34:3149–3157
Prospero JM, Ginoux P, Torres O, et al (2002) Environmental characterization of global sources of atmospheric soil dust derived from the nimbus7 toms absorbing aerosol product, rev. In: Reviews of geophysics. Citeseer
Quackenboss JJ, Lebowitz MD, Crutchfield CD (1989) Indoor-outdoor relationships for particulate matter: exposure classifications and health effects. Environ Int 15:353–360
Querol X, Alastuey A, Moreno T et al (2008) Spatial and temporal variations in airborne particulate matter (PM10 and PM2.5) across Spain 1999–2005. Atmos Environ 42:3964–3979
Querol X, Alastuey A, Rodriguez S, Plana F, Ruiz CR, Cots N et al (2001) PM10 and PM2.5 source apportionment in the Barcelona Metropolitan area, Catalonia, Spain. Atmos Environ 35(36):6407–6419
Querol X, Alastuey A, Rodrıguez S, Viana MM, Artınano B, Salvador P et al (2004a) Levels of particulate matter in rural, urban and industrial sites in Spain. Sci Total Environ 334:359–376
Querol X, Alastuey A, Ruiz CR, Artiñano B, Hansson HC, Harrison RM et al (2004b) Speciation and origin of PM10 and PM2.5 in selected European cities. Atmos environ 38(38):6547–6555
Querol X, Perez N, Reche C et al (2019) African dust and air quality over Spain: is it only dust that matters? Sci Total Environ 686:737–752
Ravi S, D'Odorico P, Over TM, Zobeck TM (2004) On the effect of air humidity on soil susceptibility to wind erosion: the case of air-dry soils. Geophysical Research Letters 31:
Rehn LP, Waked A, Charron A, Piot C, Besombes JL et al (2014) Source apportionment of traffic exhaust and nonexhaust of PM10 using Positive Matrix Factorization (PMF). Pollution Atmosphérique 221:1–9
Remoundaki E, Bourliva A, Kokkalis P et al (2011) PM10 composition during an intense Saharan dust transport event over Athens (Greece). Sci Total Environ 409:4361–4372
Sabin LD, Lim JH, Venezia MT et al (2006) Dry deposition and resuspension of particle-associated metals near a freeway in Los Angeles. Atmos Environ 40:7528–7538
Safar ZS, Labib MW (2010) Assessment of particulate matter and lead levels in the Greater Cairo area for the period 1998–2007. J Adv Res 1:53–63
Salminen R, Plant JA, Reeder S, Salminen R (2005) Geochemical atlas of Europe. Part 1, background information, methodology and maps. Geological survey of Finland Espoo
Saradhi IV, Prathibha P, Hopke PK et al (2008) Source apportionment of coarse and fine particulate matter at Navi Mumbai, India. Aeroso Air Qual Res 8:423–436
Savoie DL, Prospero JM (1980) Water-soluble potassium, calcium, and magnesium in the aerosols over the tropical North Atlantic. J Geophys Res Oceans 85:385–392
Seinfeld JH, Pandis SN (2016) Atmospheric chemistry and physics. Wiley
Shahbazi H, Taghvaee S, Hosseini V, Afshin H (2016) A GIS based emission inventory development for Tehran. Urban Climate 17:216–229
Sharma SK, Mandal TK, Saxena M et al (2014) Source apportionment of PM10 by using positive matrix factorization at an urban site of Delhi, India. Urban Climate 10:656–670
Sharma SK, Mandal TK, Jain S et al (2016) Source apportionment of PM 2.5 in Delhi, India using PMF model. Bull Environ Contam Toxicol 97:286–293
Shen Z, Sun J, Cao J, Zhang L, Zhang Q, Lei Y et al (2016) Chemical profiles of urban fugitive dust PM2.5 samples in Northern Chinese cities. Sci Total Environ 569:619–626
Shen ZX, Cao JJ, Arimoto R, et al (2007) Chemical composition and source characterization of spring aerosol over Horqin sand land in northeastern China. Journal of Geophysical Research Atmospheres 112
Singh N, Murari V, Kumar M et al (2017) Fine particulates over South Asia: review and meta-analysis of PM2.5 source apportionment through receptor model. Environ Pollut 223:121–136
Smolders E, Degryse F (2002) Fate and effect of zinc from tire debris in soil. Environ Sci Technol 36:3706–3710
Song Y, Zhang Y, Xie S et al (2006) Source apportionment of PM2.5 in Beijing by positive matrix factorization. Atmos Environ 40:1526–1537
Sudheer AK, Rengarajan R (2012) Atmospheric mineral dust and trace metals over urban environment in western India during winter. Aerosol Air Qual Res 12:923–933
Taghvaee S, Sowlat MH, Mousavi A et al (2018) Source apportionment of ambient PM2.5 in two locations in central Tehran using the positive matrix factorization (PMF) model. Sci Total Environ 628:672–686
Tahri M, Bounakhla M, Zghaïd M et al (2013) TXRF characterization and source identification by positive matrix factorization of airborne particulate matter sampled in Kenitra City (Morocco). X-Ray Spectrom 42:284–289
Taiwo AM, Harrison RM, Shi Z (2014) A review of receptor modelling of industrially emitted particulate matter. Atmos Environ 97:109–120
Talbi A, Kerchich Y, Kerbachi R, Boughedaoui M (2018) Assessment of annual air pollution levels with PM1, PM2.5, PM10 and associated heavy metals in Algiers. Algeria Environ Pollut 232:252–263
Tauler R, Viana M, Querol X et al (2009) Comparison of the results obtained by four receptor modelling methods in aerosol source apportionment studies. Atmos Environ 43:3989–3997
Terrouche A, Ali-Khodja H, Kemmouche A et al (2016) Identification of sources of atmospheric particulate matter and trace metals in Constantine, Algeria. Air Qual Atmos Health 9:69–82
Thorpe A, Harrison RM (2008) Sources and properties of non-exhaust particulate matter from road traffic: a review. Sci Total Environ 400:270–282
Tian HZ, Lu L, Cheng K et al (2012) Anthropogenic atmospheric nickel emissions and its distribution characteristics in China. Sci Total Environ 417:148–157
Tran HN, Mölders N (2011) Investigations on meteorological conditions for elevated PM2.5 in Fairbanks. Alaska Atmos Res 99:39–49
Trousset P (1995) Djerid.(Jérid, Qastîliya). Encyclopédie berbère 2461–2465
Turunen M, Peräniemi S, Ahlgrén M, Westerholm H (1995) Determination of trace elements in heavy oil samples by graphite furnace and cold vapour atomic absorption spectrometry after acid digestion. Anal Chim Acta 311:85–91
Ulbrich IM, Canagaratna MR, Zhang Q et al (2009) Interpretation of organic components from positive matrix factorization of aerosol mass spectrometric data. Atmos Chem Phys 9:2891–2918
Vale MGR, Damin IC, Klassen A et al (2004) Method development for the determination of nickel in petroleum using line-source and high-resolution continuum-source graphite furnace atomic absorption spectrometry. Microchem J 77:131–140
von Uexküll O, Skerfving S, Doyle R, Braungart M (2005) Antimony in brake pads-a carcinogenic component? J Clean Prod 13:19–31
Wadden RA, Hawkins JL, Scheff PA, Franke JE (1991) Characterization of emission factors related to source activity for

trichloroethylene degreasing and chrome plating processes. Am Ind Hyg Assoc J 52:349–356

Wang J, Ogawa S (2015) Effects of meteorological conditions on PM2.5 concentrations in Nagasaki, Japan. Int J Environ Res Public Health 12(8):9089–9101

Wang Y, Zhuang G, Sun Y, An Z (2006) The variation of characteristics and formation mechanisms of aerosols in dust, haze, and clear days in Beijing. Atmos Environ 40:6579–6591

Webb NP, Strong CL (2011) Soil erodibility dynamics and its representation for wind erosion and dust emission models. Aeol Res 3:165–179

Wen QZ (1989) Chinese loess geochemistry. Sci Press, Beijing 115–158

Westerlund K-G, Johansson C (2002) Emission of metals and particulate matter due to wear of brake linings in Stockholm. WIT Transactions on Ecology and the Environment 53:

Wimolwattanapun W, Hopke PK, Pongkiatkul P (2011) Source apportionment and potential source locations of PM2.5 and PM2.5–10 at residential sites in metropolitan Bangkok. Atmos Pollut Res 2:172–181

Xu J, Bergin MH, Greenwald R, et al (2004) Aerosol chemical, physical, and radiative characteristics near a desert source region of northwest China during ACE-Asia. Journal of Geophysical Research: Atmospheres 109:

Yin D, Nickovic S, Sprigg WA (2007) The impact of using different land cover data on wind-blown desert dust modeling results in the southwestern United States. Atmos Environ 41:2214–2224

Zainal NA, Zulkifli NWM, Gulzar M, Masjuki HH (2018) A review on the chemistry, production, and technological potential of bio-based lubricants. Renew Sustain Energy Rev 82:80–102

Zezza F, Macrì F (1995) Marine aerosol and stone decay. Sci Total Environ 167:123–143

Zghaid M, Noack Y, Boukla M, Benyaich F (2009) Atmospheric particulate pollution in Kenitra (Morocco); Pollution atmospherique particulaire dans la ville de Kenitra (Maroc). Pollution Atmospherique 13:

Zhu Y, Huang L, Li J et al (2018) Sources of particulate matter in China: insights from source apportionment studies published in 1987–2017. Environ Int 115:343–357

Source apportionment of $PM_{2.5}$ and their associated metallic elements by positive matrix factorization at traffic site in Constantine, Algeria

Lamri Naidja[a,b,c], Hocine Ali-Khodja[a*], Salah Khardi[d], Fairouz Bencharif-Madani[a], Ahmed Terrouche[a], Kanza Lokorai[a], Mokhtar Bouziane[a], Aurélie Charron[e]

[a] *Laboratory of Pollution and Water Treatment, Department of Chemistry, Faculty of Exact Sciences, University of Mentouri Brothers-, Constantine 1 25017, Algeria*
[b] *Centre de Recherche Scientifique et Technique en Analyses Physico-Chimiques (CRAPC), BP 384, Si`ege ex Pasna Zone Industrielle Bou-Ismail, CP 42004 Tipaza, Algeria*
[c] *Centre de Recherche en Sciences Pharmaceutiques, Zone d'activités ZAM, Nouvelle Ville Ali Mendjli, Constantine, Algeria*
[d] *University Lyon , INSA Lyon, CNRS, LaMCoS, UMR5259, 69621 Villeurbanne, France*
[e] *Unité Mixte de Recherche Epidémiologique et de Surveillance Transport Travail Environnement University Gustave Eiffel Lyon Campus France*
*Corresponding author : e-mail : hocine_ak@yahoo.fr; Tel: +2135 6 57 86 02 88/Fax: +213 31 79 84 60

Table of contents

Table S1

Detection limits and relative standard deviations of major and trace elements analysed by ICP-OES and ICP-MS

Element	Detection limit (µg/L)	Measurement uncertainty (%)
Na	10	1.25
Mg	0.05	1.25
P	20	5.98
K	10	1.15
Ca	10	0.97
Sr	0.01	1.17
Zr	0.01	0.93
Ba	0.05	1.56
Pb	0.01	1.33
Al	0.02	11.15
Ti	0.05	8.02
V	0.01	6.60
Cr	0.01	3.96
Mn	0.02	6.24
Fe	0.1	3.58
Ni	0.01	1.79
Cu	0.05	1.65
Zn	0.1	3.02
Mo	0.05	1.66
S	150	4.52

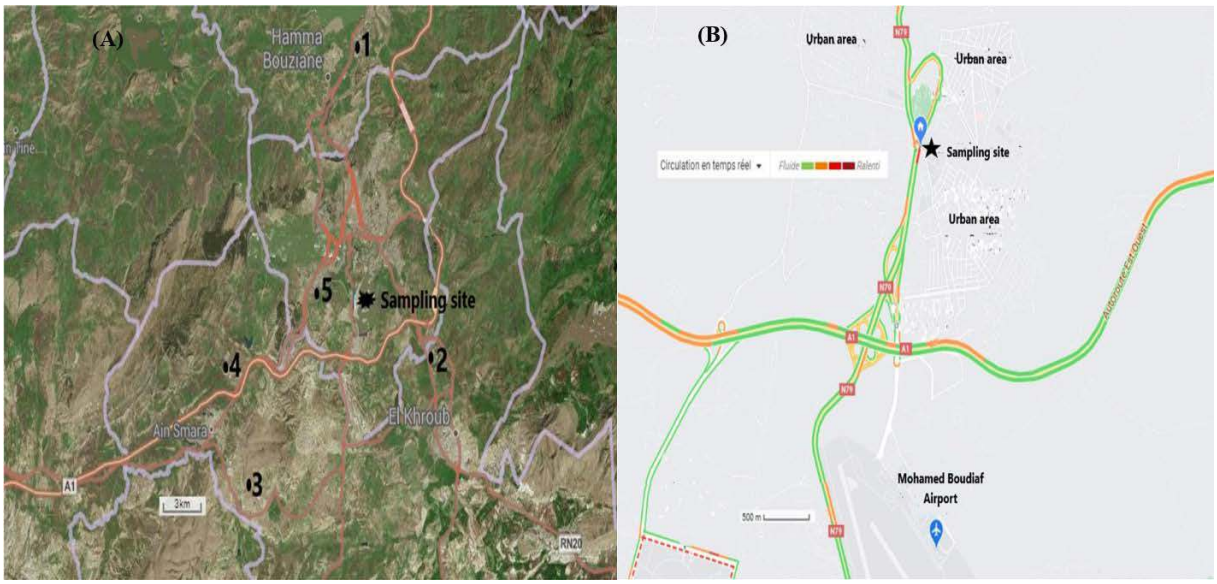

Fig. S1. Sampling site with (A) industrial emission sources and (B) nearby roads

(1) Hamma Bouziane cement plant, (2) mechanical manufacturing plant (Oued Hmeimim), (3) stone production quarries, (4) mechanical complex (Ain Smara), (5) industrial activity zone (Palma).

Fig. S2. Sampler (LVS) used for sampling aerosols at the Zouaghi site

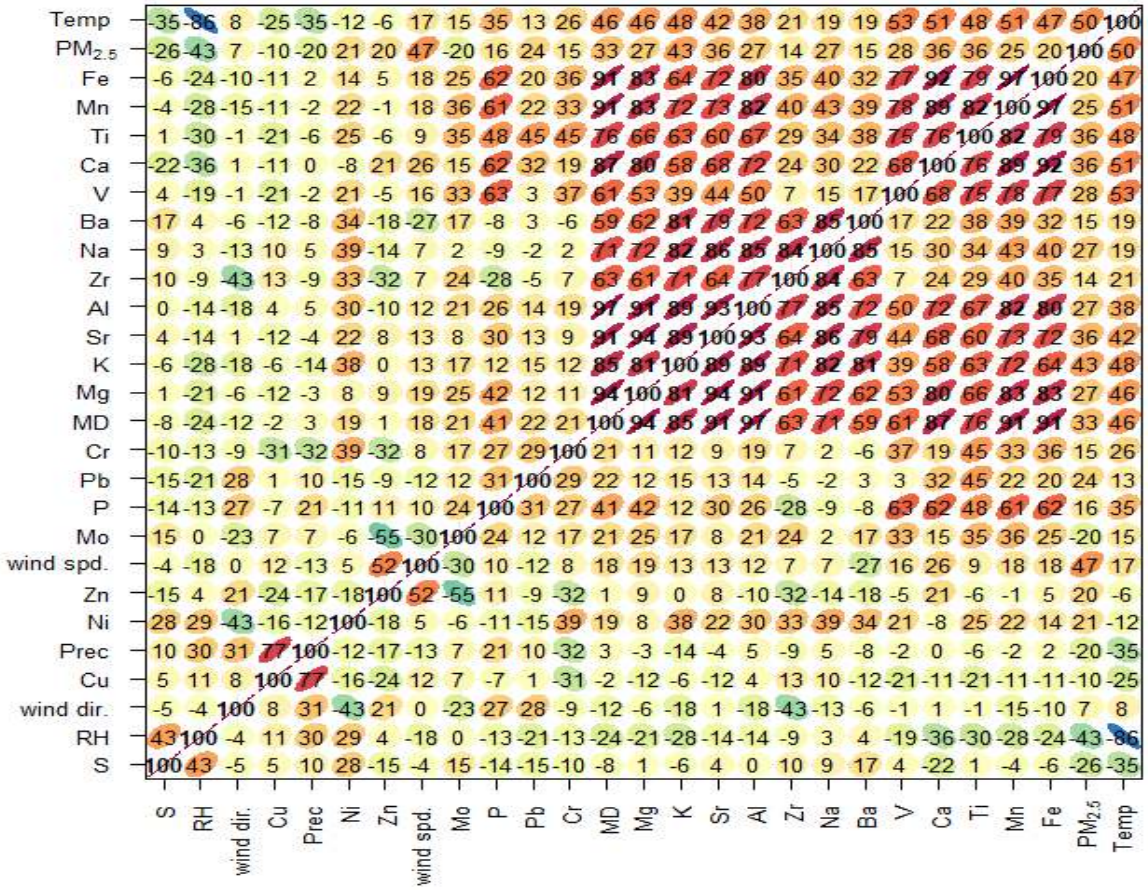

Fig. S3. Spearman correlation matrix showing the relationships between the average seasonal concentrations of $PM_{2.5}$ components and the different meteorological parameters during the summer

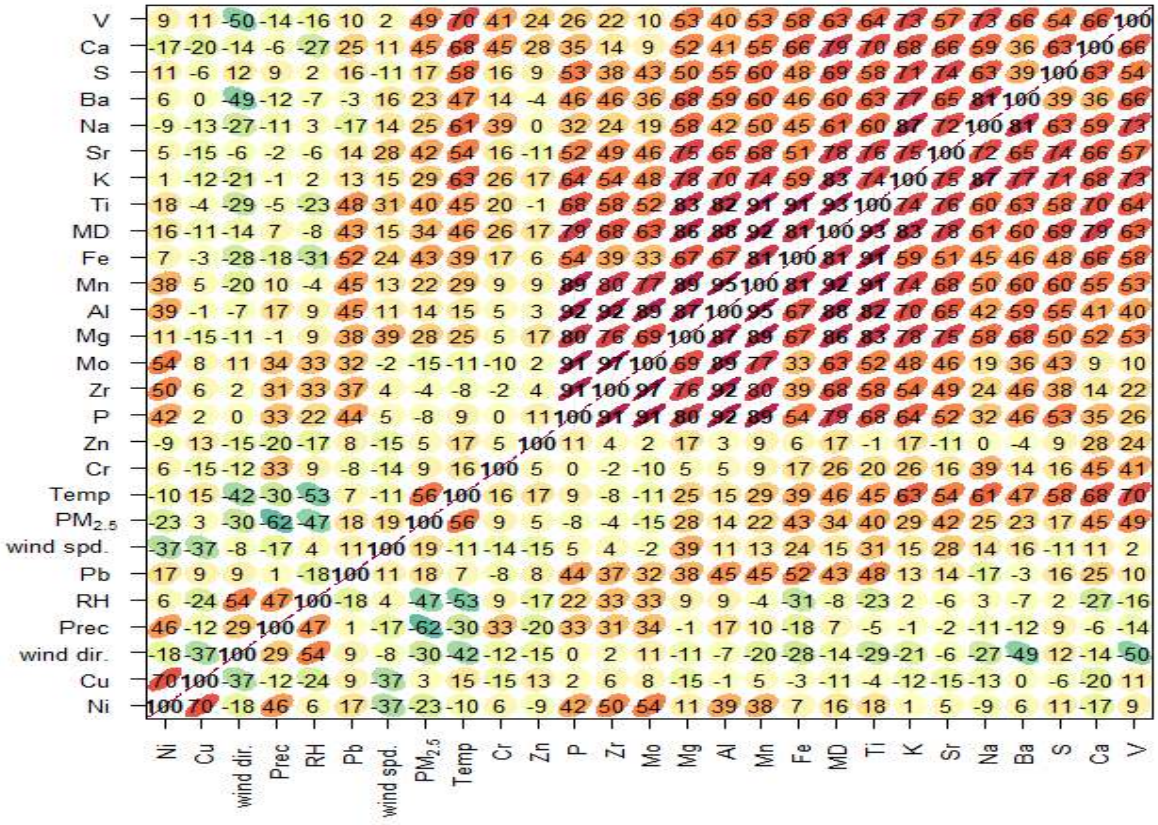

Fig. S4. Spearman correlation matrix showing the relationships between the average seasonal concentrations of $PM_{2.5}$ components and the various meteorological parameters during the autumn

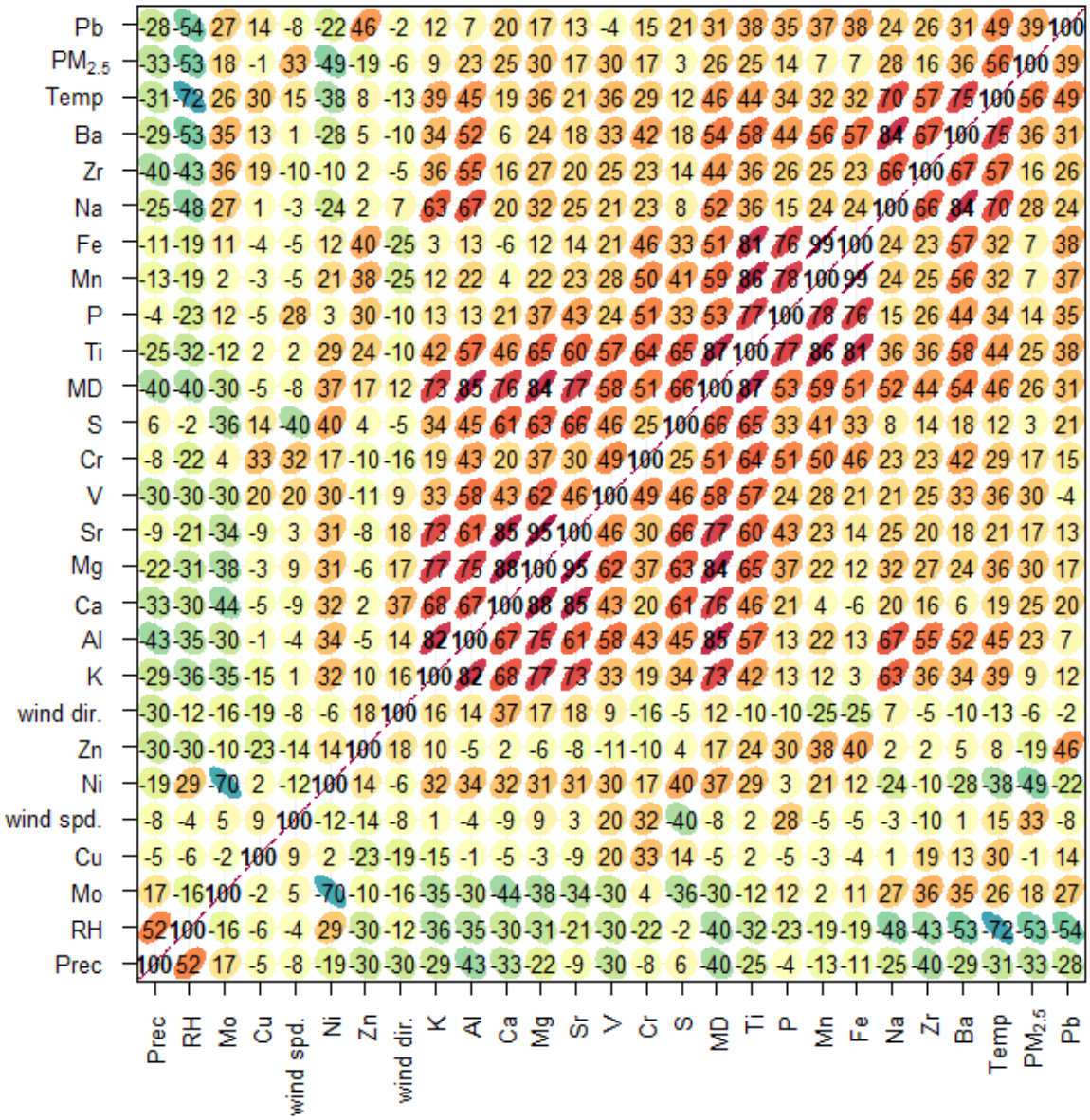

Fig. S5. Spearman correlation matrix showing the relationships between the average seasonal concentrations of $PM_{2.5}$ components and the various meteorological parameters during the spring

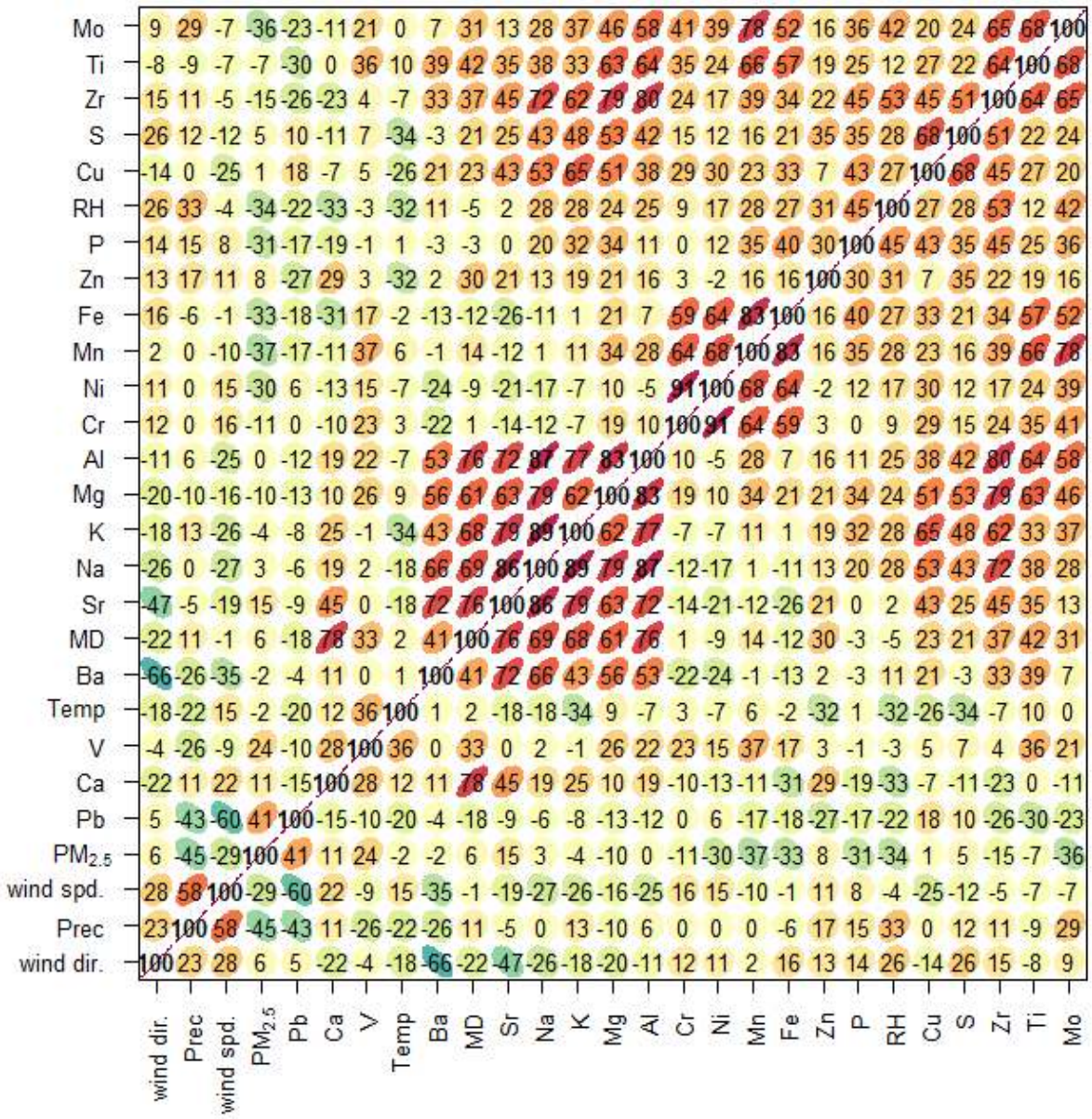

Fig. S6. Spearman correlation matrix showing the relationships between the average seasonal concentrations of $PM_{2.5}$ components and the various meteorological parameters during winter

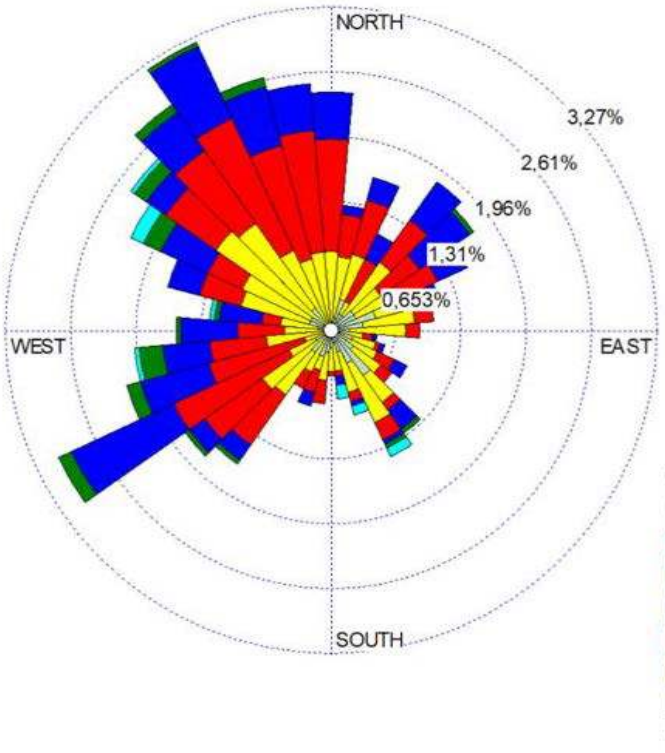

Wind direction	Frequency (%)
North	18,95
North-East	11,23
East	7,46
South-East	7,8
South	6,6
South-West	12,95
West	15,61
North-West	19,38

Fig. S7. Wind rose for the Zouaghi site for the period from 03/15/2017 to 3/15/2018

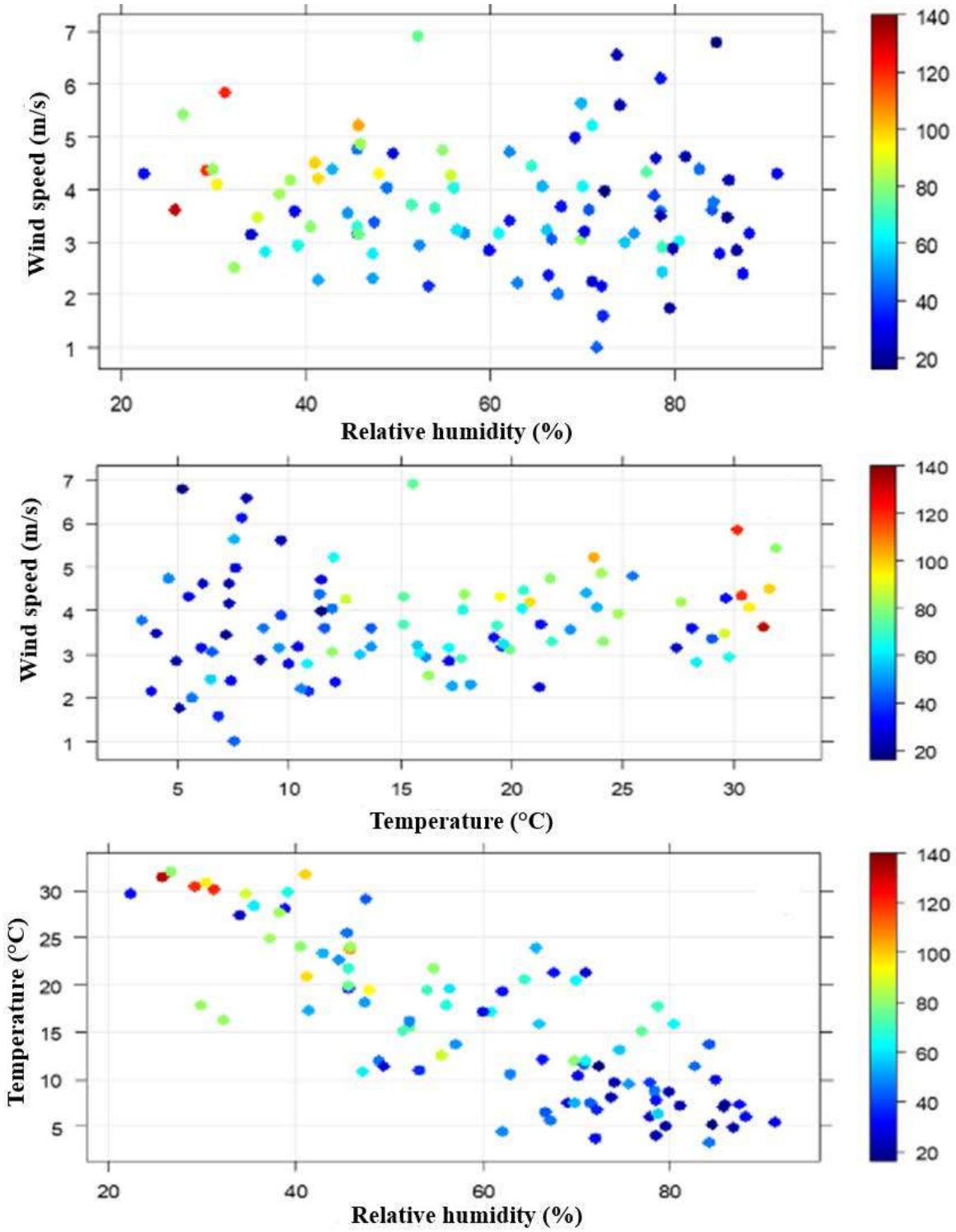

Fig. S8. Scatterplot of daily $PM_{2.5}$ concentrations versus relative humidity (%), temperature (°C) and wind speed (m/s)

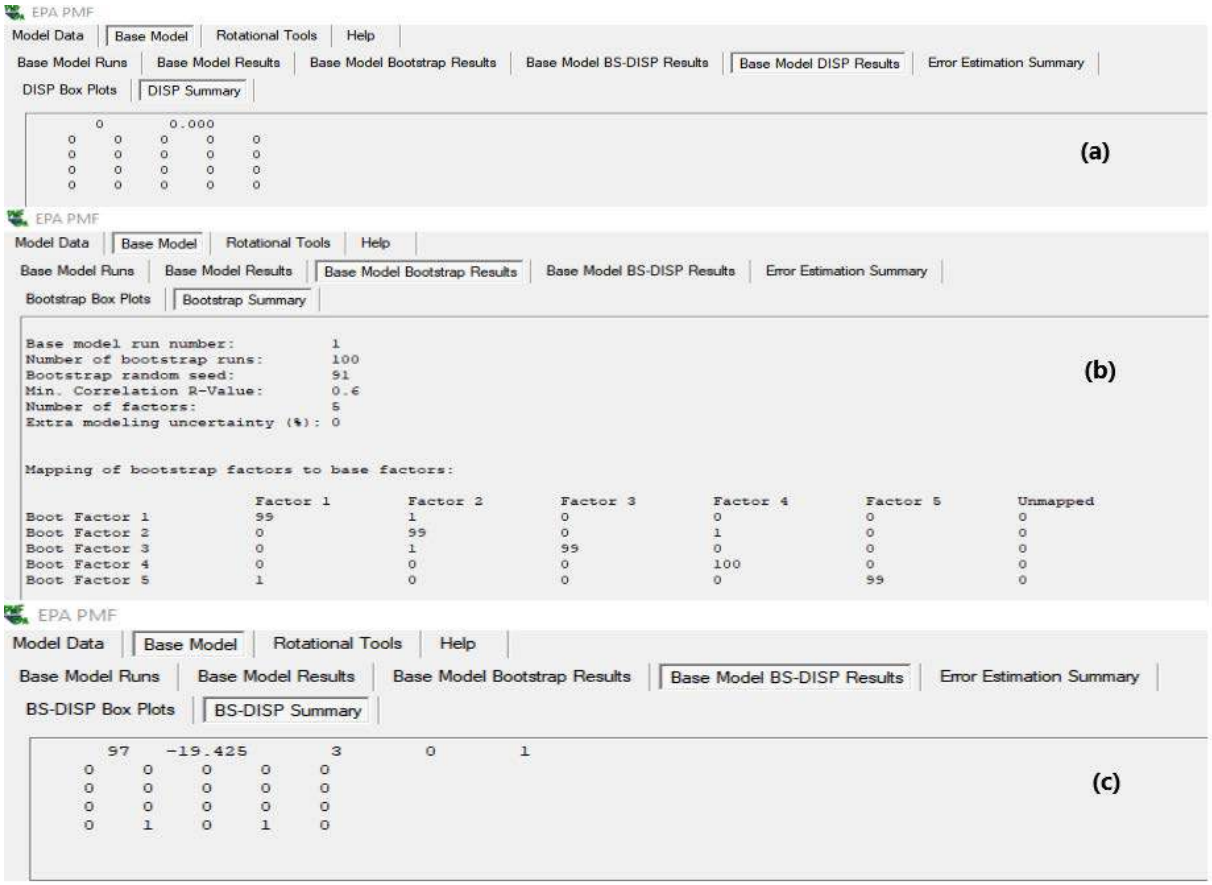

Fig. S9. The results of error estimation (a) DISP, (b) BS, and (c) BS DISP for the five-factor solution

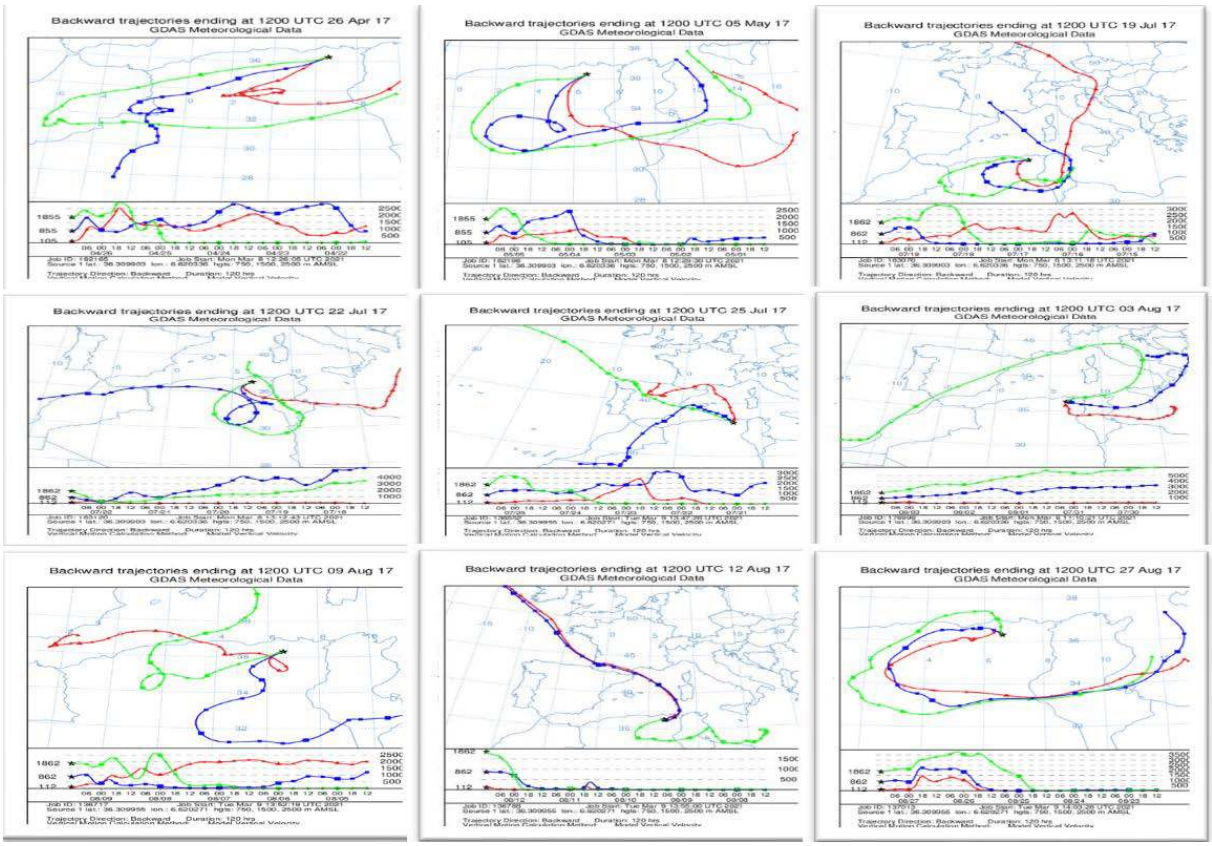

Fig. S10. 85th percentiles of sea salt back trajectories developed by HYSPLIT at altitudes of 750, 1500 and 2500 m above sea level for 5 days

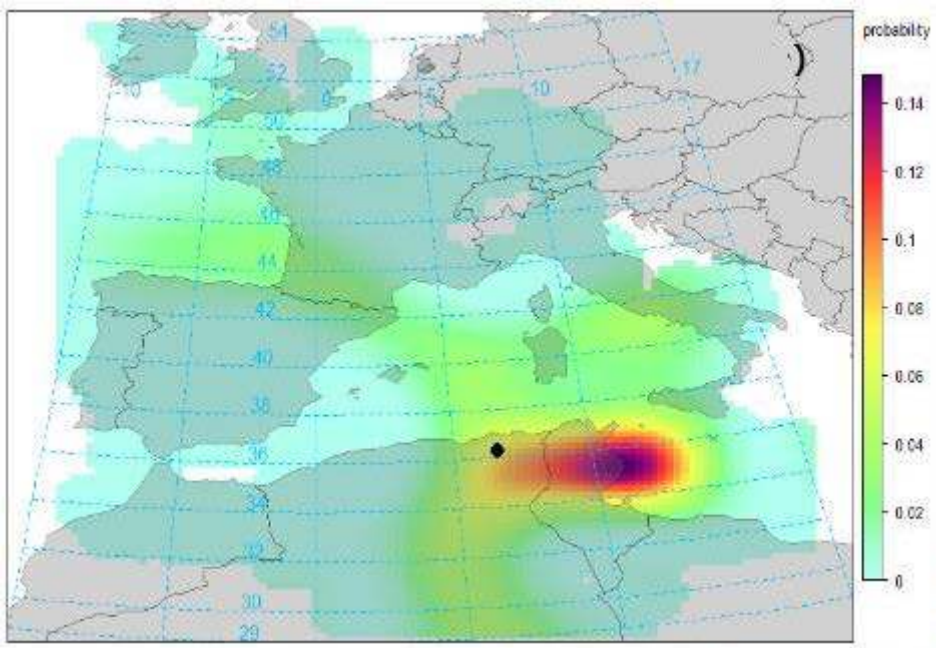

Fig. S11. PSCF probabilities (percentile 90) for sea salts contributions

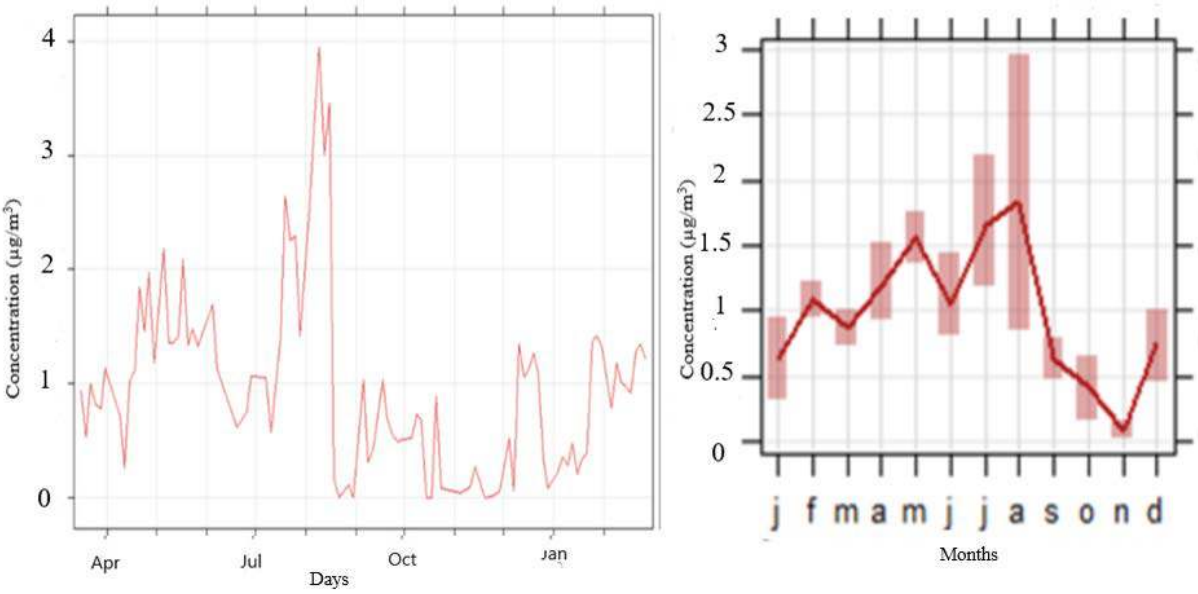

Fig. S12. Daily and monthly concentrations of the "sea salts" factor resolved by PMF

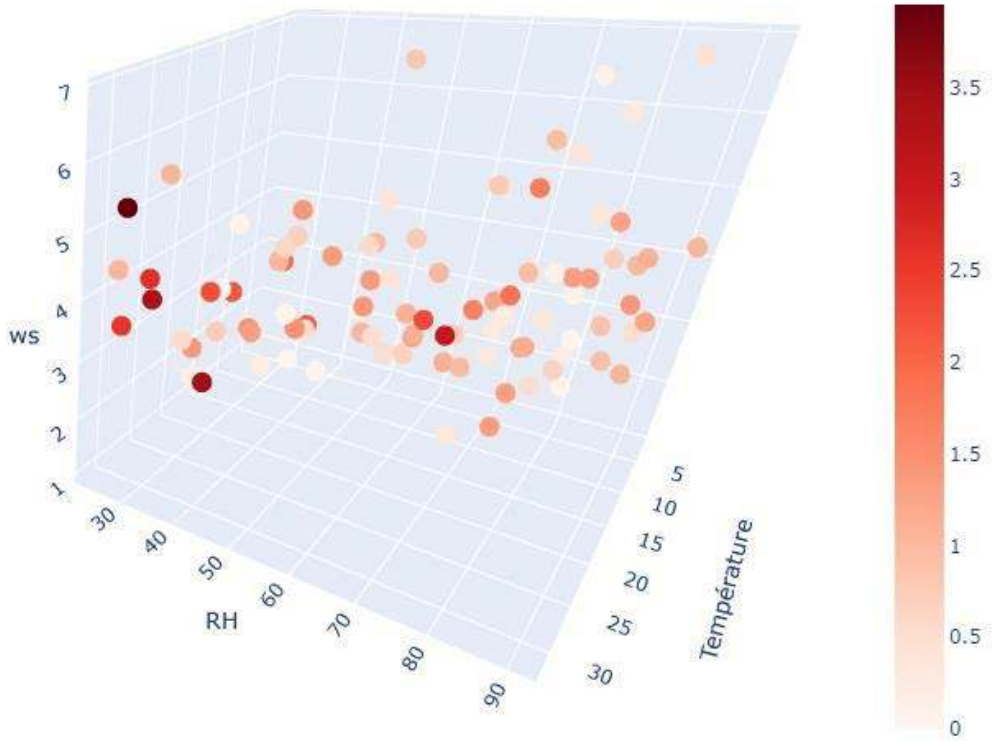

Fig. S13. Contributions (µg/m^3) of "sea salts" as a function of wind speed (m/s), relative humidity (%) and temperature (°C)

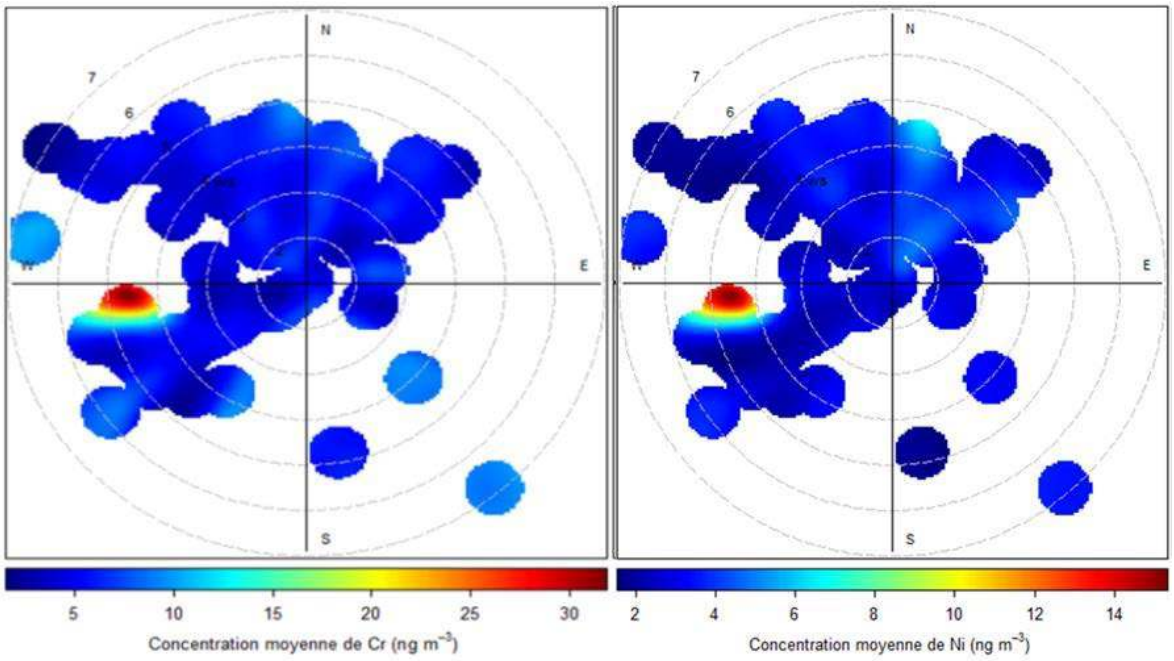

Fig. S14. Spatial distribution of Cr and Ni concentrations as a function of wind direction and speed

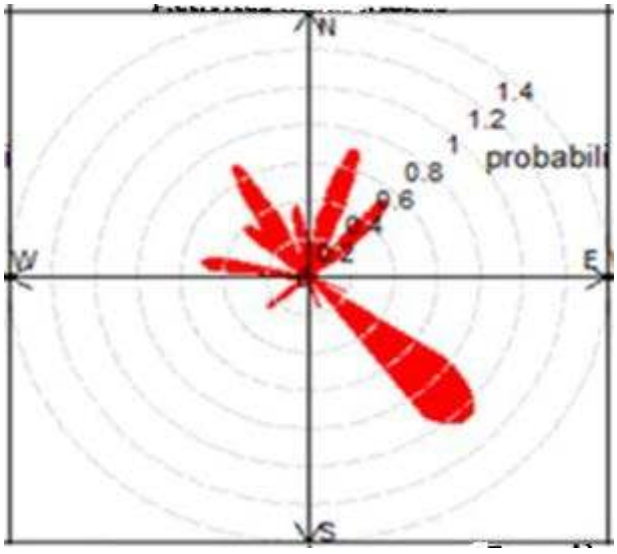

Fig. S15. 75th percentile of the conditional probability function (CPF) for the "industrial emissions" factor contributing to $PM_{2.5}$

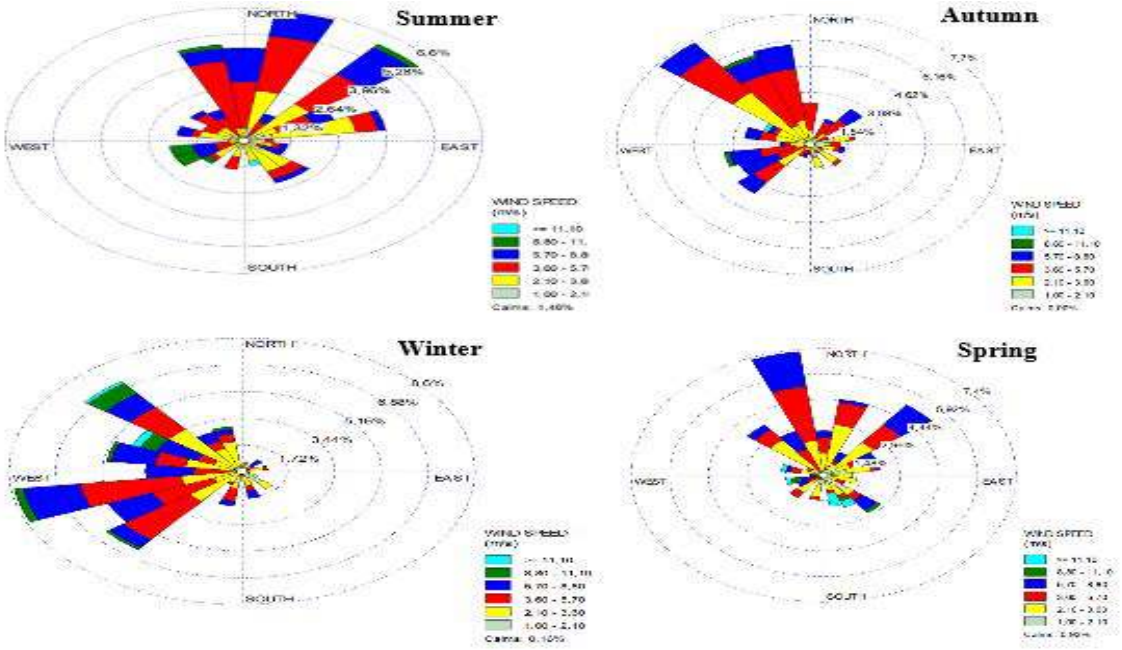

Fig. S16. Seasonal wind roses for the Zouaghi site

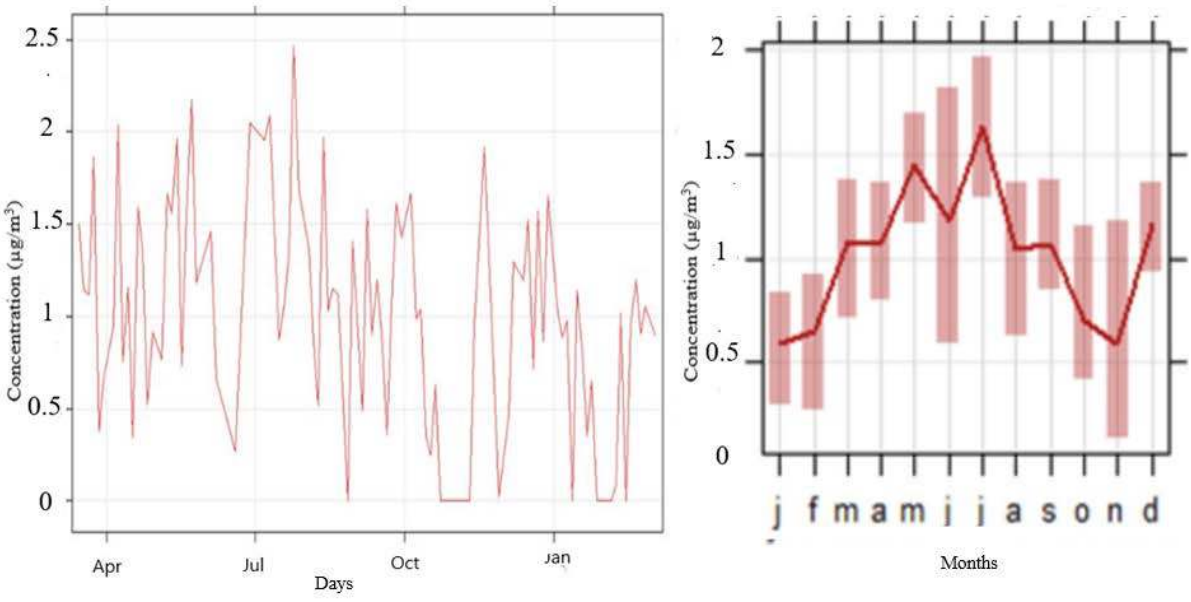

Fig. S17. Daily and monthly contribution of the "industrial activities" factor resolved by PMF

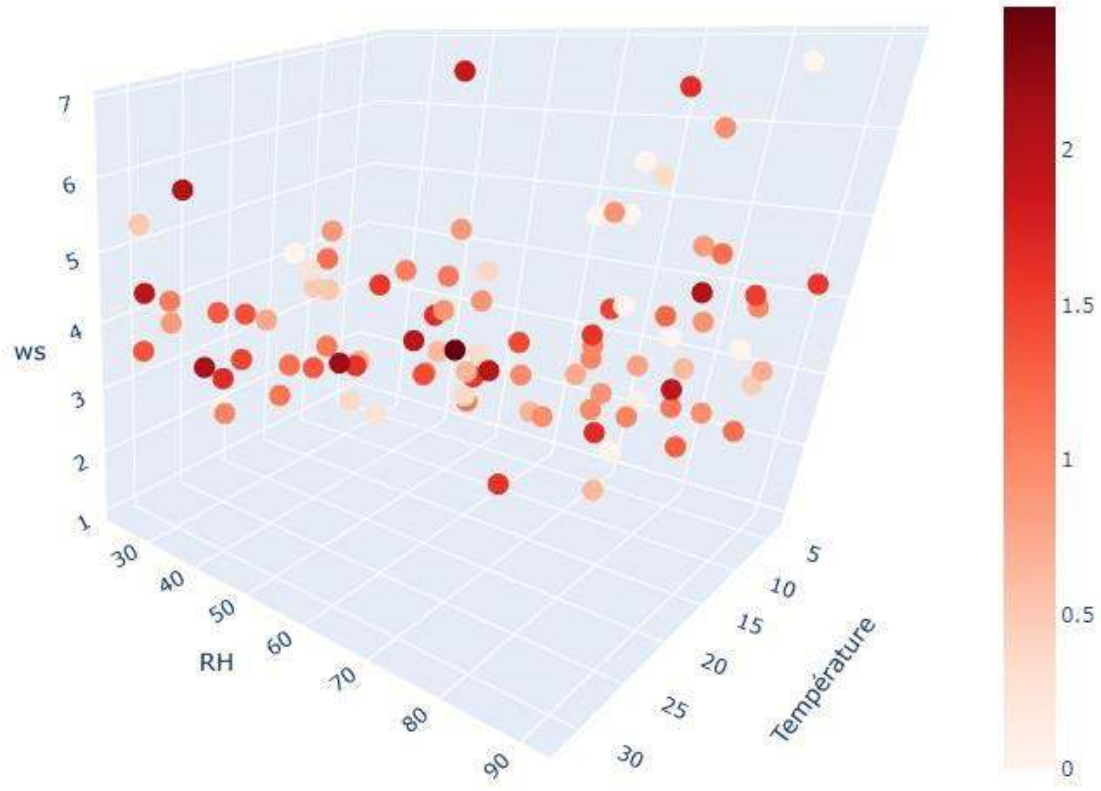

Fig. S18. Contributions (µg/m^3) of "industrial activities" as a function of wind speed (m/s), relative humidity (%) and temperature (°C)

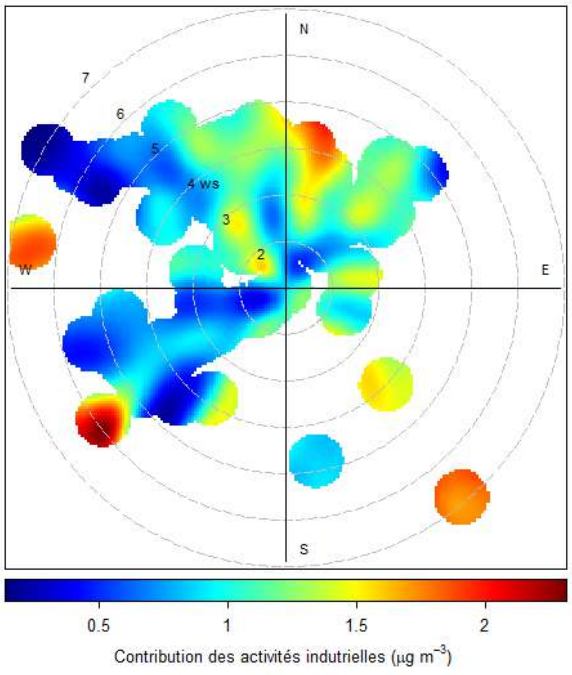

Fig. S19. Contribution of "industrial activities" as a function wind speed and direction

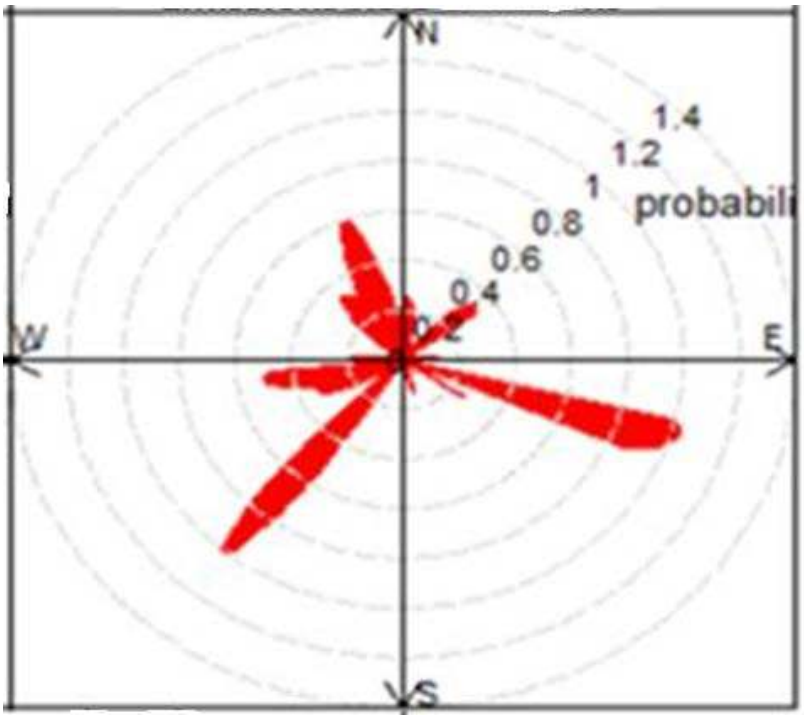

Fig. S20. 75th percentile of the conditional probability function (CPF) for the "non-exhaust emissions" factor contributing to $PM_{2.5}$

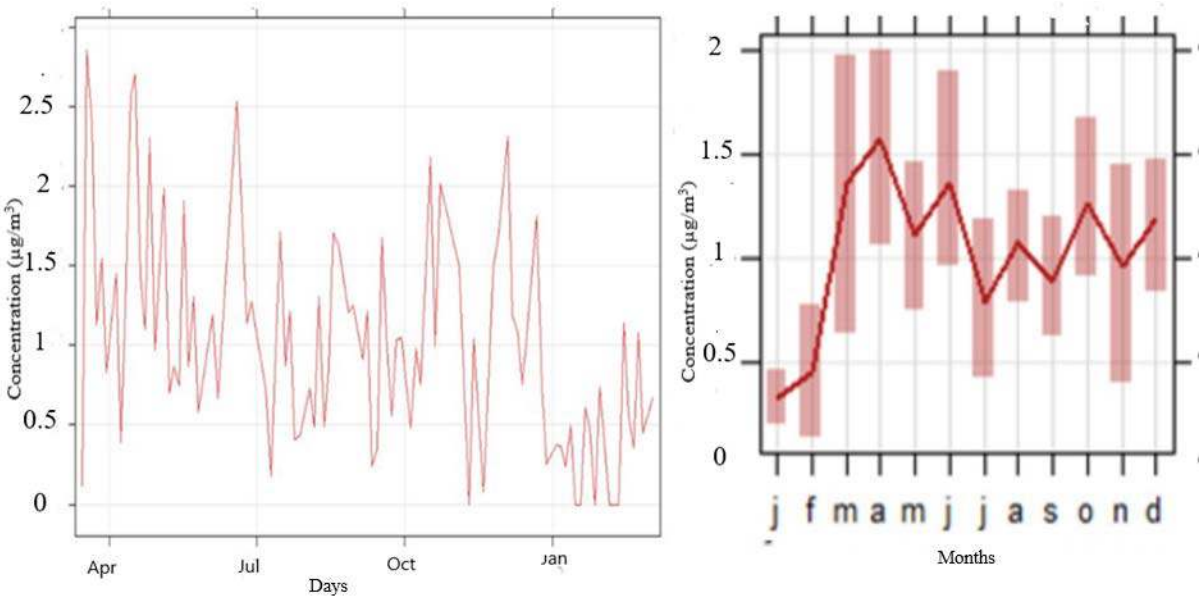

Fig. S21. Daily and monthly contribution of the "non-exhaust emissions" factor resolved by PMF

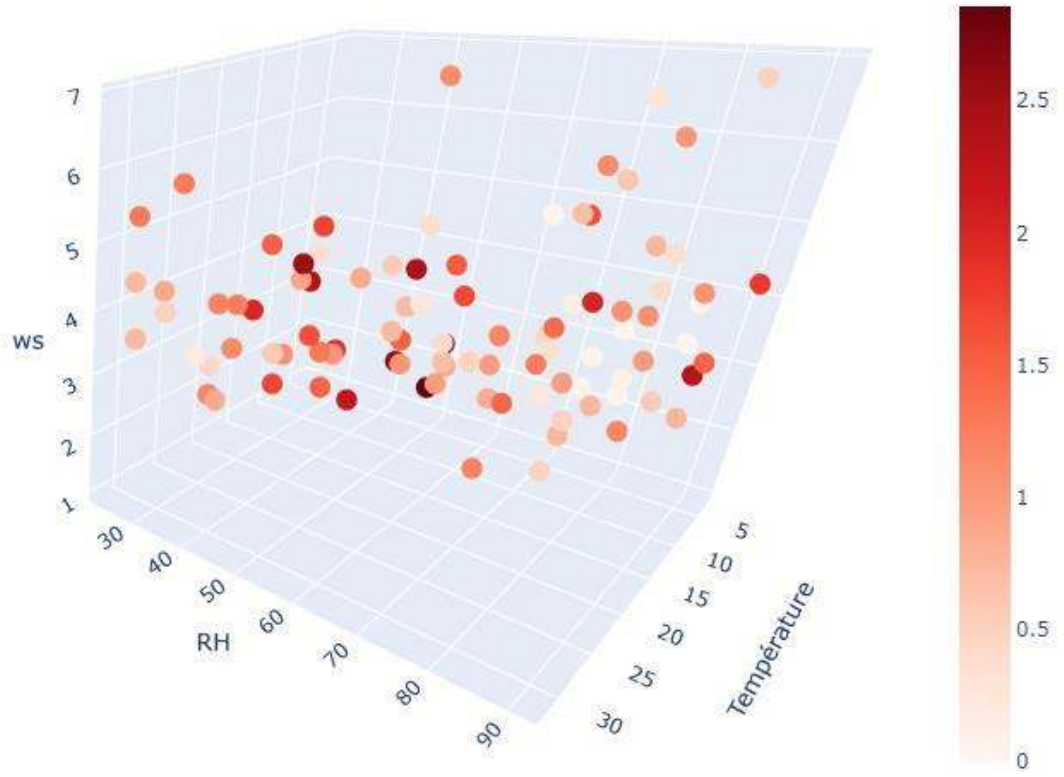

Fig. S22. Contributions (µg/m^3) of "non-exhaust emissions" as a function of wind speed (m/s), relative humidity (%) and temperature (°C)

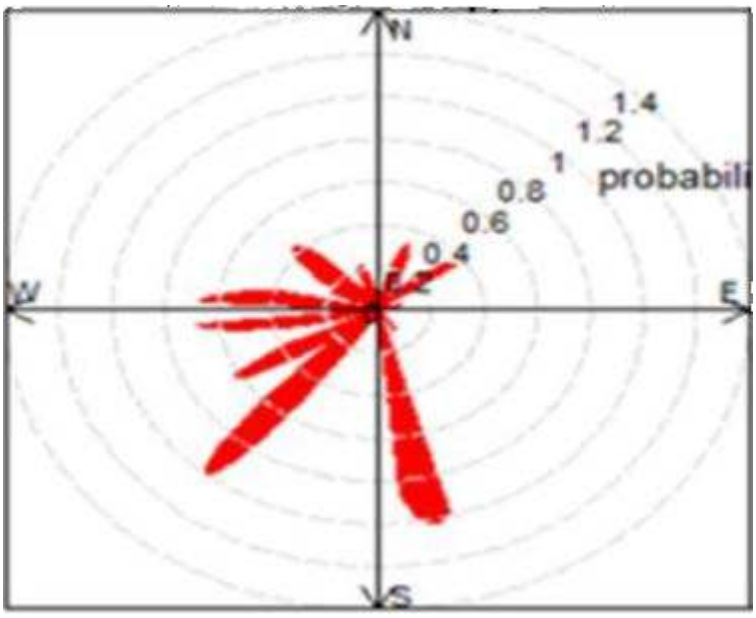

Fig. S23. 75th percentile of the conditional probability function (CPF) for "exhaust emissions" factor contributing to $PM_{2.5}$

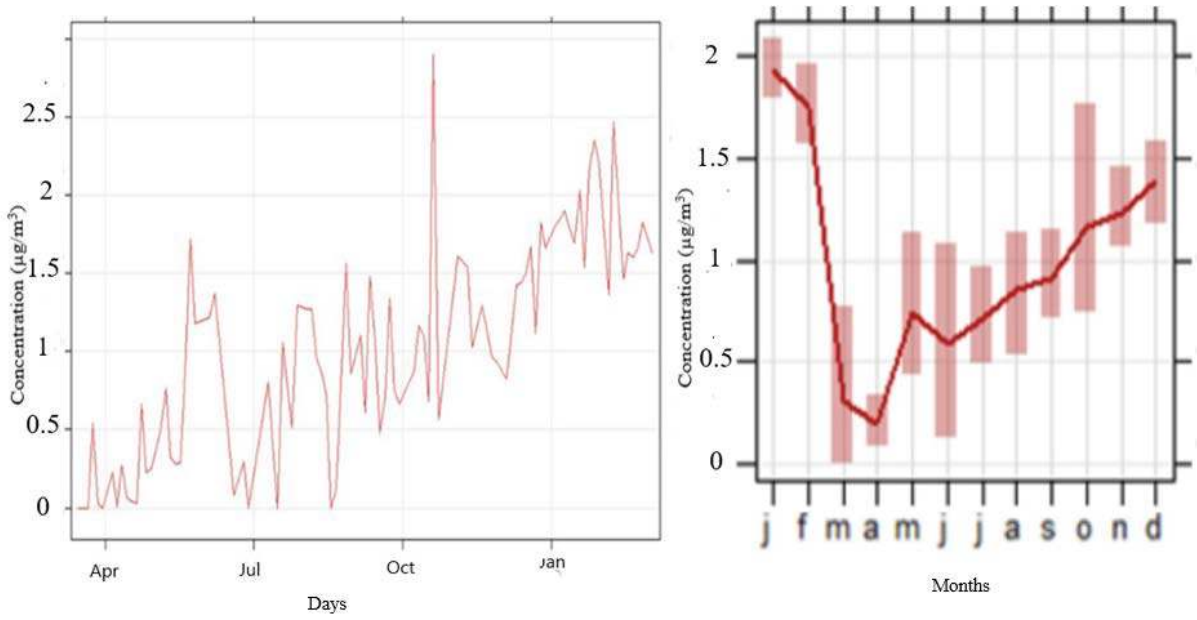

Fig. S24. Daily and monthly contribution of the "exhaust emissions" factor resolved by PMF

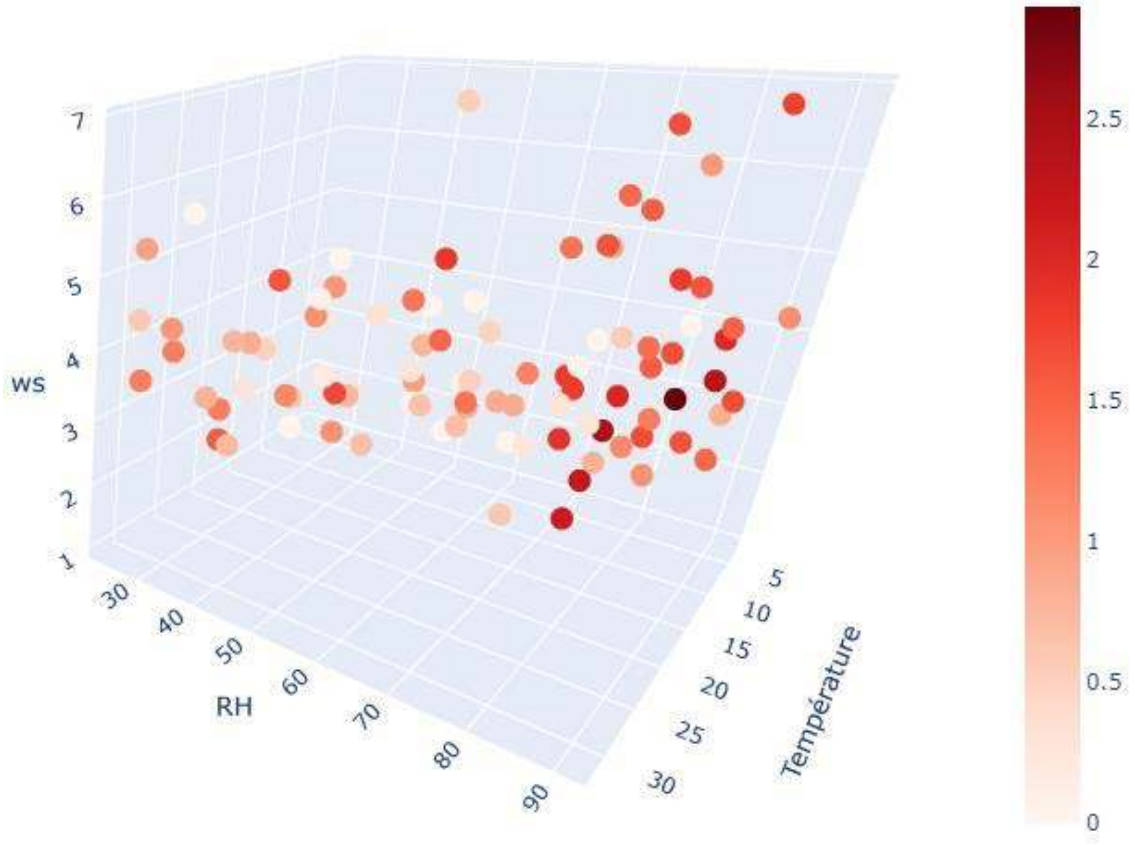

Fig. S25. Contributions (µg/m^3) of "exhaust emissions" as a function of wind speed (m/s), relative humidity (%) and temperature (°C)

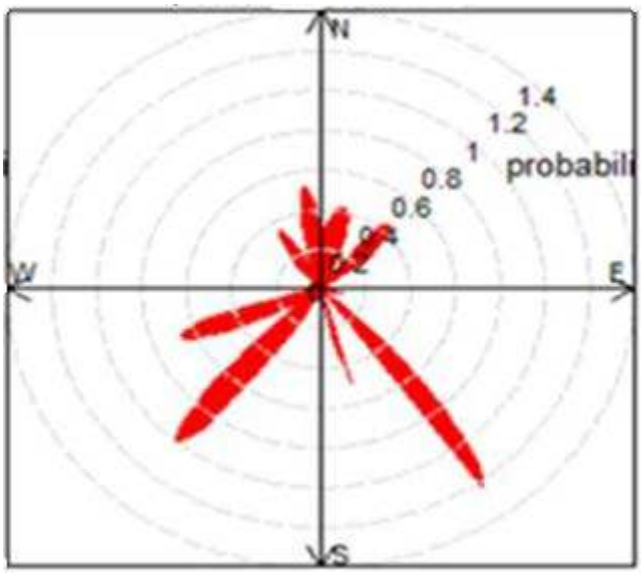

Fig. S26. 75th percentile of the conditional probability function (CPF) for the "mineral dust" factor contributing to $PM_{2.5}$

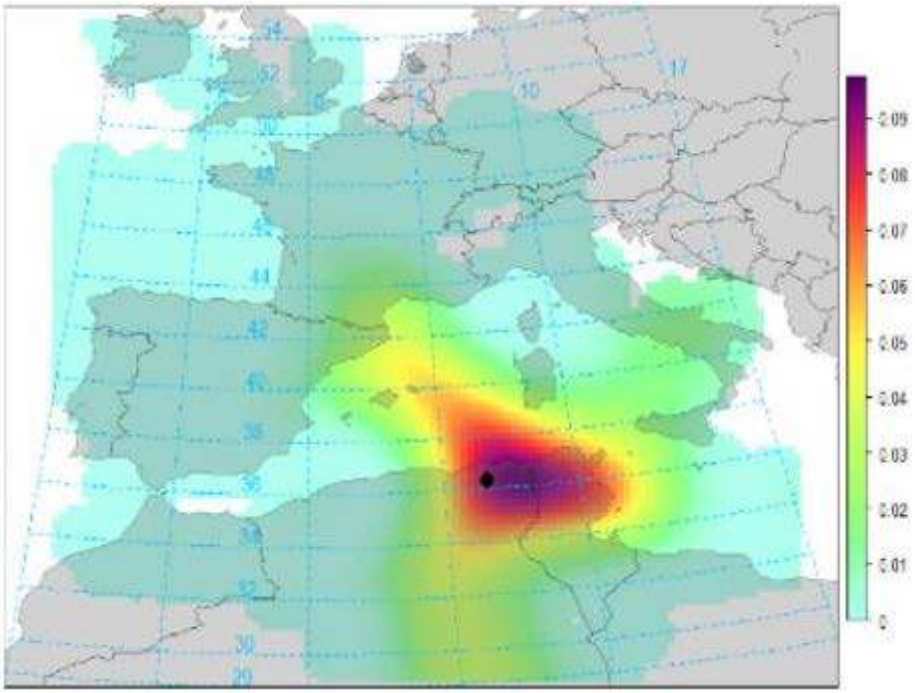

Fig. S27. 90th percentile of PSCF probabilities for the "mineral dust" contributions

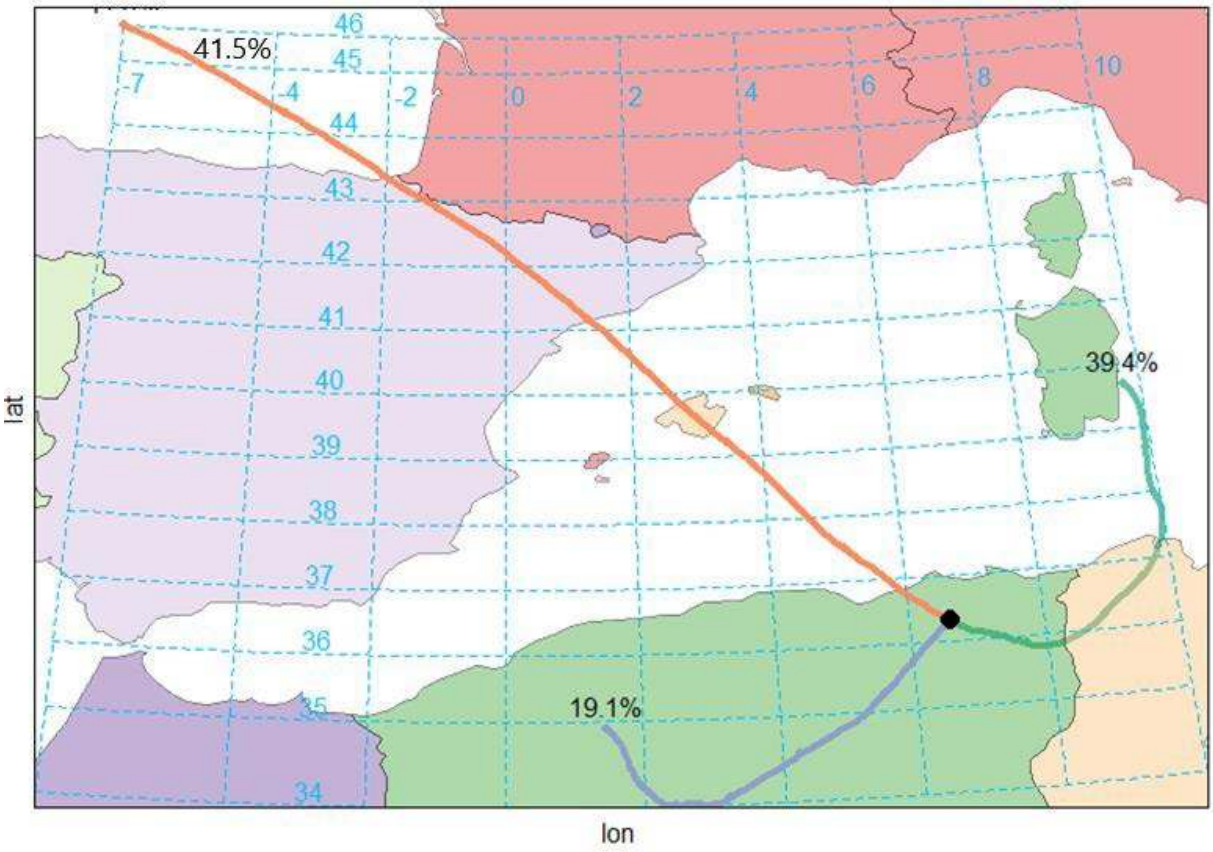

Fig. S28. Synoptic wind rose (clusters of back-trajectories calculated for our site for the study period)

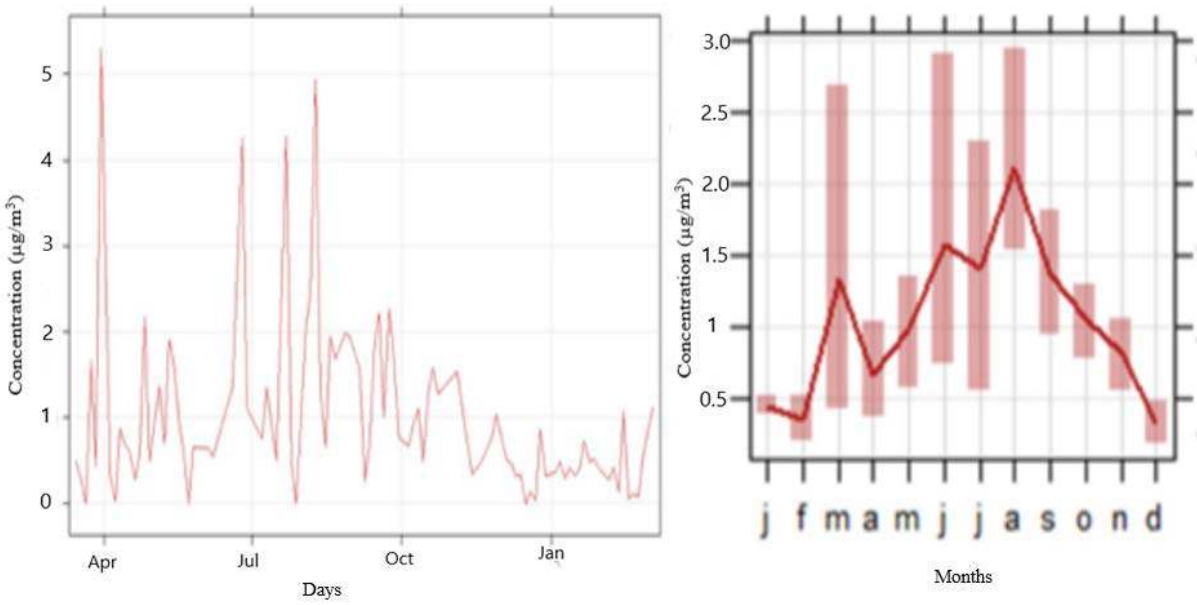

Fig. S29. Daily and monthly concentration of the "mineral dust" factor resolved by PMF

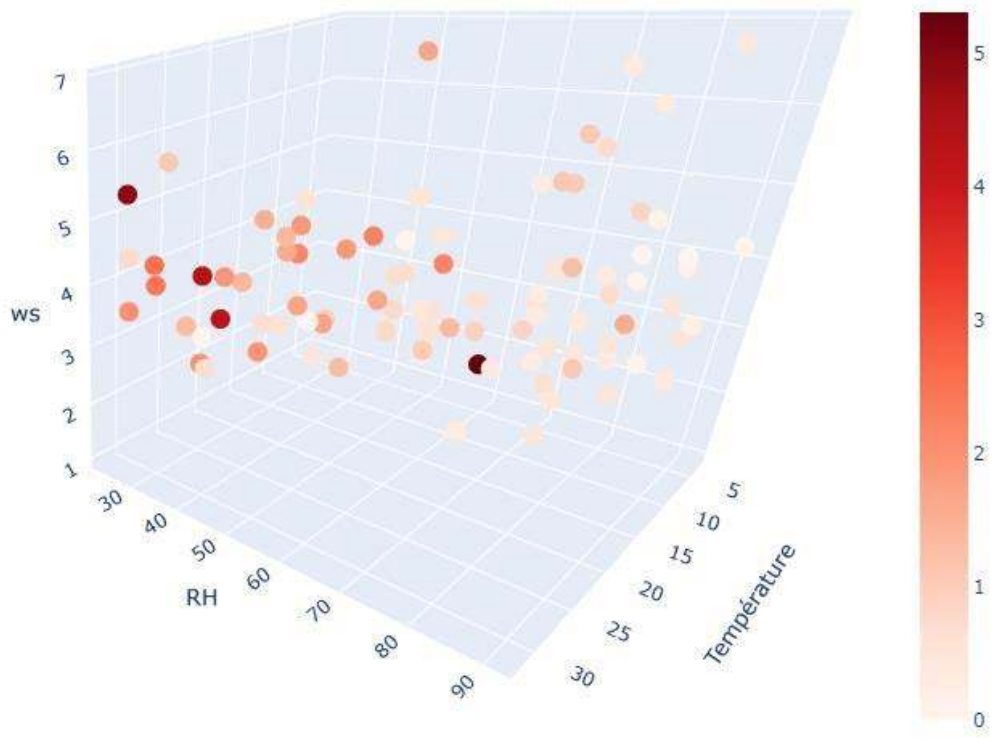

Fig. S30. Contributions (µg/m^3) of "mineral dust" as a function of wind speed (m/s), relative humidity (%) and temperature (°C)

Factor Profiles (conc. of species) from Base Run #1 (Convergent Run)

		Sea-salt	Industrial e	Non-exhaust	Exhaust	Mineral dust
1	PM2.5	5,7995	7,2829	9,3096	6,0815	9,974
1	Na	0,66525	0,10187	0	0	0
1	Mg	0,043967	0,007336	0,0046574	0,015968	0,032069
1	P	0	0,005763	0,0087976	0,004326	0,0082171
1	K	0,094687	0,013319	0,0094812	0,004778	0,046773
1	Ca	0,19822	0	0,06991	0,2533	0,57767
1	Sr	0,0021654	0,000253	0,0002923	0,001785	0,0010173
1	Zr	0,0041576	0,002918	0,0028646	0,002962	0,00058641
1	Ba	0,04214	0	0	0,057337	0
1	Pb	0	0	0,0080946	0,028764	0,0020408
1	Al	0,25673	0,12004	0,099676	0,16212	0,097498
1	Ti	0,003299	0,003242	0,0013406	0,004085	0,0062146
1	V	0,000089098	0,00014	0	0	0,00030028
1	Cr	0,00024465	0,003811	0,00013323	0,000227	0,00059013
1	Mn	0,0003818	0,001033	0,00073132	0,001111	0,001599
1	Fe	0,02247	0,037771	0,019884	0,01727	0,073576
1	Ni	0	0,00123	0,00094036	0,000197	0,00017775
1	Cu	0,00025244	0,000417	0,00034076	0	0,00032744
1	Zn	0,0023458	0	0,012926	0	0
1	Mo	0,00023708	0,007541	0,0092419	0,012087	0
1	S	0,0011189	0,066587	0,079397	0,077006	0,0033523

Factor Profiles (% of species sum) from Base Run #1 (Convergent Run)

		Factor 1	Factor 2	Factor 3	Factor 4	Factor 5
1	PM2.5	15,08420574	18,94245	24,21379804	15,81767	25,94186878
1	Na	86,72046094	13,27954	0	0	0
1	Mg	42,27722172	7,053576	4,478402722	15,3543	30,83649609
1	P	0	21,26222	32,45987529	15,95986	30,31804597
1	K	56,01521551	7,879293	5,608916338	2,826465	27,67010968
1	Ca	18,03475571	0	6,360658721	23,04613	52,55845692
1	Sr	39,2812051	4,585166	5,302436617	32,37697	18,45422091
1	Zr	30,8237281	21,63355	21,23764949	21,95753	4,347542427
1	Ba	42,36155091	0	0	57,63845	0
1	Pb	0	0	20,80906132	73,94459	5,246353414
1	Al	34,87876054	16,30836	13,54175724	22,02526	13,24585906
1	Ti	18,14541634	17,83135	7,37367237	22,46753	34,18202619
1	V	16,83101359	26,44474	0	0	56,72424476
1	Cr	4,886930432	76,12945	2,661294672	4,534368	11,78795935
1	Mn	7,862729673	21,2652	15,06069006	22,88182	32,9295567
1	Fe	13,14257974	22,09205	11,63004252	10,10113	43,03419878
1	Ni	0	48,3196	36,95032869	7,745596	6,984475015
1	Cu	18,8720433	31,17431	25,47471667	0	24,47893305
1	Zn	15,36033735	0	84,63966265	0	0
1	Mo	0,814523726	25,90686	31,75192688	41,52669	0
1	S	0,49190807	29,274	34,90573337	33,85457	1,473789816

Factor Profiles (% of factor total) from Base Run #1 (Convergent Run)

		Factor 1	Factor 2	Factor 3	Factor 4	Factor 5
1	PM2.5	81,25672091	95,1246	96,58955866	90,43362	92,12997974
1	Na	9,320809309	1,330561	0	0	0
1	Mg	0,616021079	0,095812	0,048321755	0,237449	0,296221809
1	P	0	0,075269	0,091277423	0,064323	0,075901469
1	K	1,326658356	0,173964	0,098369954	0,071047	0,432042866
1	Ca	2,777257905	0	0,725334713	3,766642	5,335945999
1	Sr	0,030339392	0,003301	0,00303269	0,02654	0,009396815
1	Zr	0,058252081	0,038113	0,029720982	0,044041	0,005416678
1	Ba	0,590423005	0	0	0,852617	0
1	Pb	0	0	0,083983613	0,427729	0,018850899
1	Al	3,597040772	1,567886	1,034164824	2,41077	0,900590412
1	Ti	0,046222247	0,042344	0,013909079	0,060742	0,057404349
1	V	0,001248351	0,001828	0	0	0,002773691
1	Cr	0,003427788	0,049779	0,001382296	0,003376	0,005451039
1	Mn	0,005349395	0,013487	0,007587638	0,016522	0,014769986
1	Fe	0,314826885	0,493341	0,206301751	0,25681	0,679622558
1	Ni	0	0,016062	0,009756483	0,002931	0,001641879
1	Cu	0,003536934	0,005447	0,003535475	0	0,003024568
1	Zn	0,032866974	0	0,134110664	0	0
1	Mo	0,003321725	0,098491	0,095887153	0,179737	0
1	S	0,015676894	0,869717	0,823764844	1,145101	0,030965243

	0,027338	0,036779	0,064337	0,021733	

	Sea-salt	Industrial e	Non-exhau	Exhaust	Mineral dust
Ca/Al	0,772095	0	0,701372	1,562423	5,92494205
Ti/Al	0,01285	0,027007	0,01345	0,025196	0,063740795
Mn/Al	0,001487	0,008602	0,007337	0,006854	0,016400336
Fe/Al	0,087524	0,314653	0,199486	0,106526	0,754641121
Zn/Al	0,009137	0	0,12968	0	0
Pb/Al	0	0	0,081209	0,177424	0,020931711
Zn/Pb	#DIV/0!	#DIV/0!	1,596867	0	0
V/Ni	#DIV/0!	0,113841	0	0	1,689338959
Mn/Fe	0,016992	0,027338	0,036779	0,064337	0,02173263
Fe/Ca	0,113359	#DIV/0!	0,284423	0,06818	0,127366836
Na/Mg	15,13067	13,88726	0	0	0
Na/Sr	307,2181	403,0305	0	0	0
Sr/Mg	0,049251	0,034457	0,06276	0,111774	0,031722224
K/Fe	4,21393	0,352625	0,476826	0,276653	0,635710014
k/Al					0,479732918

Factor Contributions (avg = 1) from Base Run #1 (Convergent Run)

		Factor 1	Factor 2	Factor 3	Factor 4	Factor 5
1	03/15/17 00:00	0,93715	1,4984	0,11435	-0,2	0,47951
1	03/18/17 00:00	0,52385	1,1434	2,858	-0,2	0,26622
1	03/21/17 00:00	0,99544	1,1193	2,3837	-0,08507	-0,02621
1	03/24/17 00:00	0,81526	1,8623	1,1277	0,53744	1,6621
1	03/27/17 00:00	0,78304	0,37965	1,5466	0,02531	0,4353
1	03/30/17 00:00	1,1348	0,65938	0,83198	-0,2	5,3051
1	04/05/17 00:00	0,98103	0,95328	1,4495	0,22683	0,31756
1	04/08/17 00:00	0,71112	2,0384	0,38657	0,002102	0,02629
1	04/11/17 00:00	0,25796	0,75311	1,2367	0,27056	0,8706
1	04/14/17 00:00	1,0213	1,1582	2,5707	0,063247	0,67492
1	04/17/17 00:00	1,1165	0,34443	2,7012	0,045225	0,60349
1	04/20/17 00:00	1,8487	1,5917	1,4327	0,026261	0,27075
1	04/23/17 00:00	1,4618	1,3573	1,0976	0,66658	0,55577
1	04/26/17 00:00	1,9763	0,52581	2,3063	0,22356	2,1654
1	04/29/17 00:00	1,1742	0,91238	0,96905	0,25254	0,48131
1	05/05/17 00:00	2,1851	0,7672	1,9837	0,49408	1,3727
1	05/08/17 00:00	1,3608	1,6652	0,7019	0,76625	0,70186
1	05/11/17 00:00	1,3589	1,563	0,86635	0,32125	1,8989
1	05/14/17 00:00	1,4202	1,965	0,74219	0,28068	1,656
1	05/17/17 00:00	2,0926	0,73193	1,9089	0,28978	0,96572
1	05/20/17 00:00	1,3359	1,5556	0,86396	0,87856	0,60757
1	05/23/17 00:00	1,4809	2,1739	1,3083	1,7182	-0,06721
1	05/26/17 00:00	1,3235	1,184	0,58105	1,1752	0,64791
1	06/04/17 00:00	1,6949	1,4638	1,1923	1,2203	0,64
1	06/07/17 00:00	1,1288	0,6624	0,67129	1,3721	0,53894
1	06/19/17 00:00	0,60801	0,26618	2,5335	0,082798	1,3506
1	06/25/17 00:00	0,7492	1,469	1,1391	0,29259	4,2639
1	06/28/17 00:00	1,0655	2,046	1,2757	-0,2	1,1016
1	07/07/17 00:00	1,054	1,9566	0,71997	0,58861	0,74941
1	07/10/17 00:00	0,56699	2,0862	0,17481	0,80526	1,3505
1	07/16/17 00:00	1,4164	0,87679	1,7157	-0,17947	0,49944
1	07/19/17 00:00	2,6392	1,0747	0,87465	1,0534	2,5299
1	07/22/17 00:00	2,2553	1,3368	1,2125	0,78214	4,273
1	07/25/17 00:00	2,3021	2,4626	0,40385	0,50698	0,45765
1	07/28/17 00:00	1,4236	1,6782	0,43323	1,2925	-0,00714
1	08/03/17 00:00	2,5532	1,3723	0,73031	1,2705	2,0465
1	08/06/17 00:00	3,3523	0,86483	0,48617	1,2684	2,4291
1	08/09/17 00:00	3,9549	0,51984	1,3022	0,95831	4,9371
1	08/12/17 00:00	3,0057	1,9693	0,48436	0,86339	1,3287
1	08/15/17 00:00	3,4636	1,031	0,86107	0,72388	0,65667
1	08/18/17 00:00	0,15934	1,1515	1,7025	-0,00011	1,9498
1	08/21/17 00:00	-0,15608	1,1172	1,6292	0,13028	1,679
1	08/27/17 00:00	0,1057	-0,03606	1,2073	1,5641	1,9938
1	08/30/17 00:00	-0,2	1,4111	1,253	0,85778	1,939
1	09/05/17 00:00	1,0341	0,49112	0,90837	1,1039	1,583
1	09/08/17 00:00	0,31234	1,5803	1,2149	0,60974	0,25427
1	09/11/17 00:00	0,42517	0,90328	0,24051	1,4741	0,66438
1	09/14/17 00:00	0,71059	1,2001	0,34979	1,0591	1,8876
1	09/17/17 00:00	1,0331	0,9081	1,6755	0,48258	2,2076
1	09/20/17 00:00	0,68132	0,3603	0,98283	0,70023	0,99901
1	09/23/17 00:00	0,55183	1,0662	0,55491	1,3409	2,261
1	09/26/17 00:00	0,4856	1,6144	1,035	0,74748	1,7224
1	09/29/17 00:00	0,5088	1,4314	1,0473	0,66025	0,76331
1	10/05/17 00:00	0,51793	1,6672	0,48331	0,80293	0,66176
1	10/08/17 00:00	0,72921	0,98718	0,98201	0,86858	0,92607

1	10/11/17 00:00	0,68027	1,0374	0,74918	1,1656	1,0979
1	10/14/17 00:00	-0,03952	0,35242	1,4791	1,1052	0,47947
1	10/17/17 00:00	-0,02238	0,24553	2,1811	0,68237	1,2991
1	10/20/17 00:00	0,88274	0,63216	0,99228	2,9001	1,5746
1	10/23/17 00:00	0,07709	-0,2	2,0167	0,56208	1,274
1	11/04/17 00:00	0,040628	-0,16409	1,4919	1,6077	1,5423
1	11/10/17 00:00	0,085167	-0,19811	-0,19126	1,5404	0,73106
1	11/13/17 00:00	0,26406	0,95832	1,0364	1,0262	0,3236
1	11/19/17 00:00	-0,2	1,9166	0,078076	1,2953	0,49822
1	11/25/17 00:00	0,015858	0,63012	1,5035	0,96284	0,76455
1	11/28/17 00:00	0,061548	0,021175	1,6593	0,93622	1,0309
1	12/04/17 00:00	0,51746	0,46225	2,3128	0,82172	0,51477
1	12/07/17 00:00	0,058561	1,2975	1,184	1,0909	0,4635
1	12/10/17 00:00	1,3456	1,2405	1,0868	1,4208	0,31263
1	12/13/17 00:00	1,051	1,1949	0,7524	1,437	0,33626
1	12/16/17 00:00	1,1221	1,5223	1,0653	1,4926	-0,2
1	12/19/17 00:00	1,2599	0,71255	1,4694	1,6694	0,13583
1	12/22/17 00:00	1,0803	1,5763	1,8078	1,116	0,029742
1	12/25/17 00:00	0,33827	0,86636	0,73815	1,8251	0,86499
1	12/28/17 00:00	0,082406	1,6535	0,25041	1,659	0,31853
1	01/03/18 00:00	0,22467	1,022	0,37087	1,8067	0,35138
1	01/06/18 00:00	0,34943	0,88891	0,36664	1,8487	0,48096
1	01/09/18 00:00	0,28235	0,97626	0,23797	1,9026	0,28217
1	01/12/18 00:00	0,4782	-0,05929	0,49506	1,7751	0,41457
1	01/15/18 00:00	0,20102	1,1394	-0,2	1,6911	0,31277
1	01/18/18 00:00	0,32572	0,80309	-0,2	2,031	0,3836
1	01/21/18 00:00	0,39137	0,35355	0,60927	1,5367	0,7286
1	01/24/18 00:00	1,3682	0,64605	0,47797	2,1517	0,47974
1	01/27/18 00:00	1,4218	-0,15233	-0,17412	2,356	0,50585
1	01/30/18 00:00	1,329	-0,2	0,7369	2,2032	0,40507
1	02/05/18 00:00	0,77747	-0,14064	-0,04998	1,3658	0,26728
1	02/08/18 00:00	1,1813	0,080923	-0,05342	2,4706	0,41848
1	02/11/18 00:00	1,0073	1,0197	-0,05395	1,9838	0,13387
1	02/14/18 00:00	0,96775	-0,02375	1,1387	1,4658	1,0745
1	02/17/18 00:00	0,92064	0,95505	0,57306	1,634	0,054568
1	02/20/18 00:00	1,2785	1,1944	0,35167	1,5977	0,10355
1	02/23/18 00:00	1,3466	0,90795	1,078	1,6581	0,071953
1	02/26/18 00:00	1,2241	1,0547	0,44765	1,8229	0,5492
1	03/04/18 00:00	1,7405	0,89931	0,67116	1,6301	1,1145

Residuals from Base Run #1 (Convergent Run)

Run	Date_Time	PM2.5	Na	Mg	P	K	Ca	Sr	Zr	Ba	Pb	Al	Ti
1	03/15/17 00:00	-4,07	-0,05485	0,01208	0,005458	0,08575	-0,07237	0,0002592	0,003892	-0,00467	-0,0005983	0,4276	0,001125
1	03/18/17 00:00	-1,936	0,09018	-0,01324	-0,01062	0,0143	0,06719	-0,00005964	0,001172	-0,00007522	0,02745	0,08263	-0,0002048
1	03/21/17 00:00	11,63	-0,01444	-0,00141	-0,006003	-0,0139	-0,01436	-0,0004487	-0,0001171	0,009584	-0,001144	0,02979	0,003512
1	03/24/17 00:00	27,04	-0,01874	0,06685	0,05123	-0,01103	0,0672	0,002248	0,003089	-0,01024	0,002174	0,02189	0,00225
1	03/27/17 00:00	62,34	0,0567	0,01857	0,01575	0,02185	0,282	0,002409	-0,001026	-0,004588	0,01664	0,009998	-0,001719
1	03/30/17 00:00	-22,27	-0,02023	0,1125	-0,004461	-0,04128	0,474	0,005707	0,003263	-0,002144	0,0001505	0,3124	0,001551
1	04/05/17 00:00	3,165	0,05929	0,03284	0,02419	0,000665	0,02658	0,002491	0,003654	-0,01084	-0,0003241	0,03288	0,0004746
1	04/08/17 00:00	22,25	0,01422	0,006437	0,01719	0,007019	-0,00883	0,001277	-0,003302	-0,0021	0,00004657	0,06702	-0,0008982
1	04/11/17 00:00	51,99	0,4125	0,009102	-0,01312	-0,00481	0,03849	0,00001064	0,00779	-0,002985	0,009372	0,2893	-0,001725
1	04/14/17 00:00	3,923	0,05374	0,01473	0,009763	-0,0201	0,8856	0,0004779	-0,0002651	-0,002386	0,06503	-0,00826	0,0002069
1	04/17/17 00:00	10,48	0,0033	0,000296	0,02791	-0,04197	0,8289	0,0003796	0,0002442	0,01345	-0,003715	0,0026	0,001053
1	04/20/17 00:00	4,7	0,07158	-0,02657	0,01459	-0,00186	0,135	-0,0003286	0,00473	0,03663	-0,001133	0,1068	-0,002288
1	04/23/17 00:00	43,02	0,09186	-0,00433	0,001015	0,0144	0,3883	-0,001248	0,0006806	0,008352	0,001189	0,0896	-0,001525
1	04/26/17 00:00	38,19	-0,01007	0,06875	-0,000405	-0,01025	0,2873	0,000733	-0,002907	0,001935	0,05279	-0,00673	0,002485
1	04/29/17 00:00	27,87	0,1073	0,007095	0,007562	-0,01193	-0,05552	-0,0006834	0,004671	-0,003018	-0,001237	0,181	0,001188
1	05/05/17 00:00	29,56	0,1766	0,007686	0,004539	0,01779	0,2153	-0,001613	0,0004391	-0,003278	0,002041	0,09044	-0,0004818
1	05/08/17 00:00	33,73	0,1988	-0,01027	-0,007404	-0,01971	0,1373	-0,001352	0,0002024	0,02989	-0,0007443	0,2325	-0,0006152
1	05/11/17 00:00	45,89	-0,09078	0,032	0,0256	-0,09164	-0,08337	-0,0005273	0,001058	0,02134	-0,002437	0,08276	0,0002928
1	05/14/17 00:00	22,73	-0,05073	0,01393	-0,002363	-0,08692	0,1266	-0,0008754	0,000484	0,02326	-0,001404	0,05739	0,0001943
1	05/17/17 00:00	-14,22	-0,09518	0,01627	0,01288	-0,00614	0,07991	0,0002669	0,0008624	0,01642	-0,001447	-0,07305	-0,003559
1	05/20/17 00:00	24,14	0,07752	0,007064	0,003181	-0,01537	-0,06252	-0,0009127	0,002431	0,009201	-0,003202	0,04052	0,003566
1	05/23/17 00:00	22,58	0,09913	0,03	0,09804	-0,01188	-0,0586	-0,0009227	-0,002136	0,03743	0,01154	-0,1417	0,04166
1	05/26/17 00:00	45,62	0,1004	0,0134	0,008913	-0,01661	-0,1821	-0,001128	0,00699	0,001577	0,00373	0,04404	-0,001518
1	06/04/17 00:00	17,81	0,05075	0,01481	0,003313	-0,02733	0,02905	-0,0007443	0,0004268	0,0133	0,01164	-0,00563	0,001022
1	06/07/17 00:00	2,972	0,3788	-0,00679	0,01075	-0,01766	-0,1117	-0,001249	0,003651	0,006032	-0,001618	0,1738	-0,001135
1	06/19/17 00:00	3,289	0,02311	0,0376	0,001165	-0,02192	-0,01661	0,0008032	0,004635	-0,003754	0,00457	0,01928	-0,0008787
1	06/25/17 00:00	-36,99	0,1658	0,06192	-0,007947	-0,01907	0,1907	0,0003277	0,006408	-0,008481	0,01468	0,3937	0,01328
1	06/28/17 00:00	78,34	0,08769	0,04702	-0,000594	0,03146	0,04044	0,001734	0,004279	-0,005644	0,02189	0,00095	-0,002848
1	07/07/17 00:00	-5,056	0,000823	0,004544	-0,00123	0,06159	-0,05849	-0,0006862	0,005047	-0,01194	0,008909	0,115	-0,00008829
1	07/10/17 00:00	51,05	0,2545	0,01882	0,00208	-0,0381	0,135	-0,0003344	0,00874	-0,00716	0,0002751	0,1938	0,001201
1	07/16/17 00:00	69,4	-0,1073	0,008939	-0,009534	-0,02031	0,675	0,001897	-0,0007376	-0,0008258	0,0214	0,007954	-0,00003978
1	07/19/17 00:00	55,85	-0,171	-0,01075	0,001096	0,03074	0,1322	-0,001012	0,0008456	0,05203	-0,0001615	0,06073	0,004528
1	07/22/17 00:00	18,04	0,1028	0,04356	0,03822	-0,09108	-0,3608	0,0009016	-0,007434	0,05252	0,001513	0,1078	0,00973
1	07/25/17 00:00	11,24	0,01169	-0,02649	0,008334	0,06199	-0,1176	-0,0001183	0,001272	0,1178	-0,0004217	0,0659	0,002896
1	07/28/17 00:00	-7,133	0,1612	0,004338	-0,000104	-0,03554	-0,02191	-0,0001828	0,002555	0,04308	0,003147	-0,01281	0,001873
1	08/03/17 00:00	72,77	0,06322	-0,01947	-0,007799	0,2364	-0,2896	-0,0007474	0,00139	0,1482	0,01629	0,1258	0,02602
1	08/06/17 00:00	33,27	-0,2454	0,008338	-0,006536	-0,01295	-0,1209	-0,001203	-0,0005487	0,1019	-0,003772	0,04293	0,004594
1	08/09/17 00:00	-13,81	-0,8386	-0,0139	-0,002781	-0,06627	-0,6133	-0,003234	-0,004291	0,03214	-0,00101	-0,07747	0,008019
1	08/12/17 00:00	-20,37	-0,2586	0,03806	-0,006557	-0,02121	-0,2414	0,0001774	0,0008734	0,1361	-0,0005509	0,05005	0,007626
1	08/15/17 00:00	19,5	0,03069	0,08036	0,002471	0,1055	-0,1098	0,001723	0,001767	0,2547	-0,003012	0,04884	0,008728
1	08/18/17 00:00	-1,901	-0,01914	0,003432	-0,001776	0,02168	-0,2299	0,001444	0,0002085	0,1312	-0,00205	0,04971	0,00003203
1	08/21/17 00:00	9,941	-0,000402	0,01021	0,002997	-0,00402	-0,04198	0,0005146	0,0000322	0,07281	-0,002826	0,006678	0,0000444
1	08/27/17 00:00	21,06	-0,000289	0,01068	0,02508	0,02593	-0,1513	-0,0002863	-0,0004163	-0,0002201	0,01463	-0,04539	-0,001388
1	08/30/17 00:00	38,03	-0,001085	-0,00129	0,006	0,002101	0,1059	-0,0004875	-0,0004018	-0,002707	0,02243	0,009763	0,04132
1	09/05/17 00:00	13,15	0,0771	-0,00358	0,008826	0,0547	-0,08413	0,00005036	-0,001678	0,132	-0,001341	-0,1398	0,000436
1	09/08/17 00:00	-4,059	0,01511	-0,01181	0,01647	0,1126	1,364	0,000977	-0,002021	0,02288	-0,004142	-0,05729	0,0007834
1	09/11/17 00:00	39,75	0,02423	-0,01848	0,005762	0,02368	0,2894	0,002757	0,0000864	-0,005784	-0,005809	-0,06589	0,001426
1	09/14/17 00:00	41,27	0,09601	-0,01316	-0,00138	0,02104	0,6569	0,004079	-0,003109	0,02133	-0,000946	-0,1292	0,001866
1	09/17/17 00:00	15,62	0,04634	0,001616	0,006309	0,02611	-0,00898	0,001274	-0,002069	0,1426	-0,0004492	-0,1887	-0,001687
1	09/20/17 00:00	0,411	0,07573	-0,01616	0,01294	0,03289	-0,07155	-0,0001883	-0,002169	0,03725	-0,004848	-0,04634	0,00187
1	09/23/17 00:00	33,57	0,02376	-0,01221	0,01096	0,02711	0,216	-0,0006525	-0,001657	0,01872	0,07606	-0,1084	0,002398
1	09/26/17 00:00	30,42	0,07278	-0,02601	0,001967	0,06234	0,3903	-0,0005927	-0,001968	0,06552	0,002519	-0,0587	0,0006214
1	09/29/17 00:00	26,23	0,001827	-0,0135	-0,000721	0,04913	0,0931	0,0004393	-0,0009393	0,07603	0,001195	-0,08934	0,0007657
1	10/05/17 00:00	39,09	0,04749	-0,0197	-0,003565	0,06215	0,1173	0,0001768	-0,0008289	0,06107	0,0007663	-0,05962	-0,001609
1	10/08/17 00:00	21,69	-0,01056	-0,00791	-0,002782	0,04228	0,0561	0,0003938	-0,001655	0,02592	-0,003535	-0,1217	-0,0009657
1	10/11/17 00:00	25,88	-0,03727	0,003348	0,000509	0,03118	0,4523	0,0006472	-0,0008919	0,029	-0,003379	-0,1392	-0,002187
1	10/14/17 00:00	25,38	0,000223	-0,00729	0,00373	0,002988	-0,1742	-0,0005824	0,001464	0,02186	0,007772	0,04868	0,002915
1	10/17/17 00:00	12,17	-0,000283	-0,00463	-0,002843	0,02376	0,1398	-0,0000786	0,000005231	0,0008341	0,05395	0,02067	-0,001642
1	10/20/17 00:00	-8,841	-0,04539	0,05577	0,07084	0,1261	-0,4477	0,00007297	0,009372	-0,01211	-0,008971	0,1935	0,002834
1	10/23/17 00:00	39,77	-0,000506	0,02016	0,004745	0,02323	-0,1725	0,00008933	0,002382	-0,004095	0,001854	0,03313	-0,001166
1	11/04/17 00:00	43,78	-0,000441	0,001011	-0,002724	0,03176	-0,2973	-0,0001256	0,0008547	0,005878	-0,0006208	0,04724	0,00145
1	11/10/17 00:00	32,83	0,00012	-0,00135	0,01582	-0,00191	-0,4552	-0,0005496	0,005931	0,01313	-0,009605	0,1554	0,0002368
1	11/13/17 00:00	6,115	-0,01396	0,02437	0,007664	0,05799	0,01804	-0,0003432	0,00005458	0,001394	0,003572	-0,03648	0,0003291
1	11/19/17 00:00	-3,96	-0,000779	-0,00181	0,00461	0,001712	0,03344	0,00008821	0,0008729	-0,005114	0,006555	0,01032	-0,001129
1	11/25/17 00:00	29,67	0,005369	0,01062	0,000459	-0,01591	0,4771	-0,0006282	-0,0004075	0,003999	0,001726	0,03559	0,00236
1	11/28/17 00:00	-3,973	0,001426	-0,00104	-0,003545	-0,02829	-0,07972	-0,001356	0,001114	-0,004757	0,002301	0,05023	0,003667
1	12/04/17 00:00	-15,88	-0,04273	0,000848	-0,004911	0,02966	-0,07829	0,0008064	-0,0004935	0,06159	-0,005383	-0,04161	0,005308
1	12/07/17 00:00	-11,77	-0,006866	0,02639	-0,0068	0,001472	-0,08482	-0,0002071	-0,001572	0,01665	0,04528	-0,0051	-0,00127
1	12/10/17 00:00	0,5968	-0,07352	0,0183	-0,000305	0,01692	0,2234	-0,0001776	-0,0009277	0,007855	0,004166	-0,06564	-0,001588
1	12/13/17 00:00	-2,27	-0,09135	0,02011	-0,000694	0,000556	-0,1524	-0,00005146	0,0006795	0,007358	0,01026	0,02708	0,0001256
1	12/16/17 00:00	-10,27	-0,1198	0,03653	-0,003554	-0,01636	-0,1248	0,001392	0,0005292	0,06466	-0,0006627	0,01184	0,004604
1	12/19/17 00:00	-4,286	-0,04884	0,03252	-0,001063	0,009203	-0,1513	0,0004769	0,0008289	-0,01847	0,01744	-0,04209	0,000653
1	12/22/17 00:00	-12,09	-0,01194	0,02593	0,004575	0,1342	0,09094	0,002035	-0,001409	-0,01796	0,01696	-0,1096	-0,0009567
1	12/25/17 00:00	-8,947	0,01929	0,008429	-0,01238	-0,0113	0,1043	0,0001457	0,001058	-0,01859	0,0146	-0,02614	-0,000551
1	12/28/17 00:00	-5,607	-0,004404	0,01864	0,001948	-0,00232	0,3177	0,0001043	0,000719	-0,00735	-0,005002	0,003362	0,000751
1	01/03/18 00:00	3,182	0,03697	0,008876	0,003272	-0,01063	-0,0687	-0,00008232	0,001371	-0,01823	0,02695	0,005484	0,0007872
1	01/06/18 00:00	0,05739	-0,005696	0,02591	-0,003885	-0,01119	0,411	0,0009901	0,0003689	0,001704	-0,01102	0,0235	0,0004763
1	01/09/18 00:00	21,07	-0,01621	0,008444	-0,005123	0,006241	0,05998	0,000009436	0,0001428	-0,01949	0,04022	0,05248	0,00162
1	01/12/18 00:00	-5,161	0,04094	-0,00738	0,006168	-0,00348	0,04168	-0,0002956	0,002847	-0,02026	-0,004954	0,04081	0,000402
1	01/15/18 00:00	36,58	0,01073	-0,00423	-0,001064	-0,00178	-0,00994	0,000004937	0,001608	-0,01078	0,05484	0,08785	-0,0009427
1	01/18/18 00:00	28,38	0,03681	0,002236	-0,00368	-0,00667	0,006195	0,0000327	0,001597	-0,003941	-0,006786	0,03639	-0,00008472
1	01/21/18 00:00	-4,688	0,02878	0,007989	-0,000441	-0,00863	1,959	0,0004758	-0,0006952	-0,01292	0,004238	0,03334	-0,001379
1	01/24/18 00:00	9,595	-0,05034	0,004694	-0,002844	0,01427	0,4099	0,002002	-0,003388	0,05133	0,02437	-0,09571	-0,001875
1	01/27/18 00:00	-6,27	-0,06932	-0,00828	0,008935	0,02036	0,008471	0,001655	0,0009627	0,05739	-0,02786	-0,05733	-0,000326
1	01/30/18 00:00	6,511	0,006348	-0,01016	-5,92E-05	0,04438	0,4258	0,001188	-0,001799	0,02819	0,03804	-0,04746	-0,002385
1	02/05/18 00:00	35,13	-0,04091	-0,00594	-0,001771	-0,01771	0,5851	0,002187	0,001661	-0,0006192	0,03566	0,02271	0,000147
1	02/08/18 00:00	5,379	0,1313	-0,02188	0,008141	0,1521	0,2932	0,001131	0,0009531	-0,06015	0,002713	-0,0016	-0,002772
1	02/11/18 00:00	20,14	-0,1166	0,00423	0,003422	0,03967	0,9804	0,002137	0,0004589	-0,01321	-0,004365	-0,00361	-0,0008573
1	02/14/18 00:00	18,42	-0,03518	-0,00727	-0,001207	0,000811	0,6586	0,002187	0,0006734	-0,005055	-0,006148	-0,00019	0,0008265
1	02/17/18 00:00	1,853	-0,0978	0,001895	-0,001205	0,03123	0,6736	0,001657	0,0001372	-0,01362	-0,0006923	0,004287	-0,0002089
1	02/20/18 00:00	-7,676	-0,1772	0,00324	-0,01016	0,04731	0,764	0,001596	-0,0007021	-0,003264	-0,004293	0,07011	-0,0004039
1	02/23/18 00:00	-12,86	-0,1184	-0,00076	-0,006095	0,0645	0,4741	0,001549	-0,002228	-0,01052	-0,002218	-0,00247	-0,0002954
1	02/26/18 00:00	7,559	-0,09916	-0,00447	-0,01007	0,04341	0,8715	0,001363	-0,001048	-0,01989	0,00653	0,05967	0,0014
1	03/04/18 00:00	20,65	-0,241	0,002864	-0,0119	0,06041	0,5656	0,001803	-0,00143	0,0172	-0,007989	0,09138	0,002049

Run	Date_Time	V	Cr	Mn	Fe	Ni	Cu	Zn	Mo	S
1	03/15/17 00:00	0,0001065	-0,001698	0,004076	0,12	0,00616	0,004531	0,03538	-0,00005231	0,09607
1	03/18/17 00:00	0,00000827	0,0005516	-0,000209	0,07324	-0,00058	0,0001559	0,02187	-0,001307	-0,06822
1	03/21/17 00:00	0,0007892	-0,0004197	0,0004173	0,08809	0,0007238	0,004191	0,008805	-0,001676	-0,06955
1	03/24/17 00:00	-0,0001601	0,0008296	-0,0008115	-0,01014	-0,0001159	0,004178	-0,0008698	0,001917	-0,1108
1	03/27/17 00:00	-0,00001332	0,00005092	-0,0001862	-0,01585	0,0002127	0,0002787	-0,004328	0,008284	0,02247
1	03/30/17 00:00	-0,0006151	0,0008476	0,0009255	-0,03855	0,005615	-0,0001156	0,001443	-0,001432	0,4386
1	04/05/17 00:00	-0,00004539	-0,0006442	0,00008354	-0,0056	0,0002263	0,0009955	-0,005165	0,01173	0,1406
1	04/08/17 00:00	0,0001343	-0,001014	0,0002379	-0,01769	-0,00008617	0,005849	-0,0002962	0,01026	0,06178
1	04/11/17 00:00	0,0001088	-0,0003822	-0,0006759	0,01476	0,00134	0,00009235	-0,002146	0,01532	0,01967
1	04/14/17 00:00	-0,00004998	0,0001255	-0,00006776	0,004683	0,0003653	0,01091	-0,002312	-0,003427	0,001676
1	04/17/17 00:00	-0,0000321	0,00006376	0,0002625	0,04565	-0,0002078	0,0003875	0,02092	-0,003993	0,03012
1	04/20/17 00:00	0,00003212	-0,001134	0,0001686	0,00196	0,0005794	0,003571	-0,003096	0,006969	-0,00257
1	04/23/17 00:00	-0,00005017	0,0007903	-0,0003156	0,0117	-0,00008643	0,00184	-0,0001827	0,0007916	-0,03792
1	04/26/17 00:00	-0,0001245	0,001028	-0,0005937	0,01255	-0,0004448	-0,00006358	0,02088	-0,003561	0,07612
1	04/29/17 00:00	-0,00001246	-0,0008994	0,0004468	0,01872	0,0001202	-0,0002504	-0,002744	0,00895	0,02226
1	05/05/17 00:00	-0,00008423	0,0004618	-0,0002403	0,03214	-0,0004253	0,0001869	0,0005569	0,0006961	-0,01042
1	05/08/17 00:00	0,00008777	-0,0004563	-0,00002252	0,01905	0,0000029	-0,0001338	0,0002192	0,002156	-0,0062
1	05/11/17 00:00	0,0003934	-0,0009897	-0,0004185	0,002903	-0,0001707	-0,0001982	-0,0003694	0,00384	0,08766
1	05/14/17 00:00	-0,000008628	-0,0003558	-0,0005369	0,1067	-0,0002345	0,01507	0,0001784	0,001022	0,07045
1	05/17/17 00:00	0,000008013	0,000168	0,00004593	0,1366	-0,0000292	-0,0002673	0,0007198	0,00951	-0,08285
1	05/20/17 00:00	0,0001024	-0,001628	-0,000297	-0,00226	0,0008278	0,007433	-0,001612	0,005273	0,1135
1	05/23/17 00:00	0,0004272	0,0003695	0,04363	5,233	0,00001837	0,002216	0,03697	-0,01638	0,004244
1	05/26/17 00:00	0,0003701	-0,0006704	0,000196	0,01966	-0,0002781	0,01425	-0,0004007	-0,0009132	0,0778
1	06/04/17 00:00	-0,00002725	0,002096	-0,0005027	0,01265	-0,0001144	0,0005137	0,002528	-0,007112	-0,1451
1	06/07/17 00:00	0,0001218	-0,000761	0,0002664	0,01169	0,000747	0,01434	-0,001678	0,00155	0,09903
1	06/19/17 00:00	0,0001287	0,0001649	-0,0001656	-0,03565	-0,0007738	0,002338	0,001294	0,001149	0,1215
1	06/25/17 00:00	-0,00001578	0,0002734	0,0002343	0,08431	-0,0005074	0,0007956	-0,0005327	0,007222	-0,08126
1	06/28/17 00:00	0,0001155	-0,000857	-0,0001338	-0,05116	-0,00001797	0,00342	-0,002532	0,005195	0,05024
1	07/07/17 00:00	-0,00007651	0,001252	0,0006212	0,03052	-0,0003759	0,005665	-0,0001749	-0,0005994	-0,09026
1	07/10/17 00:00	0,0005366	-0,001913	0,000128	-0,00824	0,000749	0,0001254	-0,00009179	0,003007	-0,03307
1	07/16/17 00:00	-0,00003483	0,001321	-0,0002719	0,003526	0,001068	0,0002004	0,01814	-0,004415	-0,04061
1	07/19/17 00:00	-0,0001671	0,0006192	-0,00006773	0,03459	0,0000577	0,004641	0,0008554	-0,00229	-0,04934
1	07/22/17 00:00	0,0005016	0,000932	-0,00007924	0,06145	0,00073	-0,0003156	0,00253	-0,00433	-0,03886
1	07/25/17 00:00	0,0005455	-0,002145	0,001379	0,01131	0,004489	0,002205	-0,0005301	-0,0006927	0,01315
1	07/28/17 00:00	0,00004065	0,0003665	-0,0002449	0,01491	0,000165	-0,0003925	0,0006701	-0,007539	0,01595
1	08/03/17 00:00	0,000172	0,0007017	0,001284	0,03069	0,004525	-0,0002115	0,001442	-0,004305	-0,0589
1	08/06/17 00:00	0,0003739	-0,0006655	0,0002622	0,02159	0,0001955	0,002028	-0,0006878	0,001601	0,05558
1	08/09/17 00:00	-0,0001154	0,0003516	0,00107	0,03333	-0,0000167	-0,0008174	0,002256	0,002063	-0,05801
1	08/12/17 00:00	0,00006869	-0,0009703	0,001335	0,0813	0,003194	-0,0006408	0,0002035	-0,000553	0,3568
1	08/15/17 00:00	-0,00002073	-0,0007725	0,0006927	-0,00898	0,000357	-0,00055	-0,001929	0,006682	-0,01214
1	08/18/17 00:00	0,000882	0,000322	0,0001276	0,01026	-0,0006134	-0,0003783	0,00177	0,004843	0,03648
1	08/21/17 00:00	0,000006242	0,000001161	-0,00003716	-0,0241	0,0003034	-0,0005738	0,0008279	0,0041	-0,0229
1	08/27/17 00:00	-0,00003581	0,005402	-0,0001809	-0,00903	-0,0000291	0,0004789	-0,0002982	-0,0004609	-0,02863
1	08/30/17 00:00	0,0008927	0,003168	-0,0004184	-0,01285	-0,0001659	0,0001261	-0,0007732	-0,0009251	0,04308
1	09/05/17 00:00	0,00003829	-0,0001397	0,0002336	-0,01511	0,00006859	-0,00005841	-0,0006576	0,004615	0,0571
1	09/08/17 00:00	0,0001321	0,0009693	0,0003738	-0,01347	-0,0004933	0,001018	0,005095	-0,001354	0,1139
1	09/11/17 00:00	-0,0000535	-0,0005897	0,0002472	0,01418	0,0006062	0,0004915	-0,0002234	0,00213	0,1946
1	09/14/17 00:00	-0,0000512	0,0005938	-0,0002567	-0,0116	0,000522	0,0001979	0,0001586	0,002687	0,2369
1	09/17/17 00:00	0,00009625	0,001257	-0,0001757	-0,01752	-0,0005775	0,0007533	0,003896	0,002072	0,1567
1	09/20/17 00:00	-0,00003671	-0,0002918	0,001069	0,0541	0,000688	0,001355	-0,001667	0,008338	0,2426
1	09/23/17 00:00	-0,0001461	0,00122	-0,0003958	0,08108	-0,0002141	0,001287	0,0002268	-0,002953	0,1027
1	09/26/17 00:00	-0,00003051	-0,0001242	0,00005401	0,03965	0,0002445	0,001059	-0,0002419	-0,0007744	0,05638
1	09/29/17 00:00	0,0001731	0,0009997	-0,0002799	-0,03173	-0,00004931	0,001021	0,0009769	0,001458	0,008613
1	10/05/17 00:00	0,0001972	-0,000009988	-0,0002371	0,002837	-0,000162	0,002057	0,00001745	0,001823	0,1345
1	10/08/17 00:00	0,00002066	-0,000262	0,0002097	-0,009	0,0008433	0,001749	-0,0002951	0,002637	0,05324
1	10/11/17 00:00	0,0001192	0,001408	-0,0004668	-0,0379	-0,00006304	0,001651	0,01585	0,00135	0,06257
1	10/14/17 00:00	0,000281	-0,0003291	0,001029	0,0312	0,005636	0,01695	-0,002092	0,001093	-0,02893
1	10/17/17 00:00	0,00005856	0,0001414	-0,0003308	-0,02457	-0,0003274	0,000509	0,002828	-0,0008155	0,1049
1	10/20/17 00:00	-0,00005122	-0,0003631	0,002186	0,04967	0,004157	0,002071	-0,0009205	0,03169	0,1283
1	10/23/17 00:00	0,00003052	-0,00001598	0,0004217	-0,02397	0,0003029	0,0007321	-0,007171	0,007867	0,04089
1	11/04/17 00:00	-0,00002655	-0,00002201	-0,0003678	0,04319	0,0002828	0,0003696	-0,00197	-0,002417	-0,01448
1	11/10/17 00:00	-0,00001099	-0,00001162	0,001038	0,0174	0,001701	0,0003349	-0,002133	0,01286	0,04403
1	11/13/17 00:00	-0,0000122	0,001922	0,00006189	-0,01745	-0,0001769	-0,000132	0,001424	-0,0007777	-0,07022
1	11/19/17 00:00	0,00003844	0,0005747	-0,00007918	-0,01874	0,003006	0,00003351	-0,000003007	-0,001293	-0,01263
1	11/25/17 00:00	-0,00003744	0,006638	0,0005679	0,05534	-0,00001481	0,0001099	0,002562	-0,003953	-0,06865
1	11/28/17 00:00	0,00004357	-0,0000856	0,0005133	0,06985	0,0002837	0,0002696	-0,003175	0,002561	-0,00442
1	12/04/17 00:00	-0,00002803	0,0001499	0,001199	0,1179	-0,00008631	0,0002123	0,008971	-0,0002983	-0,06035
1	12/07/17 00:00	0,00001937	-0,00001757	0,0001544	0,02132	0,0008533	0,0001768	0,001396	-0,003828	0,02384
1	12/10/17 00:00	-0,00005285	0,002265	-0,0001965	0,005163	0,0001139	0,0002178	0,0009973	-0,004922	-0,03074
1	12/13/17 00:00	0,00009283	0,001181	-0,00006434	0,004386	-0,0004757	-0,00005145	0,001948	-0,002517	-0,02729
1	12/16/17 00:00	0,0000032	0,001674	0,00007335	0,05708	-0,0006899	-0,0001182	0,007721	-0,005265	-0,02809
1	12/19/17 00:00	0,00001305	-0,000328	-0,00006426	0,009723	0,0003349	0,0002211	-0,001861	-0,001748	0,02258
1	12/22/17 00:00	-0,00004958	0,003272	-0,0006207	0,01169	0,0005664	0,002773	-0,0006888	-0,007949	0,06909
1	12/25/17 00:00	-0,00003928	0,0239	0,0008154	0,06711	0,01168	0,0008844	0,00009264	0,0005457	-0,04346
1	12/28/17 00:00	-0,00007888	0,002878	-0,0001997	0,0166	0,001035	-0,0002378	-0,00001667	-0,001718	-0,09271
1	01/03/18 00:00	0,00002776	-0,0008202	-0,00005274	0,01433	0,0006548	-0,00005749	-0,0002136	-0,0007197	-0,04858
1	01/06/18 00:00	-0,00004209	0,001711	-0,00008672	0,009868	-0,0001217	-0,000239	0,0003111	-0,001778	-0,02534
1	01/09/18 00:00	-0,00003752	0,001466	0,00004488	0,003434	-0,0001369	-0,0000737	0,0000357	-0,001141	-0,03834
1	01/12/18 00:00	0,00001044	-0,00001685	0,0003802	0,004223	0,001067	-0,0002043	-0,000236	0,00422	0,009295
1	01/15/18 00:00	0,00001601	0,0001034	-0,000006493	0,006895	-0,0002361	0,0001442	-0,0002106	0,002652	-0,0031
1	01/18/18 00:00	0,000258	-0,0005538	0,000139	-0,00191	0,0001559	-0,00002231	-0,000449	0,001096	0,00772
1	01/21/18 00:00	0,0001263	-0,00006874	0,0001182	-0,00866	0,0004747	-0,0003839	0,02041	0,001898	-0,0048
1	01/24/18 00:00	0,000007002	0,002189	-0,0005021	-0,01808	-0,00008958	0,001518	0,001472	-0,004164	-0,02463
1	01/27/18 00:00	0,00002711	-0,00001464	0,00005659	-0,01402	0,001286	0,001006	-0,00001567	0,005682	-0,00251
1	01/30/18 00:00	0,00003229	-0,00001684	-0,0003799	-0,01854	0,0004725	0,00112	-0,001148	-0,004653	0,03892
1	02/05/18 00:00	0,000009504	0,00003083	-0,0003244	0,002852	-0,0000175	0,0009591	0,0001583	-0,0007782	0,1338
1	02/08/18 00:00	-0,000009559	-0,00004541	-0,0001255	0,01324	0,001403	0,0009172	-0,0000521	0,002841	-0,01054
1	02/11/18 00:00	-0,000005032	0,0007838	-0,0001413	-0,01507	-0,000105	0,00009569	0,09644	0,0007721	0,03995
1	02/14/18 00:00	0,00002476	0,004048	-0,0005929	-0,02407	-0,00007013	0,0001544	0,02233	0,002157	0,04853
1	02/17/18 00:00	-0,00001937	0,001581	0,0001381	-0,00736	-0,0001973	0,00006726	0,000424	0,00000112	-0,04123
1	02/20/18 00:00	-0,00002215	0,001121	0,000002143	0,001269	-0,00006592	-0,00003631	0,000311	0,004748	-0,02676
1	02/23/18 00:00	-0,00001951	0,001937	0,0002387	-0,01837	-0,0001296	0,00006223	0,002527	-0,0008325	0,03853
1	02/26/18 00:00	0,00004841	0,0008931	-0,000418	-0,02366	-0,0001592	0,0007851	0,0004355	0,001573	0,03401
1	03/04/18 00:00	-0,00007525	0,001391	-0,0001198	-0,0079	-0,0001541	-0,0002519	0,001481	0,004495	-0,01481

Scaled Residuals from Base Run #1 (Convergent Run)

Run	Date_Time	PM2.5	Na	Mg	P	K	Ca	Sr	Zr	Ba	Pb	Al	Ti
1	03/15/17 00:00	-0,512	-0,506	1,045	0,885	2,623	-1,383	0,609	2,13	-1,304	-0,862	1,604	0,65
1	03/18/17 00:00	-0,111	1,081	-2,387	-1,637	0,799	0,943	-0,188	0,541	-0,043	2,015	0,852	-0,136
1	03/21/17 00:00	0,531	-0,126	-0,157	-0,944	-0,787	-0,305	-1,191	-0,056	1,361	-0,486	0,303	1,773
1	03/24/17 00:00	0,779	-0,175	2,428	1,236	-0,403	0,319	2,008	1,163	-1,241	0,48	0,177	0,597
1	03/27/17 00:00	1,512	0,612	1,599	2,061	1,059	2,339	1,561	-0,844	-1,01	1,801	0,141	-1,608
1	03/30/17 00:00	-0,984	-0,168	0,74	-0,481	-0,832	0,279	0,931	1,469	-0,413	0,083	1,643	0,252
1	04/05/17 00:00	0,2	0,488	2,114	1,367	0,032	0,314	1,381	1,568	-1,65	-0,116	0,35	0,269
1	04/08/17 00:00	1,059	0,136	0,774	2,329	0,432	-0,332	1,224	-1,633	-0,493	0,088	0,81	-0,674
1	04/11/17 00:00	1,382	2,078	0,947	-2,282	-0,374	0,343	0,028	1,631	-0,832	2,157	1,353	-1,163
1	04/14/17 00:00	0,171	0,421	0,955	1,125	-0,896	1,176	0,702	-0,115	-0,357	1,652	-0,075	0,09
1	04/17/17 00:00	0,442	0,028	0,023	1,341	-2,258	1,727	0,579	0,115	1,416	-1,195	0,025	0,519
1	04/20/17 00:00	0,233	0,326	-2,154	1,812	-0,056	1,176	-0,454	1,473	2,102	-0,638	0,74	-1,196
1	04/23/17 00:00	1,138	0,509	-0,279	0,151	0,454	2,079	-1,918	0,281	0,514	0,261	0,653	-0,656
1	04/26/17 00:00	0,839	-0,049	0,628	-0,049	-0,221	0,892	0,58	-1,26	0,131	1,452	-0,042	0,584
1	04/29/17 00:00	1,191	0,729	0,529	1,116	-0,546	-0,63	-1,373	1,943	-0,329	-0,553	1,527	0,585
1	05/05/17 00:00	0,766	0,689	0,3	0,564	0,37	0,842	-1,743	0,148	-0,186	0,387	0,515	-0,143
1	05/08/17 00:00	1,007	1,04	-0,686	-1,217	-0,748	0,867	-2,093	0,088	1,518	-0,174	1,462	-0,229
1	05/11/17 00:00	1,049	-0,622	1,231	1,23	-1,938	-0,39	-0,631	0,446	1,464	-0,916	0,576	0,08
1	05/14/17 00:00	0,694	-0,309	0,611	-0,332	-1,802	0,567	-1,144	0,201	1,561	-0,581	0,401	0,054
1	05/17/17 00:00	-0,942	-0,463	0,686	1,521	-0,153	0,423	0,253	0,309	0,902	-0,396	-0,543	-1,511
1	05/20/17 00:00	0,828	0,459	0,41	0,458	-0,59	-0,498	-1,264	0,902	0,529	-0,704	0,31	1,097
1	05/23/17 00:00	0,704	0,506	1,404	1,626	-0,451	-0,54	-0,99	-0,743	1,258	1,077	-1,026	1,479
1	05/26/17 00:00	1,213	0,607	0,729	1,245	-0,663	-1,531	-1,514	2,17	0,084	0,571	0,344	-0,613
1	06/04/17 00:00	0,606	0,255	0,678	0,452	-0,908	0,172	-0,766	0,149	0,573	1,345	-0,038	0,309
1	06/07/17 00:00	0,186	2,108	-0,503	1,504	-0,856	-0,911	-1,827	1,468	0,304	-0,243	1,289	-0,513
1	06/19/17 00:00	0,153	0,338	2,042	0,152	-1,14	-0,102	1,203	1,903	-0,925	1,007	0,208	-0,407
1	06/25/17 00:00	-2,41	1,357	0,545	-0,897	-0,448	0,143	0,29	2,089	-1,408	2,385	0,644	0,591
1	06/28/17 00:00	1,393	0,581	2,132	-0,085	0,94	0,291	2,03	1,551	-1,334	1,778	0,009	-1,254
1	07/07/17 00:00	-0,328	0,006	0,297	-0,188	1,763	-0,498	-1,111	1,735	-1,199	1,787	0,878	-0,033
1	07/10/17 00:00	1,227	2,007	1,081	0,297	-2,235	0,724	-0,52	1,396	-0,756	0,066	1,463	0,366
1	07/16/17 00:00	1,437	-0,774	0,603	-1,644	-0,819	1,706	2,152	-0,397	-0,113	2,288	0,078	-0,022
1	07/19/17 00:00	1,012	-0,673	-0,333	0,136	0,16	0,361	-0,697	0,255	1,55	-0,025	0,097	0,791
1	07/22/17 00:00	0,39	0,394	0,314	0,836	-1,706	-0,283	0,164	-1,752	1,819	0,237	0,157	0,408
1	07/25/17 00:00	0,448	0,043	-1,504	1,153	1,212	-1,031	-0,113	0,405	1,61	-0,153	0,387	0,803
1	07/28/17 00:00	-0,607	0,84	0,284	-0,017	-1,783	-0,238	-0,212	0,924	1,62	0,479	-0,104	0,689
1	08/03/17 00:00	1,183	0,074	-0,675	-1,135	0,868	-1,09	-0,514	0,134	1,002	1,726	0,194	0,996
1	08/06/17 00:00	0,75	-0,263	0,071	-0,96	-0,065	-0,35	-0,24	-0,163	0,717	-0,604	0,063	0,776
1	08/09/17 00:00	-0,371	-1,01	-0,09	-0,278	-0,261	-0,406	-0,571	-0,412	0,844	-0,143	-0,096	0,301
1	08/12/17 00:00	-1,27	-0,296	0,348	-1,009	-0,392	-1,171	0,116	0,081	0,968	-0,119	0,08	1,392
1	08/15/17 00:00	0,635	0,028	0,645	0,38	0,479	-0,61	0,327	0,162	0,435	-0,768	0,081	1,83
1	08/18/17 00:00	-0,096	-0,616	0,256	-0,234	0,9	-1,464	2,109	0,136	2,162	-0,867	0,551	0,011
1	08/21/17 00:00	0,428	-0,075	0,906	0,38	-0,289	-0,268	1,191	0,025	2,201	-1,071	0,096	0,018
1	08/27/17 00:00	0,73	-0,026	0,65	2,435	1,161	-0,672	-0,374	-0,302	-0,016	1,328	-0,541	-0,48
1	08/30/17 00:00	0,982	-0,205	-0,105	0,698	0,127	0,474	-0,982	-0,264	-0,471	2,443	0,109	0,491
1	09/05/17 00:00	0,527	0,63	-0,202	1,129	1,471	-0,407	0,054	-1,03	1,247	-0,218	-1,499	0,138
1	09/08/17 00:00	-0,324	0,261	-2,116	2,004	1,313	1,673	1,733	-1,444	2,143	-1,161	-0,808	0,409
1	09/11/17 00:00	1,282	0,403	-2,328	0,87	1,338	1,681	2,523	0,058	-0,398	-0,97	-0,889	0,581
1	09/14/17 00:00	1,074	0,925	-0,828	-0,2	0,695	2,008	1,382	-2,41	1,268	-0,174	-1,431	0,503
1	09/17/17 00:00	0,488	0,374	0,077	0,713	0,674	-0,035	1,157	-1,112	1,485	-0,095	-1,91	-0,496
1	09/20/17 00:00	0,029	0,891	-1,675	1,705	1,347	-0,538	-0,319	-2,009	2,338	-1,276	-0,625	0,791
1	09/23/17 00:00	0,898	0,316	-0,699	1,239	0,853	0,716	-0,767	-1,038	1,049	1,394	-1,083	0,572
1	09/26/17 00:00	0,857	0,864	-2,189	0,25	1,85	1,492	-0,928	-1,198	1,694	0,467	-0,587	0,183
1	09/29/17 00:00	0,924	0,025	-1,516	-0,108	1,97	0,709	0,703	-0,582	1,261	0,264	-1,162	0,319
1	10/05/17 00:00	1,196	0,562	-2,54	-0,576	2,382	0,931	0,297	-0,534	1,577	0,175	-0,75	-0,784
1	10/08/17 00:00	0,821	-0,122	-0,662	-0,429	1,546	0,365	0,525	-1,083	1,622	-0,752	-1,543	-0,419
1	10/11/17 00:00	0,891	-0,476	0,227	0,074	1,191	1,922	0,743	-0,53	1,551	-0,585	-1,706	-0,905
1	10/14/17 00:00	1,029	0,041	-1,444	0,542	0,401	-2,424	-1,673	0,964	1,741	0,986	0,692	1,441
1	10/17/17 00:00	0,51	-0,052	-0,523	-0,394	1,423	0,769	-0,168	0,004	0,141	1,122	0,269	-0,835
1	10/20/17 00:00	-0,437	-0,498	1,851	1,37	1,332	-2,071	0,053	0,764	-0,422	-0,698	1,046	0,611
1	10/23/17 00:00	1,16	-0,073	1,652	0,63	1,395	-1,333	0,192	1,54	-0,859	0,334	0,48	-0,674
1	11/04/17 00:00	1,678	-0,082	0,08	-0,39	1,644	-1,78	-0,175	0,543	0,392	-0,068	0,515	0,502
1	11/10/17 00:00	1,506	0,016	-0,187	2,34	-0,267	-2,796	-1,211	1,311	0,832	-1,847	2,196	0,149
1	11/13/17 00:00	0,388	-0,356	2,176	1,082	1,52	0,204	-0,779	0,036	0,13	0,565	-0,525	0,182
1	11/19/17 00:00	-0,377	-0,073	-0,296	0,677	0,264	0,362	0,197	0,582	-0,559	0,961	0,146	-0,576
1	11/25/17 00:00	1,03	0,409	1,125	0,066	-2,024	2,502	-1,671	-0,298	0,444	0,266	0,465	1,032
1	11/28/17 00:00	-0,304	0,167	-0,12	-0,536	-1,875	-0,603	-1,491	0,776	-0,613	0,342	0,668	1,475
1	12/04/17 00:00	-1,53	-0,813	0,084	-0,717	1,452	-0,754	1,141	-0,266	1,572	-0,943	-0,482	1,933
1	12/07/17 00:00	-1,236	-0,272	2,303	-1,069	0,15	-1,02	-0,458	-1,12	1,357	1,159	-0,065	-0,694
1	12/10/17 00:00	0,033	-0,517	0,981	-0,045	0,583	1,346	-0,19	-0,392	0,358	0,51	-0,539	-0,654
1	12/13/17 00:00	-0,154	-0,834	1,193	-0,107	0,025	-1,523	-0,061	0,299	0,366	1,172	0,226	0,05
1	12/16/17 00:00	-0,903	-1,021	2,038	-0,566	-0,911	-1,91	1,329	0,208	2,181	-0,087	0,096	1,554
1	12/19/17 00:00	-0,275	-0,377	1,654	-0,159	0,366	-1,435	0,458	0,318	-0,944	1,497	-0,346	0,258
1	12/22/17 00:00	-0,875	-0,092	1,54	0,597	1,586	0,828	1,852	-0,58	-1,306	1,773	-0,992	-0,423
1	12/25/17 00:00	-0,738	0,385	0,624	-2,063	-0,831	0,587	0,178	0,541	-1,234	1,301	-0,275	-0,211
1	12/28/17 00:00	-0,532	-0,132	1,717	0,296	-0,275	2,215	0,171	0,409	-0,536	-0,734	0,04	0,322
1	01/03/18 00:00	0,228	0,842	0,868	0,499	-1,257	-0,691	-0,126	0,767	-1,28	2,174	0,065	0,349
1	01/06/18 00:00	0,004	-0,119	1,828	-0,638	-1,047	2,188	1,125	0,219	0,093	-1,593	0,254	0,203
1	01/09/18 00:00	0,973	-0,395	0,82	-0,863	0,568	0,514	0,014	0,089	-1,279	1,376	0,567	0,687
1	01/12/18 00:00	-0,656	0,769	-0,859	0,957	-0,305	0,323	-0,442	1,638	-1,318	-0,648	0,496	0,217
1	01/15/18 00:00	1,363	0,272	-0,573	-0,179	-0,209	-0,106	0,008	1,031	-0,759	1,191	1,017	-0,519
1	01/18/18 00:00	1,207	0,728	0,225	-0,633	-0,698	0,052	0,044	0,971	-0,208	-0,89	0,419	-0,04
1	01/21/18 00:00	-0,446	0,587	0,677	-0,07	-0,695	1,507	0,625	-0,533	-0,938	0,515	0,389	-0,714
1	01/24/18 00:00	0,462	-0,362	0,257	-0,455	0,499	1,778	1,391	-1,849	1,472	1,783	-0,807	-0,723
1	01/27/18 00:00	-0,717	-0,536	-0,52	1,395	0,725	0,048	1,178	0,486	1,516	-2,348	-0,533	-0,132
1	01/30/18 00:00	0,376	0,049	-0,688	-0,009	1,443	1,851	0,924	-0,998	0,892	2,344	-0,42	-1,141
1	02/05/18 00:00	0,422	-0,589	-0,689	-0,318	-1,571	1,577	2,233	1,295	-0,037	1,061	0,328	0,103
1	02/08/18 00:00	0,365	0,946	-1,75	1,247	1,71	1,405	0,884	0,47	-1,526	0,244	-0,014	-1,304
1	02/11/18 00:00	0,932	-1,181	0,307	0,546	1,602	1,86	1,729	0,228	-0,616	-0,554	-0,033	-0,387
1	02/14/18 00:00	0,731	-0,386	-0,493	-0,182	0,034	2,284	1,753	0,349	-0,281	-0,864	-0,002	0,3
1	02/17/18 00:00	0,132	-1,063	0,158	-0,198	1,405	1,672	1,57	0,069	-0,763	-0,09	0,041	-0,101
1	02/20/18 00:00	-0,73	-1,485	0,219	-1,792	1,569	1,69	1,377	-0,337	-0,153	-0,64	0,543	-0,175
1	02/23/18 00:00	-1,226	-0,907	-0,051	-1,001	1,898	2,472	1,284	-1,056	-0,496	-0,272	-0,019	-0,123
1	02/26/18 00:00	0,376	-0,803	-0,281	-1,721	1,359	1,509	1,105	-0,495	-0,973	0,683	0,438	0,456
1	03/04/18 00:00	0,687	-1,592	0,127	-2,003	1,324	1,872	1,198	-0,602	0,623	-1,142	0,552	0,539
Q(true)/Qexp:		1,1293	0,71233	1,945534	1,656817	1,99683	2,324666	1,83173993	1,500256009	1,921150778	1,802540993	0,857217	0,844530024

Run	Date_Time	V	Cr	Mn	Fe	Ni	Cu	Zn	Mo	S	Q(true)/Qexp
1	03/15/17 00:00	1,297	-2,509	1,355	1,723	1,7	1,801	1,891	-0,034	1,894	3,695785
1	03/18/17 00:00	0,186	0,663	-0,396	2,421	-1,096	0,19	2,425	-0,277	-1,276	2,447853
1	03/21/17 00:00	1,736	-0,638	0,771	1,49	1,116	1,63	1,399	-0,399	-1,378	1,771672
1	03/24/17 00:00	-1,585	0,589	-0,979	-0,291	-0,213	1,525	-0,371	0,386	-1,443	1,902473
1	03/27/17 00:00	-0,366	0,155	-0,513	-1,323	0,639	0,474	-1,646	2,129	0,457	2,820093
1	03/30/17 00:00	-1,205	0,825	0,563	-0,618	1,553	-0,104	0,646	-1,047	1,571	1,377505
1	04/05/17 00:00	-1,109	-1,168	0,168	-0,343	0,527	0,987	-2,162	2,216	2,139	2,496639
1	04/08/17 00:00	1,819	-0,964	0,53	-1,379	-0,206	1,851	-0,306	1,163	1,142	1,989119
1	04/11/17 00:00	1,449	-0,77	-1,579	0,69	2,455	0,174	-0,988	1,427	0,388	3,000938
1	04/14/17 00:00	-0,816	0,15	-0,099	0,18	0,561	0,634	-0,462	-0,759	0,028	0,790483
1	04/17/17 00:00	-0,717	0,177	0,428	1,662	-0,482	0,445	2,384	-1,091	0,515	1,955118
1	04/20/17 00:00	0,423	-1,313	0,275	0,085	0,98	1,503	-1,042	1,408	-0,048	2,089946
1	04/23/17 00:00	-0,762	0,757	-0,51	0,458	-0,202	1,227	-0,07	0,178	-0,747	1,156127
1	04/26/17 00:00	-1,068	1,327	-0,644	0,292	-1,058	-0,066	2,513	-0,953	1,205	1,516774
1	04/29/17 00:00	-0,227	-1,788	0,817	0,897	0,349	-0,605	-1,454	2,121	0,448	1,935925
1	05/05/17 00:00	-0,885	0,601	-0,285	0,825	-1,04	0,19	0,118	0,148	-0,191	0,694072
1	05/08/17 00:00	0,89	-0,439	-0,032	0,662	0,006	-0,216	0,117	0,467	-0,116	1,240972
1	05/11/17 00:00	2,003	-0,996	-0,482	0,076	-0,383	-0,257	-0,175	0,919	1,461	1,614973
1	05/14/17 00:00	-0,064	-0,274	-0,641	2,005	-0,484	0,655	0,09	0,258	1,178	1,20719
1	05/17/17 00:00	0,091	0,256	0,063	1,399	-0,067	-0,387	0,158	1,728	-1,78	1,254724
1	05/20/17 00:00	1,092	-2,041	-0,446	-0,092	1,439	1,853	-0,845	0,978	1,678	1,700891
1	05/23/17 00:00	1,679	0,258	1,963	2,15	0,029	1,256	2,147	-1,643	0,06	2,610345
1	05/26/17 00:00	2,899	-0,911	0,276	0,753	-0,894	0,681	-0,26	-0,218	1,289	2,130723
1	06/04/17 00:00	-0,346	1,567	-0,676	0,425	-0,241	0,526	0,768	-1,575	-1,563	1,075412
1	06/07/17 00:00	1,698	-1,824	0,413	0,56	1,944	0,694	-1,153	0,349	1,609	2,415611
1	06/19/17 00:00	1,366	0,439	-0,246	-1,703	-2,35	1,329	0,243	0,276	1,823	2,216446
1	06/25/17 00:00	-0,023	0,207	0,155	1,127	-1,061	0,523	-0,222	1,479	-1,76	2,322923
1	06/28/17 00:00	0,925	-0,715	-0,182	-2,223	-0,031	1,424	-1,023	1,144	0,868	2,508582
1	07/07/17 00:00	-0,979	0,865	0,759	0,978	-0,847	1,739	-0,1	-0,142	-1,965	1,871228
1	07/10/17 00:00	1,39	-1,774	0,149	-0,274	1,287	0,17	-0,169	0,663	-0,674	1,953221
1	07/16/17 00:00	-0,632	1,599	-0,589	0,172	1,867	0,266	2,77	-1,812	-0,875	2,94696
1	07/19/17 00:00	-1,132	0,571	-0,057	0,647	0,134	1,498	0,31	-0,56	-1,01	0,859468
1	07/22/17 00:00	0,511	0,657	-0,049	0,795	1,098	-0,267	0,717	-1,071	-0,742	1,208073
1	07/25/17 00:00	1,473	-1,732	1,43	0,365	1,243	1,195	-0,348	-0,163	0,237	1,586385
1	07/28/17 00:00	0,675	0,327	-0,429	0,705	0,38	-1,066	0,463	-2,003	0,282	1,199963
1	08/03/17 00:00	0,95	0,573	0,96	0,625	1,36	-0,244	0,569	-0,998	-1,178	1,361864
1	08/06/17 00:00	0,545	-0,845	0,215	0,423	0,543	1,073	-0,34	0,371	0,988	0,556239
1	08/09/17 00:00	-0,143	0,354	0,545	0,405	-0,038	-0,738	0,53	0,45	-1,21	0,458347
1	08/12/17 00:00	0,449	-0,777	1,114	1,566	1,643	-0,923	0,1	-0,123	1,201	1,303849
1	08/15/17 00:00	-0,219	-1,1	0,826	-0,322	0,882	-0,965	-0,741	1,392	-0,247	0,9419
1	08/18/17 00:00	0,474	0,35	0,147	0,291	-1,485	-0,616	0,488	1,102	0,655	1,442059
1	08/21/17 00:00	0,064	0,001	-0,048	-0,929	0,572	-1,325	0,256	0,938	-0,455	0,996209
1	08/27/17 00:00	-0,42	1,771	-0,212	-0,317	-0,112	0,683	-0,127	-0,105	-0,577	1,203153
1	08/30/17 00:00	0,479	2,108	-0,467	-0,392	-0,339	0,162	-0,344	-0,195	0,7	1,168584
1	09/05/17 00:00	0,376	-0,282	0,278	-0,558	0,225	-0,105	-0,323	1,015	1,023	0,939553
1	09/08/17 00:00	1,919	0,857	0,602	-0,838	-1,191	1,003	1,575	-0,309	1,67	2,973657
1	09/11/17 00:00	-1,141	-1,054	0,387	0,688	1,716	0,854	-0,372	0,488	1,36	2,338785
1	09/14/17 00:00	-0,455	0,586	-0,297	-0,361	1,211	0,272	0,164	0,641	1,028	1,762844
1	09/17/17 00:00	0,655	1,267	-0,181	-0,478	-1,478	0,622	0,926	0,453	2,17	1,604434
1	09/20/17 00:00	-0,65	-0,905	1,473	1,913	1,932	1,286	-0,877	1,932	1,657	3,148685
1	09/23/17 00:00	-1,33	1,139	-0,408	1,615	-0,624	1,021	0,173	-0,741	1,601	1,614116
1	09/26/17 00:00	-0,268	-0,11	0,057	0,97	0,446	0,848	-0,113	-0,171	0,909	1,595926
1	09/29/17 00:00	1,757	0,909	-0,45	-1,726	-0,111	0,964	0,413	0,324	0,157	1,539192
1	10/05/17 00:00	1,928	-0,009	-0,392	0,126	-0,412	1,399	0,015	0,423	2,019	2,282676
1	10/08/17 00:00	0,273	-0,382	0,297	-0,406	1,694	1,302	-0,139	0,589	0,923	1,342265
1	10/11/17 00:00	1,207	1,431	-0,692	-1,904	-0,179	1,277	1,944	0,297	1,05	2,15335
1	10/14/17 00:00	3,965	-1,244	1,523	1,628	1,675	0,707	-0,821	0,237	-0,567	3,598445
1	10/17/17 00:00	0,805	0,409	-0,502	-1,211	-0,912	0,636	0,608	-0,185	1,567	0,93254
1	10/20/17 00:00	-0,578	-0,606	1,506	1,185	1,375	1,349	-0,438	0,87	0,516	1,849229
1	10/23/17 00:00	0,515	-0,216	0,635	-1,4	0,881	0,916	-2,501	1,648	0,751	2,015656
1	11/04/17 00:00	-0,423	-0,165	-0,504	1,377	0,907	0,618	-0,753	-0,545	-0,273	1,114065
1	11/10/17 00:00	-0,381	-0,255	1,893	1,305	2,236	1,622	-1,571	1,517	0,943	3,616173
1	11/13/17 00:00	-0,329	2,062	0,114	-1,332	-0,527	-0,367	0,614	-0,182	-1,464	1,467141
1	11/19/17 00:00	0,58	0,453	-0,127	-1,134	1,199	0,076	-0,018	-0,292	-0,236	0,488173
1	11/25/17 00:00	-0,874	1,486	0,811	2,018	-0,039	0,214	0,774	-1	-1,402	2,219909
1	11/28/17 00:00	0,792	-0,52	0,76	1,18	0,844	0,499	-1,147	0,581	-0,085	1,221027
1	12/04/17 00:00	-0,771	0,35	1,494	1,114	-0,198	0,315	1,491	-0,057	-1,122	1,763205
1	12/07/17 00:00	0,368	-0,021	0,235	0,957	1,473	0,304	0,551	-0,847	0,392	1,458487
1	12/10/17 00:00	-1,043	1,889	-0,29	0,227	0,253	0,312	0,365	-1,026	-0,546	0,862984
1	12/13/17 00:00	1,349	1,187	-0,1	0,212	-1,548	-0,106	0,915	-0,54	-0,504	1,024798
1	12/16/17 00:00	0,082	1,374	0,115	2,208	-1,881	-0,238	2,13	-1,021	-0,479	2,793943
1	12/19/17 00:00	0,323	-0,649	-0,099	0,486	0,757	0,355	-0,617	-0,309	0,355	0,844063
1	12/22/17 00:00	-1,179	2,163	-1,017	0,508	0,851	1,423	-0,182	-1,54	0,933	2,318318
1	12/25/17 00:00	-0,696	0,65	0,933	2,055	1,918	1,052	0,059	0,101	-0,814	1,668508
1	12/28/17 00:00	-2,04	1,956	-0,323	0,8	1,87	-0,79	-0,031	-0,346	-1,905	2,021926
1	01/03/18 00:00	0,619	-1,435	-0,088	0,778	1,628	-0,189	-0,274	-0,148	-0,958	1,371735
1	01/06/18 00:00	-1,076	1,917	-0,141	0,521	-0,458	-1,037	0,348	-0,385	-0,485	1,593237
1	01/09/18 00:00	-1,166	1,656	0,076	0,217	-0,532	-0,279	0,061	-0,242	-0,749	0,976206
1	01/12/18 00:00	0,403	-0,169	0,714	0,334	1,975	-2,067	-0,214	0,94	0,184	1,408836
1	01/15/18 00:00	0,368	0,137	-0,012	0,446	-1,149	0,45	-0,556	0,591	-0,061	0,71772
1	01/18/18 00:00	1,666	-1,132	0,24	-0,133	0,728	-0,107	-1,21	0,244	0,149	0,861982
1	01/21/18 00:00	1,945	-0,203	0,197	-0,544	1,65	-2,635	1,551	0,438	-0,095	1,759908
1	01/24/18 00:00	0,128	2,501	-0,788	-1,01	-0,358	1,374	0,9	-0,882	-0,455	2,144287
1	01/27/18 00:00	0,622	-0,152	0,099	-1,073	1,936	1,584	-0,072	1,193	-0,052	1,749743
1	01/30/18 00:00	0,867	-0,228	-0,701	-1,425	2,202	1,415	-0,663	-1,123	0,68	2,179895
1	02/05/18 00:00	0,442	0,613	-1,194	0,328	-0,845	1,818	0,638	-0,36	2,488	2,081406
1	02/08/18 00:00	-0,27	-0,218	-0,218	0,763	1,555	1,486	-0,154	0,572	-0,209	1,661562
1	02/11/18 00:00	-0,124	0,958	-0,253	-1,122	-0,461	0,264	0,726	0,16	0,695	1,252378
1	02/14/18 00:00	0,382	1,68	-0,994	-1,293	-0,321	0,303	1,237	0,472	0,854	1,443218
1	02/17/18 00:00	-0,599	1,775	0,24	-0,525	-0,711	0,163	0,281	0	-0,808	1,09909
1	02/20/18 00:00	-0,504	1,155	0,004	0,072	-0,212	-0,086	0,262	0,864	-0,515	1,304771
1	02/23/18 00:00	-0,516	2,047	0,355	-1,2	-0,368	0,118	0,857	-0,153	0,61	1,819812
1	02/26/18 00:00	0,681	0,989	-0,632	-1,262	-0,525	0,933	0,317	0,291	0,57	1,266798
1	03/04/18 00:00	-0,927	1,454	-0,143	-0,279	-0,488	-0,483	0,692	0,797	-0,275	1,63859
Q(true)/Qexp:		1,73711825	1,871585912	0,69691306	1,717936	1,897064002	1,440151101	1,475715948	1,25349309	1,707741	

**** Run Comparison Statistics ****

Concentration of Species — Lowest Q (Robust) Run = Run 1

Statistics Over All Runs

Factor 1	Lowest Q	Min	25th	50th	75th	Max	Mean	Std Dev	RSD % mean	RSD % Lowest Q
PM2.5	5,7995	5,7929	5,795425	5,79785	5,79965	5,8017	5,79761	0,002500295	0,000431263	0,000431122
Na	0,66525	0,66444	0,6648025	0,66498	0,66528	0,66541	0,6649915	0,000290304	0,000436553	0,000436384
Mg	0,043967	0,043919	0,043943	0,0439555	0,0439715	0,043984	0,04395495	1,75454E-05	0,000399167	0,000399057
P	0	0	0	0	0	0	0	0	0	0
K	0,094687	0,094572	0,09461975	0,094652	0,09469	0,094707	0,09465005	3,96624E-05	0,000419042	0,000418879
Ca	0,19822	0,19801	0,1980925	0,198175	0,198215	0,19845	0,198176	0,000108308	0,000546522	0,000546401
Sr	0,0021654	0,0021626	0,002163925	0,00216445	0,0021654	0,0021659	0,002164545	9,32724E-07	0,00043091	0,00043074
Zr	0,0041576	0,0041526	0,004154625	0,00415605	0,0041576	0,0041587	0,00415602	1,82197E-06	0,000438393	0,000438227
Ba	0,04214	0,042065	0,04209725	0,042107	0,04213375	0,042151	0,04211215	2,25675E-05	0,00053589	0,000535536
Pb	0	0	0	0	0	0	0	0	0	0
Al	0,25673	0,25642	0,25657	0,256635	0,2567575	0,25677	0,256638	0,000107781	0,000419975	0,000419824
Ti	0,003299	0,0032974	0,003298775	0,00329965	0,003300975	0,0033026	0,0032998	1,30465E-06	0,000395372	0,000395468
V	0,000089098	0,00008907	8,91278E-05	0,000089176	8,92163E-05	0,000089267	8,9173E-05	5,47141E-08	0,000613572	0,000614089
Cr	0,00024465	0,00024465	0,000246573	0,00024751	0,000248053	0,00024998	0,000247329	1,29209E-06	0,005224171	0,005281377
Mn	0,0003818	0,00038171	0,000381883	0,00038213	0,000382235	0,00038256	0,000382104	2,34844E-07	0,000614607	0,000615096
Fe	0,02247	0,022464	0,022472	0,022483	0,0224895	0,022505	0,02248225	1,16206E-05	0,000516881	0,000517163
Ni	0	0	0	0	0	0	0	0	0	0
Cu	0,00025244	0,0002522	0,00025234	0,000252395	0,000252498	0,00025258	0,000252401	1,042E-07	0,000412836	0,000412771
Zn	0,0023458	0,0023294	0,002333425	0,00233605	0,0023386	0,0023458	0,002336565	4,50839E-06	0,001929493	0,001921897
Mo	0,00023708	0,00023495	0,000236065	0,00023638	0,00023699	0,00023793	0,000236411	6,82626E-07	0,002887453	0,002879305
S	0,0011189	0,0010998	0,00110955	0,0011148	0,001117875	0,001127	0,001114215	6,39122E-06	0,005736072	0,005712054

Statistics Over All Runs

Factor 2	Lowest Q	Min	25th	50th	75th	Max	Mean	Std Dev	RSD % mean	RSD % Lowest Q
PM2.5	7,2829	7,277	7,278325	7,2823	7,285725	7,293	7,282455	0,004299385	0,000590376	0,00059034
Na	0,10187	0,10166	0,1017125	0,10175	0,1018575	0,10195	0,101777	8,0138E-05	0,000787388	0,00078667
Mg	0,0073355	0,0073241	0,00732625	0,00733005	0,0073338	0,0073433	0,007330545	4,97864E-06	0,000679163	0,000678704
P	0,0057627	0,0057577	0,005759625	0,00576255	0,0057663	0,0057712	0,00576294	3,64784E-06	0,000632982	0,000633009
K	0,013319	0,013295	0,01329925	0,013305	0,01331475	0,013332	0,01330755	9,81661E-06	0,000737672	0,000737038
Ca	0	0	0	0	0	0	0	0	0	0
Sr	0,00025276	0,00025235	0,00025242	0,00025258	0,000252693	0,00025301	0,000252583	1,80324E-07	0,000713921	0,000713421
Zr	0,002918	0,0029156	0,002915825	0,0029175	0,002918775	0,0029215	0,00291749	1,71154E-06	0,000586648	0,000586546
Ba	0	0	0	0	0	0	0	0	0	0
Pb	0	0	0	0	0	0	0	0	0	0
Al	0,12004	0,11993	0,11994	0,120005	0,120055	0,12018	0,120009	7,10004E-05	0,000591625	0,000591473
Ti	0,0032419	0,0032391	0,0032396	0,0032413	0,0032427	0,0032459	0,00324137	1,88459E-06	0,000581418	0,000581323
V	0,00013999	0,00013986	0,000139883	0,00013995	0,000140018	0,00014016	0,000139959	8,08442E-08	0,000577628	0,0005775
Cr	0,0038112	0,0038079	0,003808475	0,00381085	0,00381255	0,0038155	0,00381067	2,21837E-06	0,000582147	0,000582066
Mn	0,0010326	0,0010318	0,001032	0,00103255	0,001033075	0,001034	0,001032585	6,01992E-07	0,000582995	0,000582987
Fe	0,037771	0,037741	0,03774625	0,0377655	0,03778325	0,03782	0,037767	2,19185E-05	0,000580361	0,0005803
Ni	0,0012297	0,0012287	0,001229	0,00122965	0,0012302	0,0012312	0,00122967	6,96684E-07	0,000566562	0,000566548
Cu	0,000417	0,00041647	0,000416533	0,00041677	0,000417053	0,00041736	0,000416781	2,69891E-07	0,00064756	0,00064722
Zn	0	0	0	0	0	0	0	0	0	0
Mo	0,0075406	0,0075348	0,00753705	0,00754085	0,007545125	0,007551	0,00754135	4,3997E-06	0,00058341	0,000583468
S	0,066587	0,066536	0,066553	0,066588	0,06662275	0,066677	0,0665914	3,87181E-05	0,000581429	0,000581467

Statistics Over All Runs

Factor 3	Lowest Q	Min	25th	50th	75th	Max	Mean	Std Dev	RSD % mean	RSD % Lowest Q
PM2.5	9,3096	9,2981	9,303475	9,3075	9,30945	9,3143	9,30668	0,004358851	0,000468357	0,00046821
Na	0	0	0	0	0	0	0	0	0	0
Mg	0,0046574	0,0046483	0,004650925	0,00465175	0,004654775	0,0046593	0,004652795	2,95892E-06	0,000635946	0,000635317
P	0,0087976	0,0087866	0,0087916	0,0087953	0,0087974	0,0088014	0,008794535	4,16063E-06	0,000473092	0,000472927
K	0,0094812	0,0094671	0,009470975	0,00947325	0,009479025	0,0094836	0,009474205	4,94192E-06	0,000521619	0,000521234
Ca	0,06991	0,069738	0,06976475	0,0697945	0,06983975	0,069949	0,06980935	5,78321E-05	0,00082843	0,000827237
Sr	0,0002923	0,00029179	0,00029192	0,00029201	0,000292208	0,00029235	0,00029205	1,64971E-07	0,000564874	0,00056439
Zr	0,0028646	0,0028613	0,002863075	0,0028643	0,002864775	0,0028662	0,00286394	1,35972E-06	0,000474773	0,000474664
Ba	0	0	0	0	0	0	0	0	0	0
Pb	0,0080946	0,0080826	0,008085975	0,00809005	0,008093975	0,008097	0,008089825	4,26625E-06	0,00052736	0,000527049
Al	0,099676	0,099553	0,0996135	0,099658	0,099676	0,099724	0,09964625	4,76201E-05	0,000477891	0,000477749
Ti	0,0013406	0,0013382	0,001339325	0,00133985	0,001340525	0,0013411	0,00133982	7,81766E-07	0,000583486	0,000583146
V	0	0	0	0	0	0	0	0	0	0
Cr	0,00013323	0,00013277	0,000133328	0,000133735	0,000134325	0,00013463	0,000133808	5,91019E-07	0,004416938	0,004436084
Mn	0,00073132	0,00073028	0,0007308	0,000731105	0,00073131	0,00073166	0,000731042	3,72591E-07	0,000509671	0,000509477
Fe	0,019884	0,019853	0,01986775	0,019876	0,01988325	0,019893	0,01987495	1,0704E-05	0,000538569	0,000538324
Ni	0,00094036	0,0009393	0,00093996	0,000940305	0,000940613	0,00094107	0,000940265	4,80444E-07	0,000510966	0,000510915
Cu	0,00034076	0,00034037	0,000340618	0,000340745	0,000340888	0,00034107	0,000340747	1,81696E-07	0,000533229	0,000533208
Zn	0,012926	0,012914	0,012919	0,012924	0,01292675	0,012933	0,0129236	5,20526E-06	0,000402772	0,000402697
Mo	0,0092419	0,0092311	0,00923685	0,0092406	0,0092423	0,0092466	0,00923942	4,37993E-06	0,000474048	0,000473921
S	0,079397	0,079306	0,07935375	0,0793875	0,07940275	0,07944	0,0793774	3,77867E-05	0,000476038	0,00047592

Statistics Over All Runs

Factor 4	Lowest Q	Min	25th	50th	75th	Max	Mean	Std Dev	RSD % mean	RSD % Lowest Q
PM2.5	6,0815	6,0695	6,0719	6,07395	6,0762	6,0815	6,0741	0,003070402	0,000505491	0,000504876
Na	0	0	0	0	0	0	0	0	0	0
Mg	0,015968	0,015946	0,01595	0,015955	0,0159625	0,015968	0,01595595	6,58127E-06	0,000412465	0,000412154
P	0,0043256	0,0043165	0,00431845	0,00432005	0,004321375	0,0043256	0,00431999	2,31219E-06	0,00053523	0,000534536
K	0,0047778	0,0047714	0,004775475	0,0047778	0,004780675	0,0047867	0,004778215	4,10305E-06	0,0008587	0,000858774
Ca	0,2533	0,25301	0,25306	0,25313	0,25328	0,25331	0,253158	0,000108123	0,000427096	0,000426856
Sr	0,0017848	0,0017821	0,001782625	0,00178325	0,001784	0,0017848	0,001783305	7,4302E-07	0,000416653	0,000416304
Zr	0,0029617	0,0029553	0,0029568	0,00295795	0,0029586	0,0029617	0,002957825	1,55695E-06	0,000526382	0,000525693
Ba	0,057337	0,057248	0,05726525	0,057286	0,057307	0,057337	0,05728595	2,45667E-05	0,000428844	0,000428462
Pb	0,028764	0,028718	0,0287265	0,0287375	0,0287475	0,028764	0,02873725	1,25315E-05	0,000436073	0,000435667
Al	0,16212	0,16183	0,1618825	0,16194	0,16199	0,16212	0,16194	7,58808E-05	0,000468574	0,000468053
Ti	0,0040848	0,0040778	0,0040792	0,0040805	0,0040821	0,0040848	0,00408059	1,83243E-06	0,000449059	0,000448597
V	0	0	0	0	0	0	0	0	0	0
Cr	0,000227	0,00022308	0,000224428	0,0002249	0,000225593	0,000227	0,000224973	9,49165E-07	0,004219027	0,004181344
Mn	0,0011111	0,0011091	0,001109525	0,00110985	0,0011103	0,0011111	0,00110988	5,21738E-07	0,000470085	0,000469569
Fe	0,01727	0,017237	0,0172425	0,017249	0,017254	0,01727	0,01724875	8,44097E-06	0,000489367	0,000488765
Ni	0,00019712	0,00019608	0,000196348	0,000196495	0,000196703	0,00019712	0,000196515	2,53927E-07	0,001292151	0,001288185
Cu	0	0	0	0	0	0	0	0	0	0
Zn	0	0	0	0	0	0	0	0	0	0
Mo	0,012087	0,012063	0,012068	0,012073	0,01207575	0,012087	0,01207225	6,13767E-06	0,000508412	0,000507791
S	0,077006	0,076838	0,07687575	0,0769085	0,076925	0,077006	0,07690555	4,13082E-05	0,000537129	0,000536428

Statistics Over All Runs

Factor 5	Lowest Q	Min	25th	50th	75th	Max	Mean	Std Dev	RSD % mean	RSD % Lowest Q
PM2.5	9,974	9,9693	9,971925	9,9759	9,97955	9,9869	9,97638	0,004832195	0,000484364	0,000484479
Na	0	0	0	0	0	0	0	0	0	0
Mg	0,032069	0,032053	0,03206275	0,0320775	0,03208925	0,032109	0,0320776	1,52433E-05	0,0004752	0,000475328
P	0,0082171	0,0082128	0,008215475	0,00821855	0,0082217	0,0082284	0,00821915	4,10257E-06	0,000499147	0,000499272
K	0,046773	0,046752	0,0467655	0,0467865	0,04680275	0,046833	0,04678695	2,2343E-05	0,000477547	0,000477689
Ca	0,57767	0,57739	0,57757	0,57783	0,578045	0,5784	0,5778335	0,000280325	0,00048513	0,000485268
Sr	0,0010173	0,0010167	0,00101705	0,00101755	0,0010179	0,0010185	0,00101753	4,8569E-07	0,000477322	0,00047743
Zr	0,00058641	0,00058602	0,000586275	0,00058641	0,000586605	0,00058714	0,000586459	2,82822E-07	0,000482254	0,000482294
Ba	0	0	0	0	0	0	0	0	0	0
Pb	0,0020408	0,002037	0,002039025	0,00204055	0,002041025	0,0020425	0,00204015	1,30202E-06	0,0006382	0,000637996
Al	0,097498	0,097449	0,097473	0,097511	0,09754925	0,097618	0,09751575	4,51184E-05	0,000462678	0,000462762
Ti	0,0062146	0,0062118	0,006213275	0,0062158	0,0062181	0,0062225	0,00621607	2,93421E-06	0,000472036	0,000472148
V	0,00030028	0,00030014	0,000300213	0,000300325	0,000300438	0,00030066	0,000300336	1,39752E-07	0,000465318	0,000465404
Cr	0,00059013	0,00058851	0,000589285	0,000589755	0,000590323	0,00059071	0,000589782	5,90741E-07	0,001001626	0,001001035
Mn	0,001599	0,0015983	0,00159865	0,00159935	0,0015999	0,001601	0,00159939	7,46853E-07	0,000466961	0,000467075
Fe	0,073576	0,073547	0,073562	0,0735915	0,07361975	0,07367	0,07359515	3,43623E-05	0,000466909	0,000467031
Ni	0,00017775	0,00017759	0,000177708	0,000177785	0,000177865	0,00017806	0,000177791	1,08623E-07	0,000610959	0,0006111
Cu	0,00032744	0,00032723	0,000327323	0,00032742	0,000327538	0,00032781	0,000327445	1,50035E-07	0,000458199	0,000458206
Zn	0	0	0	0	0	0	0	0	0	0
Mo	0	0	0	0	0	0	0	0	0	0
S	0,0033523	0,0033416	0,00334705	0,00335005	0,0033535	0,0033565	0,00334993	4,04801E-06	0,001208388	0,001207533

Percent of Species Sum — Statistics Over All Runs

Factor 1	Lowest Q	Min	25th	50th	75th	Max	Mean	Std Dev	RSD % mean	RSD % Lowest Q
PM2.5	15,08420574	15,06974397	15,07695308	15,08462621	15,08749425	15,09605302	15,0833215	0,006608789	0,000438152	0,000438126
Na	86,72046094	86,71072527	86,7199338	86,72659325	86,7331331	86,73884686	86,72650223	0,008741036	0,000100789	0,000100796

Mg	42,27722172	42,25060799	42,26379489	42,27753367	42,28434812	42,29617128	42,27582169	0,013149532	0,000311041	0,000311031
P	0	0	0	0	0	0	0	0	0	0
K	56,01521551	55,97731833	55,99419137	56,010151	56,01681786	56,02721491	56,00694979	0,014110224	0,000251937	0,0002519
Ca	18,03475571	18,01602617	18,02546217	18,03467786	18,03770012	18,0573577	18,03277357	0,009877715	0,000547765	0,000547704
Sr	39,2812051	39,25999332	39,27238182	39,28513743	39,29296539	39,30239563	39,28384869	0,012824337	0,000326453	0,000326475
Zr	30,8237281	30,80251808	30,81941301	30,82682359	30,83673723	30,84385359	30,82704376	0,011441461	0,00037115	0,00037119
Ba	42,36155091	42,33114022	42,35859568	42,36829376	42,37638077	42,39658694	42,36715748	0,015897595	0,000375234	0,000375284
Pb	0	0	0	0	0	0	0	0	0	0
Al	34,87876054	34,85677393	34,87201328	34,88117707	34,89048248	34,89962077	34,88118908	0,011954312	0,000342715	0,000342739
Ti	18,14541634	18,13920994	18,14591334	18,15373378	18,1582371	18,16791542	18,15306249	0,008045591	0,000443208	0,000443395
V	16,83101359	16,8288755	16,83337714	16,84274862	16,84785109	16,85948883	16,84199267	0,009230131	0,000548043	0,0005484
Cr	4,886930432	4,886930432	4,923069134	4,940709741	4,954001663	4,993198719	4,940098124	0,025787007	0,005219938	0,005276729
Mn	7,862729673	7,862729673	7,865649341	7,870591633	7,873475757	7,880620628	7,870318807	0,004909654	0,000623819	0,000624421
Fe	13,14257974	13,14044464	13,14465558	13,14994255	13,1543323	13,16374399	13,14996828	0,006594493	0,000501484	0,000501766
Ni	0	0	0	0	0	0	0	0	0	0
Cu	18,8720433	18,85872775	18,86890814	18,87402484	18,87854975	18,88518264	18,8728583	0,007349176	0,000389405	0,000389421
Zn	15,36033735	15,27335195	15,29475013	15,31276534	15,32342631	15,36033735	15,3115227	0,022562594	0,00147357	0,001468887
Mo	0,814523726	0,807925545	0,811197909	0,812731581	0,814474975	0,817743238	0,812703938	0,002268096	0,002790803	0,002784568
S	0,49190807	0,483931648	0,488190283	0,490489283	0,491637734	0,495632759	0,490112361	0,002729667	0,005569471	0,00554914

Statistics Over All Runs

Factor 2	Lowest Q	Min	25th	50th	75th	Max	Mean	Std Dev	RSD % mean	RSD % Lowest Q
PM2.5	18,942454	18,9312572	18,94254223	18,94429656	18,95271452	18,96536928	18,94635932	0,008565614	0,000452098	0,000452191
Na	13,27953906	13,26115314	13,2668669	13,27340675	13,2800662	13,28927473	13,27349777	0,008741036	0,000658533	0,000658233
Mg	7,053575635	7,045784468	7,046748763	7,050074847	7,053285293	7,060281554	7,050509744	0,004053731	0,000574956	0,000574706
P	21,26222189	21,24936808	21,26228748	21,2672723	21,2747196	21,28902792	21,26811705	0,009777014	0,000459703	0,00045983
K	7,879293413	7,868563329	7,870004824	7,87387591	7,878545995	7,88566379	7,874430713	0,004752288	0,000603509	0,000603136
Ca	0	0	0	0	0	0	0	0	0	0
Sr	4,585165513	4,58090217	4,581289726	4,584412067	4,58584066	4,590441735	4,584072933	0,002850998	0,000621936	0,000621787
Zr	21,63354786	21,62043515	21,63372066	21,63876431	21,65094154	21,65928751	21,64031694	0,01073444	0,000496039	0,000496194
Ba	0	0	0	0	0	0	0	0	0	0
Pb	0	0	0	0	0	0	0	0	0	0
Al	16,30836449	16,29781215	16,30628739	16,30920196	16,3185526	16,32725148	16,31113294	0,008122442	0,000497969	0,000498054
Ti	17,83135048	17,8200121	17,82605646	17,83105423	17,83695097	17,84903191	17,83162214	0,007649025	0,000428958	0,000428965
V	26,44474165	26,4153295	26,42612961	26,43253311	26,44226909	26,45696402	26,43389452	0,010890277	0,000411982	0,000411813
Cr	76,12944723	76,09244948	76,10658971	76,11350836	76,1211019	76,12944723	76,11352206	0,009878384	0,000129785	0,000129758
Mn	21,26520341	21,25551727	21,2632969	21,26632015	21,27443739	21,28833547	21,268483	0,008643225	0,000406387	0,000406449
Fe	22,0920507	22,07665358	22,08422799	22,08762298	22,09395143	22,11023548	22,09008502	0,008828251	0,000399648	0,000399612
Ni	48,31960015	48,30069136	48,32139761	48,33237687	48,34443104	48,35498023	48,33151442	0,015037592	0,000311134	0,000311211
Cu	31,17430699	31,13939004	31,15281338	31,16353649	31,17473593	31,18770795	31,16415369	0,013636375	0,000437566	0,000437424
Zn	0	0	0	0	0	0	0	0	0	0
Mo	25,9068568	25,90190449	25,9147834	25,92616269	25,933805	25,94621564	25,9247082	0,013090945	0,00050496	0,000505308
S	29,27400365	29,26740025	29,28192708	29,29290049	29,30317612	29,31448587	29,2917396	0,013628287	0,00046526	0,000465542

Statistics Over All Runs

Factor 3	Lowest Q	Min	25th	50th	75th	Max	Mean	Std Dev	RSD % mean	RSD % Lowest Q
PM2.5	24,21379804	24,19370367	24,20807009	24,21335965	24,21861557	24,22866923	24,21267393	0,008875068	0,000366546	0,000366529
Na	0	0	0	0	0	0	0	0	0	0
Mg	4,478402722	4,469927541	4,473067054	4,474589514	4,477371142	4,481177669	4,475053072	0,002706839	0,000604873	0,000604421
P	32,45987529	32,43688234	32,44939838	32,45518241	32,46241947	32,47927295	32,45621314	0,012046782	0,00037117	0,000371128
K	5,608916338	5,600478937	5,604075812	5,606140114	5,608508149	5,610767638	5,606139071	0,002734095	0,000487697	0,000487455
Ca	6,360658721	6,345119943	6,348892607	6,351451356	6,355990983	6,366587815	6,352213404	0,005530929	0,000870709	0,000869553
Sr	5,302436617	5,294817869	5,298293584	5,300576218	5,302188364	5,304960369	5,300341814	0,002601277	0,000490775	0,000490582
Zr	21,23764949	21,22423003	21,23772058	21,24273762	21,24893124	21,25658613	21,24311294	0,007842399	0,000369174	0,000369269
Ba	0	0	0	0	0	0	0	0	0	0
Pb	20,80906132	20,79875532	20,80650376	20,81556581	20,82071314	20,8297961	20,81400273	0,009414743	0,000452327	0,000452435
Al	13,54175724	13,53006492	13,54047815	13,54226551	13,54793351	13,5523907	13,54351135	0,005360572	0,000395804	0,000395855
Ti	7,37367237	7,361564951	7,368761309	7,370175481	7,373633738	7,377631036	7,370699848	0,00409756	0,000555925	0,000555701
V	0	0	0	0	0	0	0	0	0	0
Cr	2,661294672	2,653447063	2,663998776	2,671372974	2,683579709	2,689429887	2,672641335	0,011327296	0,00423824	0,00425631
Mn	15,06069006	15,04354776	15,05444056	15,05693354	15,06182282	15,0699524	15,05749615	0,006964083	0,000462499	0,000462401
Fe	11,63004252	11,61252208	11,62203812	11,62449784	11,63009396	11,63605522	11,62494698	0,006276775	0,00053994	0,000539704
Ni	36,95032869	36,92999206	36,94596378	36,95310347	36,96954488	36,98781969	36,95659014	0,01541569	0,00041713	0,0004172
Cu	25,47471667	25,45355289	25,47325662	25,47766159	25,48529214	25,50113274	25,47879349	0,011456117	0,000449633	0,000449705
Zn	84,63966265	84,63966265	84,67657369	84,68723466	84,70524987	84,72664805	84,6884773	0,022562594	0,000266419	0,000266572
Mo	31,75192688	31,74064272	31,75281538	31,76173422	31,7722606	31,77970252	31,76212026	0,011163577	0,000351475	0,000351587
S	34,90573337	34,89179419	34,90638309	34,91808925	34,92508265	34,93617244	34,91595229	0,011981573	0,000343155	0,000343255

Statistics Over All Runs

Factor 4	Lowest Q	Min	25th	50th	75th	Max	Mean	Std Dev	RSD % mean	RSD % Lowest Q
PM2.5	15,81767345	15,78888496	15,79616078	15,80320727	15,80760766	15,81767345	15,80265001	0,007568792	0,000478957	0,000478502
Na	0	0	0	0	0	0	0	0	0	0
Mg	15,35430383	15,3345153	15,34123068	15,34586888	15,35245715	15,35825506	15,34641551	0,006856205	0,000446763	0,000446533
P	15,95985684	15,92809997	15,93799645	15,94268142	15,94855162	15,95985684	15,94291447	0,007927091	0,000497217	0,000496689
K	2,826465055	2,822896021	2,825359902	2,827672331	2,829141683	2,832613251	2,827397205	0,002732274	0,000966357	0,000966675
Ca	23,04612865	23,01034333	23,02749739	23,03691912	23,04442961	23,05421212	23,03579114	0,010516662	0,000456536	0,000456331
Sr	32,37697186	32,3430714	32,35660143	32,36304978	32,37409572	32,38663588	32,36480862	0,011280659	0,000348547	0,000348416
Zr	21,95753211	21,9178326	21,93207138	21,93997269	21,94413132	21,95753211	21,93949957	0,009406354	0,000428741	0,000428388
Ba	57,63844909	57,60341306	57,62361923	57,63170624	57,64140432	57,66885978	57,63284252	0,015897595	0,000275843	0,000275816
Pb	73,94458526	73,91473277	73,93146732	73,93736736	73,94430689	73,95301591	73,93697292	0,010074509	0,000136258	0,000136244
Al	22,02525867	21,99138717	22,00328779	22,01003898	22,0155566	22,02589283	22,01022359	0,008853256	0,000402234	0,000401959
Ti	22,46753461	22,43236404	22,43923712	22,44871578	22,45562631	22,46753461	22,44839191	0,009921695	0,000441978	0,000441601
V	0	0	0	0	0	0	0	0	0	0
Cr	4,534368315	4,455887552	4,482181864	4,491870758	4,50488162	4,534368315	4,493553928	0,018906884	0,004207557	0,004169684
Mn	22,88182017	22,84269186	22,85127173	22,86186366	22,86878627	22,88182017	22,86055464	0,010616862	0,000464418	0,000463987
Fe	10,10112826	10,07929175	10,08393529	10,08869705	10,09351013	10,10112826	10,08887121	0,005627138	0,000557757	0,00055708
Ni	7,745596146	7,709426039	7,719680368	7,722653267	7,729874107	7,745596146	7,723915443	0,00895806	0,001159782	0,001156536
Cu	0	0	0	0	0	0	0	0	0	0
Zn	0	0	0	0	0	0	0	0	0	0
Mo	41,52669259	41,46882773	41,48926991	41,50024501	41,51314152	41,52669259	41,5004676	0,014630965	0,000352549	0,000352327
S	33,85456509	33,80046781	33,81676035	33,8283797	33,83968103	33,85456509	33,82865274	0,013886697	0,000410501	0,000410187

Statistics Over All Runs

Factor 5	Lowest Q	Min	25th	50th	75th	Max	Mean	Std Dev	RSD % mean	RSD % Lowest Q
PM2.5	25,94186878	25,94186878	25,9462972	25,95331705	25,96256061	25,97315419	25,95499523	0,009748115	0,000375578	0,000375768
Na	0	0	0	0	0	0	0	0	0	0
Mg	30,83649609	30,83340306	30,84239278	30,84923323	30,85988125	30,87962535	30,85219998	0,013028066	0,000422273	0,000422489
P	30,31804597	30,31804597	30,3249354	30,32982057	30,3434693	30,3532017	30,33275534	0,010395589	0,000342718	0,000342885
K	27,67010968	27,66454666	27,67467922	27,68183968	27,69613062	27,71224112	27,68508323	0,013513079	0,0004881	0,000488364
Ca	52,55845692	52,55845692	52,5691048	52,57696411	52,5871498	52,6132382	52,57922189	0,014653951	0,000278702	0,000278812
Sr	18,45422091	18,45422091	18,46024377	18,46540023	18,47225105	18,48661073	18,46692794	0,009287976	0,000502952	0,000503298
Zr	4,347542427	4,346981563	4,347555309	4,350309718	4,351807049	4,35443902	4,350026789	0,002398136	0,000551292	0,000551607
Ba	0	0	0	0	0	0	0	0	0	0
Pb	5,246353414	5,243335854	5,247087332	5,248600365	5,251008794	5,25554695	5,249024351	0,003199231	0,000609491	0,000609801
Al	13,24585906	13,24574863	13,2495533	13,25183858	13,25801712	13,26574589	13,25394304	0,006346687	0,000478853	0,000479145
Ti	34,18202619	34,18190221	34,18753089	34,19253344	34,20376999	34,21772113	34,19622361	0,01107876	0,000323976	0,000324111
V	56,72424476	56,69673025	56,71724104	56,72409606	56,73513487	56,74329068	56,72411281	0,011643524	0,000205266	0,000205265
Cr	11,78795935	11,75538707	11,77080919	11,78002264	11,79065171	11,80171394	11,78018456	0,012791999	0,001085891	0,001085175
Mn	32,9295567	32,9295567	32,93569093	32,94066757	32,95182685	32,96101237	32,94314741	0,010196751	0,000309526	0,000309653
Fe	43,03419878	43,0284358	43,03885773	43,04396006	43,05584421	43,06492079	43,04612852	0,010597958	0,0002462	0,000246268
Ni	6,984475015	6,97793156	6,984848288	6,988448497	6,991942922	6,995074279	6,987980001	0,004504413	0,000644594	0,000644918
Cu	24,47893305	24,46515173	24,47662914	24,48528501	24,49127203	24,50160772	24,48419452	0,009205689	0,000375985	0,000376066
Zn	0	0	0	0	0	0	0	0	0	0
Mo	0	0	0	0	0	0	0	0	0	0
S	1,473789816	1,469762246	1,472406844	1,473821148	1,47499237	1,476447916	1,473543006	0,001892617	0,001284399	0,001284183

Percent of Total Variable

Statistics Over All Runs

Factor 1	Lowest Q	Min	25th	50th	75th	Max	Mean	Std Dev	RSD % mean	RSD % Lowest Q
PM2.5	81,25672091	81,25376356	81,25561881	81,25710687	81,25846838	81,26302712	81,25713464	0,002185753	2,68992E-05	2,68994E-05
Na	9,320809309	9,316484801	9,31895782	9,320358921	9,321497499	9,323670393	9,320272445	0,001851673	0,000198672	0,00019866
Mg	0,616021079	0,615868444	0,616023166	0,616060567	0,616102166	0,616161754	0,61605616	6,43326E-05	0,000104426	0,000104432
P	0	0	0	0	0	0	0	0	0	0
K	1,326658356	1,326194893	1,326462272	1,326602732	1,326660556	1,326816694	1,326579736	0,000160271	0,000120815	0,000120808
Ca	2,777257905	2,775590884	2,776989528	2,777475021	2,778176104	2,779490172	2,777560715	0,000857208	0,000308619	0,000308653
Sr	0,030339392	0,030325475	0,030335134	0,030337394	0,030339905	0,030344666	0,030337454	4,28379E-06	0,000141205	0,000141196
Zr	0,058252081	0,058227133	0,058241172	0,058249009	0,058258386	0,058276618	0,058249224	1,18904E-05	0,00020413	0,00020412

Ba	0,590423005	0,589907203	0,590095164	0,590247524	0,59031625	0,59056062	0,590228145	0,000158468	0,000268486	0,000268398
Pb	0	0	0	0	0	0	0	0	0	0
Al	3,597040772	3,595624854	3,596632104	3,596922373	3,597436369	3,598024514	3,596942336	0,000568207	0,000157969	0,000157965
Ti	0,046222247	0,046222247	0,046244767	0,046250431	0,046257232	0,046269741	0,046248766	1,28949E-05	0,000278816	0,000278976
V	0,001248351	0,001247924	0,001249484	0,001249841	0,001250323	0,001251027	0,001249815	7,84895E-07	0,000628009	0,000628745
Cr	0,003427788	0,003427788	0,003456458	0,003468269	0,003476718	0,003505003	0,003466474	1,87429E-05	0,005406892	0,005467914
Mn	0,005349395	0,005347984	0,00535436	0,00535513	0,00535798	0,005360282	0,005355427	3,18212E-06	0,000594186	0,000594856
Fe	0,314826885	0,314734022	0,315035416	0,315109492	0,315213793	0,31533216	0,315102835	0,000151765	0,000481636	0,000482058
Ni	0	0	0	0	0	0	0	0	0	0
Cu	0,003536934	0,003535954	0,003537097	0,00353753	0,003537999	0,003538889	0,003537551	7,70284E-07	0,000217745	0,000217783
Zn	0,032866974	0,03264889	0,03270982	0,032743593	0,032771236	0,032866974	0,032748413	5,63681E-05	0,001721245	0,001715036
Mo	0,003321725	0,003290709	0,00330779	0,003312731	0,003320594	0,003334156	0,003313448	9,35617E-06	0,002823697	0,002816661
S	0,015676894	0,015403796	0,015551534	0,01562399	0,015673072	0,015792856	0,015616416	8,8466E-05	0,005664937	0,005643083

Statistics Over All Runs

Factor 2	Lowest Q	Min	25th	50th	75th	Max	Mean	Std Dev	RSD % mean	RSD % Lowest Q
PM2.5	95,12459884	95,1243592	95,12553217	95,12603376	95,12673027	95,12753534	95,12606813	0,00090993	9,56552E-06	9,56567E-06
Na	1,330561024	1,328375119	1,328867946	1,329516374	1,329873918	1,3305907	1,32944808	0,00068817	0,000517636	0,000517203
Mg	0,095811627	0,09570465	0,095719418	0,095756253	0,095778381	0,095825014	0,095754238	3,35237E-05	0,000350101	0,000349892
P	0,075268715	0,075264192	0,075270034	0,075276637	0,075283855	0,07529149	0,075277611	8,08365E-06	0,000107385	0,000107397
K	0,173964291	0,173717623	0,173743993	0,173836911	0,173880467	0,17398725	0,173828044	7,77588E-05	0,000447332	0,000446981
Ca	0	0	0	0	0	0	0	0	0	0
Sr	0,00330139	0,003296958	0,003298109	0,003299409	0,00330029	0,003302359	0,003299331	1,36922E-06	0,000415001	0,000414742
Zr	0,038113057	0,03810344	0,038106572	0,03810923	0,038111672	0,038115117	0,038109313	3,41607E-06	8,96386E-05	8,96298E-05
Ba	0	0	0	0	0	0	0	0	0	0
Pb	0	0	0	0	0	0	0	0	0	0
Al	1,567885986	1,567310294	1,567481672	1,567583304	1,567695827	1,567976761	1,567601087	0,000176276	0,00011245	0,000112429
Ti	0,042343632	0,042337587	0,042338411	0,042339625	0,04234097	0,042345176	0,042339951	2,16587E-06	5,11542E-05	5,11498E-05
V	0,00182846	0,001827895	0,001828068	0,001828197	0,001828223	0,001828585	0,001828195	1,67028E-07	9,1362E-05	9,13488E-05
Cr	0,049779466	0,049767284	0,049774457	0,049776778	0,049779115	0,049782051	0,049776354	3,86819E-06	7,77113E-05	7,77065E-05
Mn	0,013487163	0,013486847	0,013487636	0,013487975	0,013488491	0,013489039	0,013488	6,33125E-07	4,69399E-05	4,69428E-05
Fe	0,493340733	0,493300722	0,493307639	0,493324306	0,49333964	0,493386535	0,493326253	2,15582E-05	4,36996E-05	4,36984E-05
Ni	0,016061558	0,016059096	0,016061875	0,01606251	0,016062813	0,016064849	0,016062396	1,16119E-06	7,22925E-05	7,22963E-05
Cu	0,005446588	0,005441743	0,00544332	0,005443853	0,005444965	0,005446588	0,005444145	1,2269E-06	0,000225361	0,00022526
Zn	0	0	0	0	0	0	0	0	0	0
Mo	0,098490512	0,098490512	0,098502377	0,09850804	0,098514092	0,098524938	0,098507849	9,14908E-06	9,28767E-05	9,2893E-05
S	0,869716962	0,869698132	0,869786848	0,869845517	0,869891352	0,869951874	0,869841023	7,01812E-05	8,06827E-05	8,06942E-05

Statistics Over All Runs

Factor 3	Lowest Q	Min	25th	50th	75th	Max	Mean	Std Dev	RSD % mean	RSD % Lowest Q
PM2.5	96,58955866	96,58935036	96,59018965	96,59044063	96,59068797	96,59111321	96,5903784	0,000434778	4,50125E-06	4,50129E-06
Na	0	0	0	0	0	0	0	0	0	0
Mg	0,048321755	0,048261832	0,048278875	0,048283545	0,048301093	0,048334614	0,048289532	1,92057E-05	0,00039772	0,000397455
P	0,091277423	0,091271187	0,091273648	0,091274597	0,09127729	0,091279449	0,091275026	2,24022E-06	2,45437E-05	2,4543E-05
K	0,098369954	0,098293959	0,098302511	0,098325459	0,098345269	0,098387376	0,098329056	2,75105E-05	0,00027978	0,000279663
Ca	0,725334713	0,723756258	0,7241711	0,724459624	0,724729234	0,725636455	0,724523819	0,000460588	0,000635711	0,000635
Sr	0,00303269	0,003029945	0,003030558	0,003030827	0,003031506	0,003032778	0,003031067	7,58341E-07	0,00025019	0,000250056
Zr	0,029720982	0,029718843	0,029721858	0,0297238	0,029725706	0,029726648	0,029723709	2,17264E-06	7,30945E-05	7,31012E-05
Ba	0	0	0	0	0	0	0	0	0	0
Pb	0,083983613	0,083941696	0,083947686	0,083960628	0,083969257	0,083996603	0,083961117	1,50669E-05	0,000179451	0,000179403
Al	1,034164824	1,034121941	1,034164926	1,034182301	1,034226252	1,034265278	1,034189309	3,87567E-05	3,74755E-05	3,74764E-05
Ti	0,013909079	0,013901479	0,013904175	0,01390553	0,013907032	0,013909079	0,013905465	2,01996E-06	0,000145264	0,000145226
V	0	0	0	0	0	0	0	0	0	0
Cr	0,001382296	0,001378262	0,001384331	0,001388098	0,001393508	0,00139768	0,001388735	5,90084E-06	0,004249077	0,004268868
Mn	0,007587638	0,007586289	0,00758692	0,007587235	0,007587558	0,007587797	0,007587193	3,9836E-07	5,25042E-05	5,25011E-05
Fe	0,206301751	0,206236781	0,206260386	0,206272687	0,206287669	0,206302923	0,206274298	1,91287E-05	9,27345E-05	9,27222E-05
Ni	0,009756483	0,009755515	0,009757658	0,0097586	0,009759948	0,009760701	0,009758636	1,44811E-06	0,000148393	0,000148426
Cu	0,003535475	0,003534974	0,003536063	0,003536526	0,003537036	0,003537478	0,003536474	6,71859E-07	0,00018998	0,000190033
Zn	0,134110664	0,134110664	0,134120364	0,134128432	0,134138505	0,134153115	0,134128975	1,15373E-05	8,60165E-05	8,60283E-05
Mo	0,095887153	0,095881858	0,095886931	0,095893526	0,095898895	0,095900013	0,095892313	6,19902E-06	6,46456E-05	6,46491E-05
S	0,823764844	0,823720669	0,823785868	0,823841591	0,823876558	0,823903528	0,823826874	5,56636E-05	6,75671E-05	6,75722E-05

Statistics Over All Runs

Factor 4	Lowest Q	Min	25th	50th	75th	Max	Mean	Std Dev	RSD % mean	RSD % Lowest Q
PM2.5	90,43362147	90,42797491	90,42989202	90,43054547	90,43172171	90,43362147	90,43071468	0,001390874	1,53806E-05	1,53801E-05
Na	0	0	0	0	0	0	0	0	0	0
Mg	0,237448667	0,237448667	0,237506184	0,237566409	0,237581863	0,237661931	0,237550922	5,39984E-05	0,000227313	0,000227411
P	0,064322893	0,064305778	0,064311351	0,064314726	0,064319682	0,064330762	0,064315665	6,1855E-06	9,61741E-05	9,61633E-05
K	0,071047235	0,071031637	0,071082105	0,071139952	0,07118696	0,071274755	0,071137695	6,5372E-05	0,000918951	0,000920121
Ca	3,766642493	3,766642493	3,768118115	3,769156468	3,769739028	3,771530012	3,768996364	0,001230007	0,000326349	0,000326553
Sr	0,02654048	0,02654048	0,026547416	0,02655014	0,026551736	0,026556728	0,026549703	3,98353E-06	0,00015004	0,000150093
Zr	0,044041315	0,044027241	0,044032405	0,044036243	0,044039097	0,044043987	0,044035862	4,4303E-06	0,000100607	0,000100594
Ba	0,852617373	0,852617373	0,852803389	0,852892581	0,852938727	0,853018508	0,852868674	0,000101326	0,000118806	0,000118841
Pb	0,427728799	0,427728799	0,427808408	0,42784943	0,427869757	0,42791717	0,427837894	4,97151E-05	0,000116201	0,00011623
Al	2,410770158	2,41069122	2,410879317	2,410952655	2,411032817	2,411170457	2,410949804	0,000132995	5,51631E-05	5,51672E-05
Ti	0,060742129	0,060742129	0,060748441	0,060751607	0,060755218	0,060757921	0,060751499	4,13843E-06	6,81206E-05	6,81311E-05
V	0	0	0	0	0	0	0	0	0	0
Cr	0,003375554	0,003321698	0,003340471	0,003349931	0,003357711	0,003375554	0,00334937	1,33156E-05	0,003975566	0,003944728
Mn	0,016522371	0,016522371	0,016523281	0,016523924	0,016524298	0,016525013	0,016523805	7,06885E-07	4,27798E-05	4,27835E-05
Fe	0,256809774	0,256767637	0,256785902	0,256798112	0,25680906	0,25683013	0,256798012	1,53237E-05	5,96721E-05	5,96694E-05
Ni	0,00293123	0,00292011	0,002923955	0,002925292	0,002927343	0,002931246	0,002925699	2,83328E-06	0,00096841	0,000966583
Cu	0	0	0	0	0	0	0	0	0	0
Zn	0	0	0	0	0	0	0	0	0	0
Mo	0,179737101	0,179697379	0,179721561	0,17973227	0,179741346	0,179758311	0,179730692	1,44221E-05	8,0243E-05	8,02402E-05
S	1,145100955	1,144681471	1,144856609	1,144981942	1,145061564	1,145194297	1,144963663	0,000139224	0,000121597	0,000121582

Statistics Over All Runs

Factor 5	Lowest Q	Min	25th	50th	75th	Max	Mean	Std Dev	RSD % mean	RSD % Lowest Q
PM2.5	92,12997974	92,12919487	92,12951925	92,12988539	92,13000191	92,13025883	92,12980474	0,000308098	3,34418E-06	3,34417E-06
Na	0	0	0	0	0	0	0	0	0	0
Mg	0,296221809	0,296207437	0,296216533	0,29622805	0,29624329	0,296265432	0,296229999	1,65782E-05	5,59639E-05	5,59654E-05
P	0,075901469	0,075895918	0,075899688	0,075901852	0,075904189	0,075908148	0,075902149	3,1943E-06	4,20845E-05	4,20849E-05
K	0,432042866	0,432039392	0,432051543	0,432064781	0,432082934	0,43210262	0,432067803	1,99296E-05	4,61261E-05	4,61287E-05
Ca	5,335945999	5,335794659	5,335923718	5,336128704	5,336343815	5,336711601	5,336172799	0,000293513	5,50045E-05	5,50068E-05
Sr	0,009396815	0,009395496	0,009396168	0,009396816	0,009397148	0,009397791	0,009396679	6,36751E-07	6,77634E-05	6,77624E-05
Zr	0,005416678	0,005413803	0,005414559	0,005416075	0,005416672	0,005417939	0,005415828	1,20058E-06	0,000221679	0,000221645
Ba	0	0	0	0	0	0	0	0	0	0
Pb	0,018850899	0,018824675	0,018837497	0,018839738	0,018844828	0,018850899	0,018840363	6,52622E-06	0,000346395	0,000346202
Al	0,900590412	0,900442704	0,900508594	0,900538845	0,900564038	0,900616143	0,900537781	4,10701E-05	4,56061E-05	4,56035E-05
Ti	0,057404349	0,057401132	0,057403294	0,057404305	0,057405065	0,057407442	0,05740412	1,6681E-06	2,90589E-05	2,90588E-05
V	0,002773691	0,002773262	0,002773424	0,002773527	0,00277368	0,002773863	0,002773541	1,56571E-07	5,64517E-05	5,64487E-05
Cr	0,005451039	0,005436807	0,005441229	0,005446435	0,005450377	0,005457215	0,005446515	5,54224E-06	0,001017575	0,00101673
Mn	0,014769986	0,014769302	0,014769753	0,014770061	0,014770332	0,014770652	0,014770036	3,63087E-07	2,45826E-05	2,45827E-05
Fe	0,679622558	0,679602383	0,679616311	0,679636236	0,679646983	0,67967543	0,679635986	2,10057E-05	3,09073E-05	3,09079E-05
Ni	0,001641879	0,001640622	0,001641498	0,00164184	0,001642405	0,001643301	0,001641863	6,67208E-07	0,000406372	0,000406368
Cu	0,003024568	0,003023035	0,003023405	0,003023861	0,003024351	0,003024701	0,003023887	5,07212E-07	0,000167735	0,000167697
Zn	0	0	0	0	0	0	0	0	0	0
Mo	0	0	0	0	0	0	0	0	0	0
S	0,030965243	0,030870559	0,030906798	0,030942095	0,030964949	0,031000182	0,030935913	3,63006E-05	0,001173414	0,001172302